Amélia da Silva Ramos

Multilayer radiating structures for mmWaves

Estruturas radiantes multicamada para ondas milimétricas

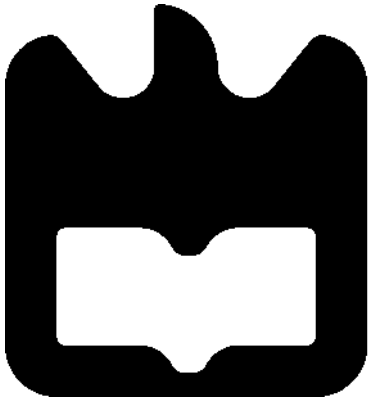

Amélia da Silva Ramos

Multilayer radiating structures for mmWaves

Estruturas radiantes multicamada para ondas milimétricas

Dissertação apresentada à Universidade de Aveiro para cumprimento dos requisitos necessários à obtenção do grau de Mestre em Engenharia de Eletrónica e Telecomunicações, realizada sob a orientação científica do Professor Doutor João Nuno Pimentel da Silva Matos, do Departamento de Eletrónica, Telecomunicações e Informática da Universidade de Aveiro e do Doutor Tiago Miguel Valente Varum, investigador no Instituto de Telecomunicações.

"A goal without a plan is just a wish"

-Antoine de Saint-Exupéry

o júri / the jury

Presidente / President

Professora Doutora Susana de Jesus Mota
Professora Auxiliar, Universidade de Aveiro

Vogais / Examiners comittee

Professor Doutor João Nuno Pimentel da Silva Matos
Professor Associado, Universidade de Aveiro (orientador)

Professor Doutor Custódio José de Oliveira Peixeiro
Professor Auxiliar, Instituto Superior Técnico da Universidade de Lisboa (arguente)

Agradecimentos / Acknowledgements

Em primeiro lugar, um obrigado muito especial aos meus pais, pela oportunidade e incentivos dados nos últimos anos. À minha irmã, Júlia, um sentido obrigado, por todas as vezes que cheguei a casa e me soube reconfortar. Que todo o meu percurso sirva para que ela aprenda e seja cada vez melhor.

Um especial agradecimento aos meus orientadores, o Professor João Nuno Matos e o Dr. Tiago Varum, por me terem proposto este tema, terem aceitado trabalhar comigo, e acima de tudo, por todos os esclarecimentos, apoio e oportunidades que me proporcionaram. Certamente sem eles este trabalho não seria possível.

Ao Instituto de Telecomunicações, e a toda a sua equipa técnica, deixo o meu especial agradecimento por todo o suporte dado durante a realização desta dissertação.

À Alexandra Figueiredo, por todas as vezes que atendeu as minhas chamadas, me ouviu, me motivou, e me fez acreditar que eu iria alcançar os meus sonhos, um grande obrigado. À Carolina e ao Rodrigo, por todo o carinho, convívio e ajuda ao longo dos anos, um enorme obrigado pela vossa amizade. Agradecer ainda a todos os outros amigos que este curso me deu, e que felizmente são demasiados para citar neste agradecimento, por todas as partilhas e união.

Por último, ao Pedro Magalhães, um obrigado, por mais uma vez me ter mostrado que não tenho razões para duvidar de mim, e por me incentivar constantemente a fazer mais e melhor.

Palavras-chave 5G, IoT, ondas milimétricas, antena multicamada, Yagi-Uda

Resumo

Nesta dissertação foram construídas três antenas Yagi-Uda, uma delas cuja frequência de operação é 2.4 GHz, enquanto as restantes operam a 24 GHz. As antenas Yagi-Uda são bastante conhecidas, no entanto, aqui, foram desenvolvidos protótipos impressos de antenas Yagi, já que, hoje em dia a maioria dos sistemas requer circuitos impressos.

Mais ainda, foi feita uma comparação entre a performance de uma antena planar e a de uma antena multicamada, ambas a operar na região das ondas milimétricas.

No decorrer do trabalho foi possível melhorar progressivamente tanto o ganho como a largura de banda das antenas, começando no protótipo de 2.4 GHz e culminando na estrutura multicamada. Estes resultados foram obtidos sem prejudicar a eficiência global das antenas, estando estes sempre em valores bastante razoáveis.

Keywords 5G, IoT, millimeter-waves, multilayer antenna, Yagi-Uda

Abstract

In this dissertation three Yagi-Uda antennas were built, one with a frequency of operation of 2.4 GHz and the others operating at 24 GHz. Yagi-Uda antennas are well known, but here, printed Yagi-like prototypes were developed since nowadays most systems require printed circuits.

Moreover, a comparison on the performance of a planar and a multilayer Yagi antenna was made, both operating in the mmWave region.

Throughout the work it was possible to progressively improve gain and bandwidth, starting in the 2.4 GHz antenna and culminating in the multilayer prototype. These results were achieved without damage of the antennas' global efficiency, which was kept at quite satisfactory values.

Contents

List of Figures

List of Tables

List of Acronyms

1G	:	*First generation of mobile communications*
2G	:	*Second generation of mobile communications*
3G	:	*Third generation of mobile communications*
4G	:	*Fourth generation of mobile communications*
5G	:	*Fifth generation of mobile communications*
CST	:	*Computer Simulation Technology*
DRA	:	*Dielectric Resonator Antenna*
GSM	:	*Global System for Mobile Communications*
HPBW	:	*Half Power Beamwidth*
IEEE	:	*Institute of Electrical and Electronics Engineers*
IoT	:	*Internet of Things*
ISM	:	*Industrial, Scientific and Medical*
LPS	:	*Local Positioning System*
LTCC	:	*Low-Temperature Co-fired Ceramic*
LTE	:	*Long Term Evolution*
SIW	:	*Substrate Integrated Waveguide*
SMS	:	*Short Message Service*
VHF	:	*Very High Frequency*
VNA	:	*Vector Network Analyser*

Chapter 1

1 Introduction

1.1 Context and Motivation

A long way has been paved since the world began conceiving communications. It is safe to say that this path was started by Maxwell (1831-1879), H. Hertz (1857-1894) and Marconi (1875-1937). Due to their respective contributions, regarding electricity and magnetism, confirmation of the existence of electromagnetic radiation and the actual prove of the feasibility of radio communications, the world of wireless communications gave its first steps [1].

Wireless communications, as defended by their name, consist on transmitting information over a specific distance, without the help of wires, cables or any electrical conductors. That distance varies, considering the application and the technology used, for example, a television's remote control works within a few meters, however, space communications operate properly, even if that means to communicate to thousands of kilometers [2].

When compared to wired communications, the wireless alternative presents several advantages. Those include ease of internet access (since it is not required to carry cables around), and it also allows people, for instance doctors, working in more remote areas, to get in touch, more easily, with professionals from other medical centres and even in urgent situations, alerts can be given promptly [2].

The usage of personal devices anywhere and anytime is very interesting and led mankind to improve many services, however, wireless communications present undesired disadvantages, starting with the threats in security. In fact, in wireless communications, an unauthorized person can (with relative ease) capture wireless signals which are spread through the air, and this might result in the misuse of the captured information [3].

Concerning the propagation issues brought by using an unguided communication medium, the biggest challenges are related to the fading of the signal, the path loss attenuation, multipath fading or shadowing by obstacles [4]. Moreover, interferences between transmitters and/or receivers can be stated [5].

As presented in [6], an antenna is a necessary element in any wireless communication system, and many radio-frequency standards, especially in this field of investigation, have been proposed or updated in the last two decades. In [6] it is said that the ultimate goal is to build a wireless world, thus the importance of new developments in antennas.

There are several innovative antenna technologies, which include reconfigurable antennas, metamaterial-based antennas and antennas suitable for software-defined radio [6]. All must be considered to design a more durable, reliable system, where proper communication is guaranteed and, in the end, each of those systems has particular requirements.

Based on the principles of traditional Yagi-Uda antennas, three printed Yagi's were built, with enhance in a multilayer prototype, an alternative design and a possible solution for the next generation of mobile communications.

1.2 Dissertation Objectives

Due to the growing evolution of wireless communications, and to the rising of information consumption, large bandwidth is each time rarer in the most commonly used areas of the electromagnetic spectrum.

The new generation of mobile communications is expected to explore frequency bands less used, where wider bandwidth is available, such as the mmWave region. Additionally, this wider bandwidth can serve as a tool to suppress the needs of the 5th generation of mobile communications (5G), for example, providing extreme data-rates (Multi-Gbps).

Since antennas represent the last and first components in any wireless communication system, there is a growing need for designing these elements in printed structures, guaranteeing efficiency, compactness and ease of integration in printed circuits.

In this framework, it is intended to test the potential of implementing multilayer radiating structures, using stacked layers of dielectric substrate. Thus, the production of a

multilayer antenna must guarantee significant efficiency values, as well as high gain and wide bandwidth, so that the prototypes developed might be considered for scenarios such as 5G.

1.3 Dissertation Outlines

In this section the structure of this dissertation is outlined, and a brief description of each chapter is presented.

This document is divided in the following 5 chapters:

- **Chapter 1** – is the current chapter. Its aim is to frame the studied topic and relevance in the everyday life, by revealing the main objectives that are intended to be achieved.

- **Chapter 2** – frames the next generation of mobile communications, its demands and requirements, especially regarding mmWave circuits. Basic concepts of antennas are also clarified. Finally, it also includes a summary of the arguments to investigate multilayer antennas as well as it shows the results already accomplished in the literature.

- **Chapter 3** – it highlights the historical frame of Yagi-Uda antennas. Then, the main principles of designing Yagi antennas are presented, emphasizing the theoretical calculations for each element: dipole, reflector and directors.

- **Chapter 4** – it shows the optimized design parameters for all Yagi antennas, comparing the calculations made in Chapter 3 with their optimal values. It also exhibits the prototypes built. Here, measured results for each antenna are exposed, and compared to the simulated ones.

- **Chapter 5** – the last chapter is where the conclusions over the developed work are presented, as well as future improvements, including different approaches of designing the antennas which could result in improving bandwidth and/or gain.

1.4 Original Contributions

Some of the results obtained in this work provided the opportunity to publish one scientific paper:

1. Ramos, A.; Varum, T.; Matos, J.N. Compact Multilayer Yagi-Uda Based Antenna for IoT/5G Sensors. *Sensors* **2018**, *18*, 2914. This paper was accepted, and it can be seen at Appendix A.
2. A. Ramos, T. Varum and J. N. Matos, "Integrated Multilayer Yagi Antenna for 5G", submitted for the 13th European Conference on Antennas and Propagation (2019 Edition of EuCAP).

Chapter 2

2 Overview on 5G and antennas

This chapter aims to frame the antennas developed in this dissertation within this field of investigation. Thus, it begins with a contextualization on the reasons why building antennas to operate in the mmWave region. Later, basic antenna concepts are clarified, in order to culminate on the Yagi-Uda's choice. Lastly, a state-of-the-art is presented regarding multilayer implementations, both in microstrip patch antennas and Yagi-Uda's.

2.1 Millimeter-Waves migration: 5G and IoT demands

2.1.1 Earlier generations of mobile communications

On April 3, 1973, Motorola's engineer, Martin Cooper, made the world's first mobile phone call using an actual handheld phone. The prototype took 10 years to be commercially available and its name was DynaTAC 8000X (Figure 2.1) [7]. The device weighed nearly 1.1 kg, measured 22.86 cm long, 12.7 cm deep and 4.44 cm wide. Moreover, the prototype's battery took 10 hours to recharge, offering a maximum talking time of 20 minutes. However, truth be told, a phone with these measurements and weight would be hard to hold for that long. A deep and great path has been paved since back then.

Figure 2.1: DynaTAC 8000x prototype [8].

Additionally to the massive weight and global dimensions, this phone was truly a luxury item. At the time it reached the market, it costed around 4000$, about 9500$ if this value is adjusted for inflation [9]. For a while now, mobile phones are no longer luxury items, on the contrary, they are seen as a necessity. The impact on people's interconnection and communication, regardless of distance, is clear. As examples, currently a mobile phone is not only used for voice calls, but it is also widely used for checking directions, reading books and news, amongst many other applications.

This invention started the mobile generations, and since the 1980's the communication systems have evolved through several stages of technological improvement. Roughly, each 10 years a new generation of mobile communications appears, introducing more efficiency, higher performance and capability [10].

In this way, the 1st generation (1G) phones emerged in 1980's. Even though at that time semiconductor technology and microprocessors were turning smaller and more sophisticated systems a reality, these 1G cellular devices transmitted only analogue voice information [11]. One example of those devices is the Sony CM-D600, shown in Figure 2.2. At this point, devices such as the one seen, were weighty and many times exposure was unreliable [13]. Apart from the restrictions of these systems, the ease of mobile communication was proven, as well as the impact in the mobile market, since it showed an annual growth of 30 to 50%, and by 1990 there were already 20 million subscribers [11].

Figure 2.2: Sony CM-D600 1G mobile phone [12].

Subsequently, the 2nd generation (2G) arose in the 1990's and it solved one of the issues of 1G. The 2G used digital modulation, solving the frequently imperceptible voice calls, since analog information is more subject to distortions than digital information [11]. Hence, at this point the great purpose of speech transmission was significantly improved and the first data services, such as the well-known Short Message Service (SMS), were provided [13],[14] (even though with a 160 characters limit at that time [15]). Despite several systems have been introduced, the Global System for Mobile Communications (GSM) became the most popular, and even now, it continues to operate in more than 200 countries [16]. In parallel, internet was emerging and, network operators wanted to include it into new mobile systems rapidly [11].

The 3rd generation (3G) started to be planned in late 1980s [15], however, only in late 1990's, early 2000's, 3G reached the market [17]. A clear statement was left by the industry here, moving towards a worldwide converged network. Once again, this generation improved the overall systems' performance, as it enhanced features for multimedia communications, and it provided extensive bandwidth, as well as high-speed capabilities (upwards of 2 Mbps) [13].

Just like 3G improved the speeds of 2G and the previous mobile generations, Long-Term Evolution (LTE), once more, increased the data capacity, data transfer speeds as well as it reduced latency [18]. It is commonly named as the 4th generation of mobile communications (4G), however, accordingly to the International Telecommunications governing body, that is the appropriate branding to use regarding LTE Advanced, where the disruptive technology arose, by reaching data transfer rates of 5 Gb/s.

In terms of mobile phones themselves, evidently these devices followed a remarkable evolution, guaranteeing each time a better user experience. As described by Tiger Mobiles, in [19], *"from simple to smart, mobile phones have transformed dramatically to become information and communication hubs fundamental to modern life"*. Figure 2.3 shows a glance of the visible changes in these devices as well as it presents a futuristic idea of what mobile phones will be, possibly within the next few years.

Figure 2.3: Evolution of mobile phones [20].

Shortly, Figure 2.4 highlights, in a timeline shaped graphic, the key milestones of mobile communications, as well as it clarifies the big improvements, from the user point of view [21]-[23].

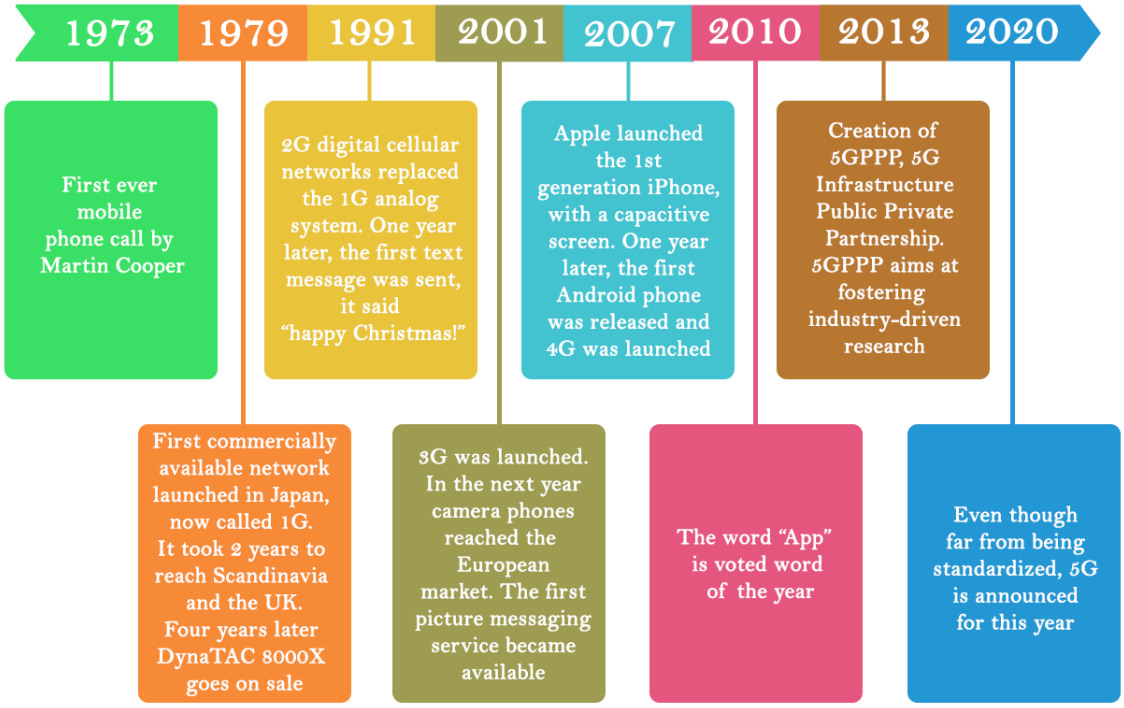

Figure 2.4: Key milestones of mobile communications.

2.1.2 5G expectations and commitments

As clearly stated earlier, 4G improved people's interconnection, and 5G intends to continue that demand and take it to the next level. Even though the evolution of mobile communications progresses naturally and arises as a response to the user needs', it is important to understand what are in fact the challenging scenarios that 5G must handle.

Powered by an explosive growth in the number of connected devices and transferred data, as depicted in Figure 2.5, 4G is now at its limit. This great demand for information, and consequently data, is forcing the mobile communications industry to *"define, develop and deliver"* 5G [24].

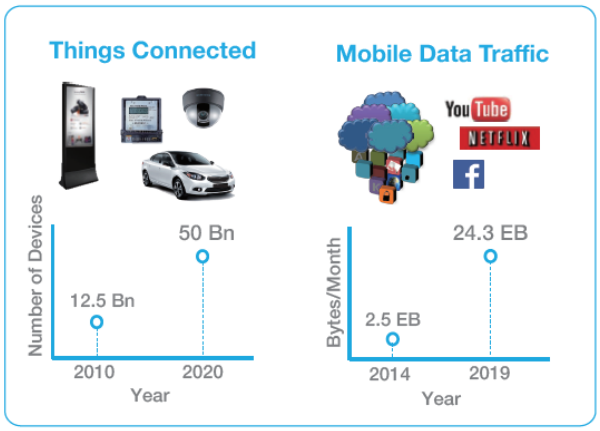

Figure 2.5: Growth in connected devices and mobile traffic [24].

Even though many of the 5G services might not be known yet, there's already a vision of what they can include. Possibly, there are four categories of services [24] within what is predicted for 5G, those categories are depicted in Figure 2.6.

Figure 2.6: 5G Service Vision.

Firstly, the Internet of Things category, frequently shortened to IoT. As stated by one of its fathers, Kevin Ashton, *"information is a great way to reduce waste and increase efficiency, and that's really what IoT provides"* [25]. This statement came after defending that the common vision of IoT is too poor, since its goal is to *"turn the world into data"*.

However, the IoT implementations that Kevin Ashton considers poor, will certainly be present on the daily life in a few years. For example, futuristic homes will include gadgets such as smart refrigerators, where they might be provided with a system capable of doing a recipe suggestion, considering what's inside the fridge.

Other possible scenario where IoT will be found is in Fitness and Healthcare. It is already common to use smart gadgets (watches for instance) to monitor the athletic performance or any type of exercise. Hereafter, these healthcare devices will be able to send vital signals such as blood pressure or brain-wave measurements to the hospital facilities, easing the prevention of medical emergencies [24].

Moreover, offices and stores will also become smart. Shopping can be customized, for example, alerts can be sent to shoppers if they are in the vicinity of a specific product that might be of their interest, or even if they're passing by a low-priced item. Surely, to support such scenarios massive connectivity and low-latency technologies are required. When it comes to the office, probably, many devices will be wirelessly connected, and will exchange data without showing a noticeable delay. Meeting warnings and documents relevant to those summits will be available instantaneously on the user's device [24].

Lastly, a big trend is now to have a connected car. Diagnosing the vehicle status can become easier, since sensors can be placed to indicate fuel level, engine status or battery level. Most importantly, IoT can facilitate the process of calling to an emergency service in case of accident. Then, the sharing of information between neighboring vehicles can be interesting, since if drivers are informed in real-time, and if the information is accurate, eventually, emergency situations can be avoided [24]. All these scenarios and possibilities are summed up in Figure 2.7, where connectivity is a key feature.

Figure 2.7: IoT cases (adapted from [26]).

Almost as a consequence of the scenarios described above, the second category arises, which is named as Immersive Multimedia Experience. In this topic, the vision for 5G is to create an immersive experience to users, almost including them in the videos and streams that they're viewing. The sensation of feeling apart of what it is being seen is also sustained by Virtual and Augmented reality. Both of these applications are a true challenge when it comes to provide a truly life-like experience [24].

Cloud-based services fit in an exclusive category and they have grown to be very popular, although the forecast is that the numbers grow higher in the coming years [27]. In fact, the idea is to offer a desktop-like experience, with everything stored in the cloud. Mobile devices would require simple interfaces for input and output, hence they could become lighter, thinner and even more eco-friendly [24].

Lastly, in the categories of the 5G Service Vision, the Remote Access is found. Correctly, Intuitive Remote Access is a more adequate expression regarding what is intended to be done in 5G. Once again, reliable connections, with near-zero latency, are necessary. As examples, users might remotely set home devices, or in a totally different scenario, remote access can help to explore unseen areas on earth in an efficient way and providing proper sets of images and video [24]. In the end, 5G will guarantee, for instance, the scenario exhibited by Figure 2.8.

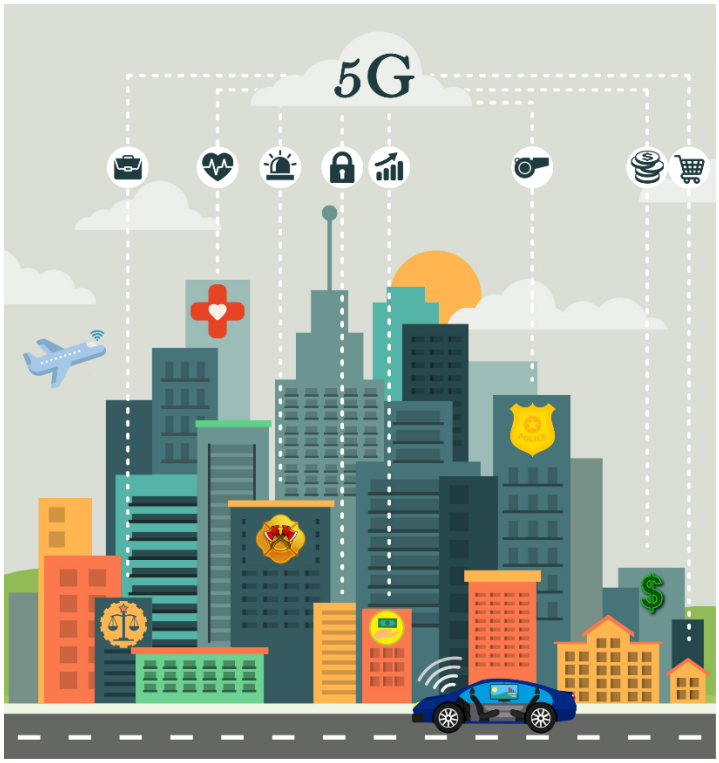

Figure 2.8: Example of 5G services scenario.

The global tendency shows that in the next years it will be witnessed an explosive growth of data traffic and it is estimated that this growth will increase around 200 times between 2010 and 2020 but from 2010 to 2030 it is expected to grow approximately 20000 times [10]. Shortly, 5G is expected to be the most reliable generation of mobile communications ever.

The 5G Vision represents, due to all exposed above, an unprecedented demand for services. It will support multiple services and devices, having a huge adaptability to several parameters such as throughput, latency and reliability, as examples. As a result, the 5G requirements can be summed up into three groups, as clarified by Figure 2.9, which are: massive internet of things, mission critical control and enhanced mobile broadband, keeping always in mind that the goal is to guarantee a unifying design [10].

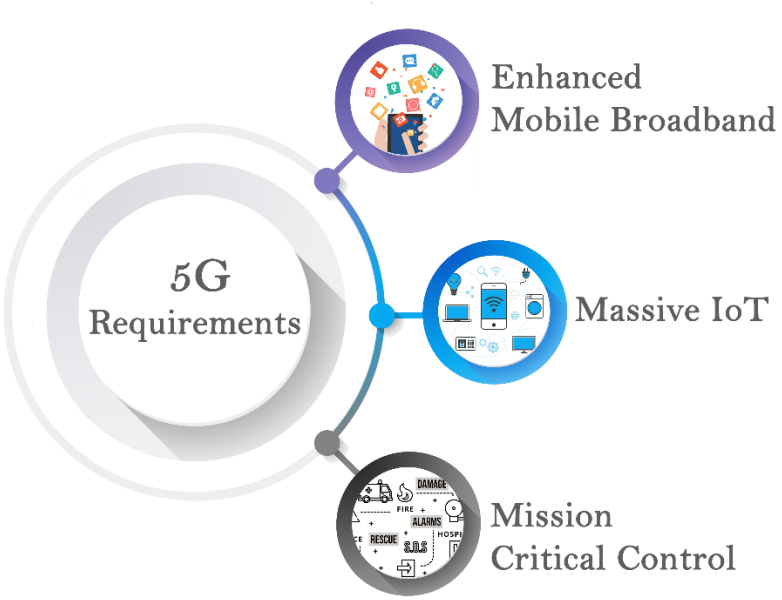

Figure 2.9: 5G requirements grouped in 3 categories.

Massive Internet of Things arises as a service and as a requirement. In the users' perspective, IoT presents itself as a service, since it will assure great interaction between users and gadgets, improving the overall users' experience. However, Smart Cities are an example of the massive IoT cases, where users will experience it as a service and at the same time, without the IoT implementation, cities would become unlivable, and within that perspective, IoT is a requirement for the next generation. In fact, half of the World's population lives in urban areas, causing several congestions. IoT can help solving issues such as waste management, air pollution, traffic congestions and even deteriorating and

aging infrastructures. This way, IoT becomes a way to conceptualize a smart city as a sustainable and livable city [28], fulfilling what is shown in Figure 2.10.

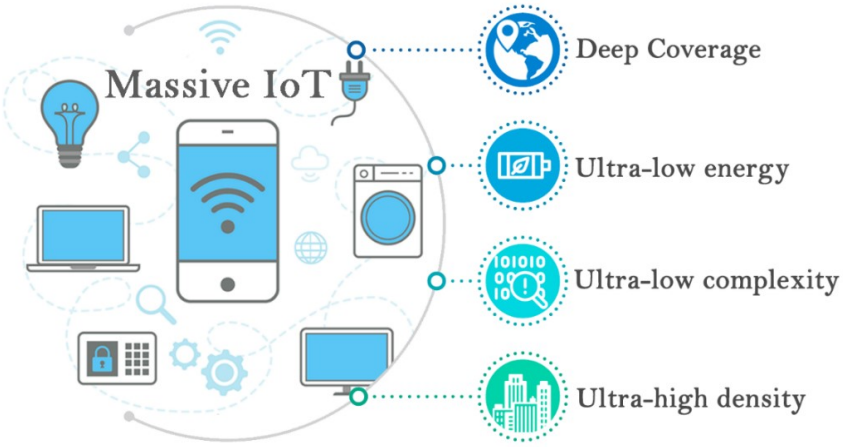

Figure 2.10: Massive IoT implementations and scenarios.

Massive IoT, as a requirement, will provide 5G with the necessary deep coverage, making possible to reach challenging locations, while fulfilling the inherent energetic efficiency. For instance, it will enable a 10 years lifetime of a powered sensor [29], but at the same time it will maintain ultra-low complexity in specific nodes, with dozens of bits per second, while simultaneously assuring ultra-high density, with up to 1 million connections per squared km [10].

On the other hand, the mission critical control requirement will change what exists nowadays. Currently, these services use specific networks, for reliability reasons, such as public safety. Predictably, the 5G infrastructure will allocate natively these mission critical services, thanks to the unprecedented performance achievable [29], assuring the topics mentioned in Figure 2.11.

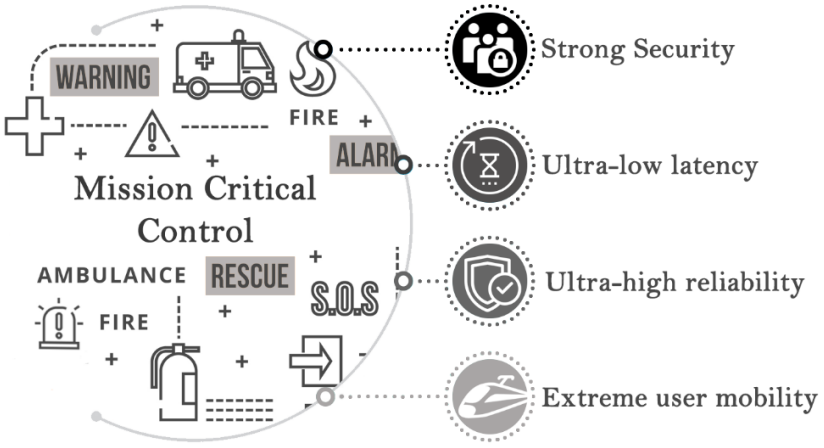

Figure 2.11: Mission critical control implementations and scenarios.

Mission critical control gathers not only medical emergencies but also financial and banking managements. New services which require real time reactivity will also be included, such as Vehicle-to-Vehicle or Vehicle-to-Road communications, paving the way towards self-driving cars or remote health services [29]. These scenarios imply clearly strong security and ultra-reliability. Ultra-low latency (under one millisecond) and extreme user mobility (trains travelling at 500 km/h) will also be a characteristic held by 5G systems [10].

Lastly, the category of enhanced mobile broadband, which as depicted by Figure 2.12, will guarantee peak data rates, allowing services such as 3D telepresence on mobile devices.

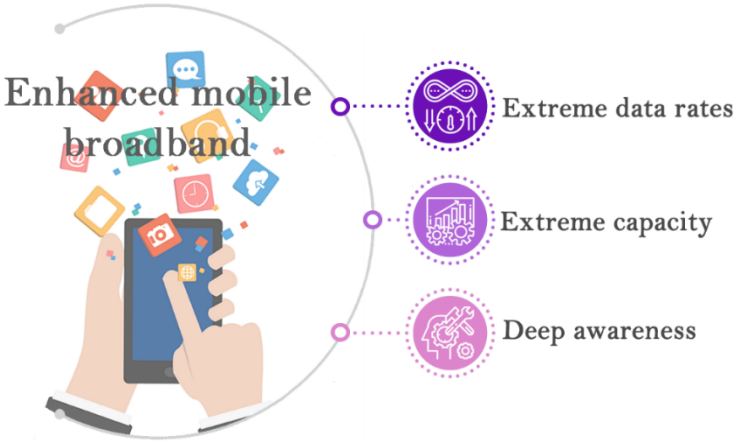

Figure 2.12: Enhanced mobile broadband implementations and scenarios.

The scaling process of 5G is expected to create deep awareness, facilitating discovery and optimization. At the same time, it will handle extreme capacities, in the order of 10 Tbps per km², or extreme data rates, such as Multi-gbps and 100+ Mbps user experienced rates [10]. Overall, these characteristics coexist in a highly flexible system to fulfill the 5G network architecture [24].

Now that the 5G requirements are introduced, it is important to highlight some concerns regarding cost and efficiency. It is mandatory to build a greener mobile communication system, capable of satisfying both cost and experience demands, while enabling much longer terminal battery life. As a comparison term, spectrum efficiency will have to improve from 3 up to 5 times, energetic efficiency will be more than 100 times better as well as the cost efficiency (the number of bits that can be transmitted per unit cost) [30]. The main capabilities of the 5G systems are summed up in Figure 2.13.

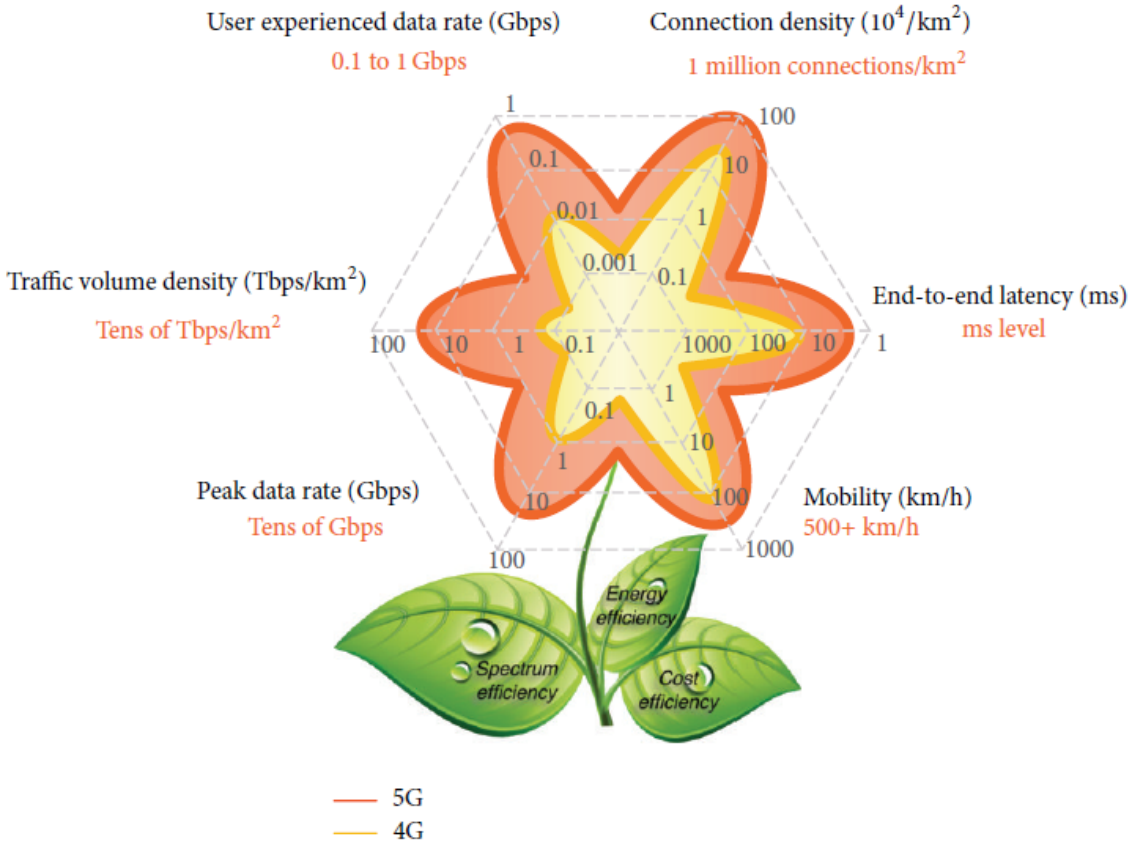

Figure 2.13: 5G key capabilities [30].

As affirmed in [29], *"the success of 5G systems and services depends inter-alia on i) a more efficient spectrum assigned to terrestrial mobile services; and ii) the timely ability to utilize certain new bands in order to support new capabilities for which demand exists."*. Also, in [31], authors defend that the most effective method to fulfill some demands for 5G cellular services, which are expected to be available in 2020, is to increase the bandwidth. Within this context, the migration to higher frequencies, in the mmWaves region, is mandatory, mainly to support the required gigabit data rate service [24].

Considering the spectrum allocation showed in Figure 2.14, it is clear that mmWave bands provide wider available bandwidths, making this spectrum region a good potential candidate for 5G operation, since it can deal with the high data rates required in the future mobile broadband access network [24].

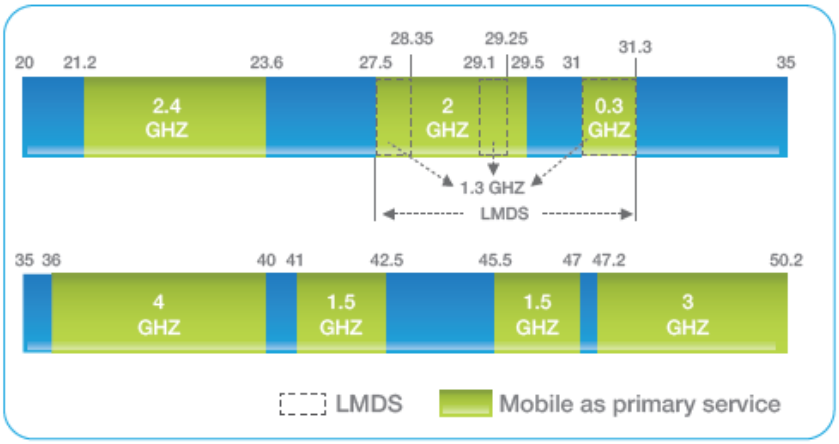

Figure 2.14: Spectrum allocation and potential bands for mobile services (20-50 GHz) [24].

Even though mmWave frequencies present advantages for the 5G implementation, there are several concerns, specially regarding propagation characteristics. The frequency ranges of mmWaves present higher path-loss resulting in fragile link, due to weak diffractions at these frequency bands. To overcome these issues, high gain antennas and highly directive antenna arrays (using several elements), as well as the application of beamforming techniques, are valid options to combat this propagation loss [24], and here mmWave wavelength naturally allows to use a large number of antenna elements.

Taking into account the full context of 5G and namely massive IoT, antennas are expected to be implemented in every small and wearable gadget, to assure the interaction between sensors (placed in the most various devices) and people. Due to their widespread usage, it is highly recommended that antennas are small and compact.

2.2 Antennas: basic concepts

Antennas are a fundamental element of all wireless communication systems [32]. It is defined as a transitional structure between free-space and a guiding device, which is clarified in Figure 2.15. Following the Institute of Electrical and Electronics Engineers (IEEE) *Standard Definitions of Terms for Antennas* an antenna is *"a means for radiating or receiving radio waves"* [32]. In practice, antennas are the first and last component of a wireless communication system, hence their importance. Also, they are used in television, radars, satellites, radio systems, among others [32].

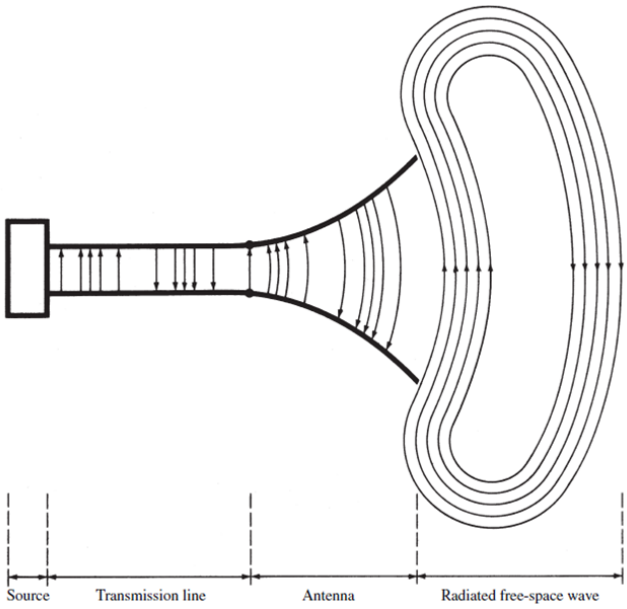

Figure 2.15: Antenna as a transition element [32].

Throughout the last 60 years, the importance of the antennas' design has been an indispensable partner of the communication revolution [32], thus, with the arise of new devices, several types of antennas were created, each one suitable for different scenarios. Clearly, it is not important in the context of this work to discuss extensively each type of antenna, however it is important to clarify their main differences and typical applications.

Firstly, wire antennas, they are very common in automobiles, buildings and ships, among others. They vary in shape, starting with the dipole, which is a straight wire, but there are also, loops and helixes [32]. Then, aperture antennas, such as the waveguide apertures and the horns, are more recent and typically used for higher frequencies than the wire antennas [32]. These antennas are typically used in spacecraft and aircraft applications.

Later, in the 1970s, microstrip antennas emerged, and became very popular. They consist on a metallic patch placed on a grounded substrate [32]. Nowadays, this type of antenna is widely used mainly due to their low-profile and ease of fabrication and normally, they're inexpensive. Also, their compact size and robustness allow them to be mounted on rigid surfaces. Additionally, they are also very versatile concerning the frequency of operation and impedance [32]. Despite the advantages, microstrip antennas present limitations regarding the gain achieved, hence their implementation in array antennas became common. Array antennas came up as a way to achieve radiation characteristics that were not achievable by a single element [32].

Even though many applications require small size antennas, when it comes to further explore the outer space, and communication at great distances, for instance, millions of miles. In these cases, it is necessary to build antennas which have high gain, and in those scenarios reflector antennas seem the best choice, as major examples, parabolic antennas and corner reflectors [32]. Finally, used in most of the same applications of the parabolic reflectors, lens antennas intend to prevent the energy from spreading in undesired directions. A disadvantage of both reflector and lens antennas is that they become extremely large in lower frequencies [32]. Examples of all these types of antennas are presented in Figure 2.16.

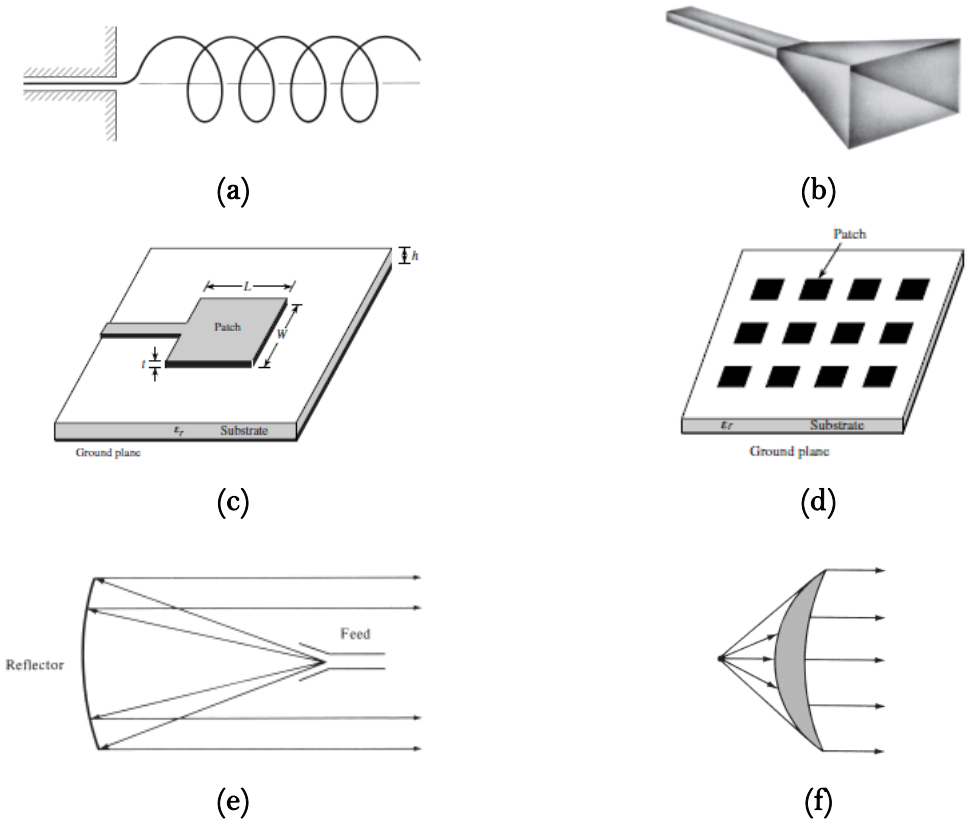

Figure 2.16: Types of antennas: (a) wire antenna: helix; (b) aperture antenna: pyramidal horn; (c) microstrip antenna: rectangular; (d) array antenna: microstrip patch array; (e) reflector antenna: parabolic with front feed; (f) lens antenna: convex-concave (all adapted from [32]).

Ultimately, as said by Constantine A. Balanis in [32], *"an ideal antenna is one that will radiate all the power delivered to it from the transmitter in a desired direction or directions"*. Evidently, this is an utopic idea, and in practice the antenna's performance can be evaluated considering certain parameters which are held in account when designing an antenna for specific applications.

2.2.1 Antenna's fundamental parameters

As said above, when designing an antenna, it is required to have in account several needs, caused by each specific application of an antenna. There are plenty others, but only a few will be named:

- **Bandwidth:** can be explained as the range of frequencies, on both sides of the central frequency, where an antenna presents characteristics (such as gain, beam direction, radiation efficiency) within an acceptable value of those at the operation frequency. In this dissertation, the range of frequencies which defines the bandwidth are those where the S_{11} parameter is lower than -10 dB.

- **Directivity:** this parameter describes the capacity of an antenna to radiate energy in a specific direction. It can be also defined as the ratio between the radiation intensity in a given direction and the average radiation intensity of an isotropic antenna (which radiates equally in every direction), both radiating the same power.

- **Efficiency:** this characteristic has in account all the losses in the antenna, whatever their nature (mismatch, antenna losses, etc.). Basically, it is the relation between the power delivered to the antenna's terminals and the amount of radiated energy by the antenna.

- **Gain:** the combination of both concepts above leads to the concept of gain. Directivity and gain are directly connected, since the first measures the directional capabilities of an antenna, and the second one, gain, has those characteristics in account as well as the antenna's efficiency, and thus, the antenna's losses.

- **Radiation pattern:** it consists of *"a graphical representation of the radiation properties of the antenna as a function of space coordinates (…) Radiation properties include power flux, density, field strength, phase and polarization*" as clarified in the IEEE Standard definitions for antennas [32]. Normally, when analysing this parameter, the 3D view of the radiation pattern can be important, but as an alternative, two planar radiation patterns (the two main planes of radiation) can be exhibited. Figure 2.17 shows three different types of radiation patterns.

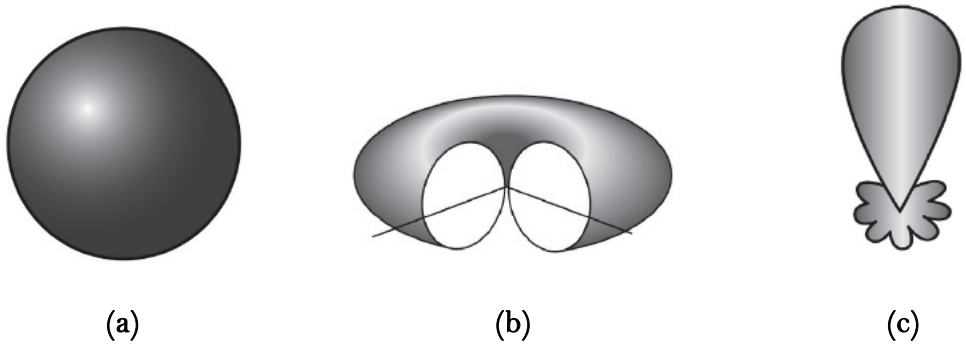

Figure 2.17: Examples of radiation patterns: (a) isotropic; (b) omnidirectional; (c) directional [33].

2.2.2 The choice of Yagi-Uda antennas

As explained earlier, one of the main parameters when designing antennas is their radiation pattern. Yagi-Uda antennas are included in the group of directional antennas, once they are highly directive. In the context of 5G and massive IoT scenarios explored in chapter 2.1, one of the strategies to overcome the 5G challenges, regarding the propagation issues (namely the higher path-loss in the mmWave region), is the usage of highly directive antennas, antenna arrays, as well as the application of beamforming techniques, in order to guarantee that the antenna is transmitting the wave in the right direction.

The structure of a Yagi antenna will be promptly analysed when presenting the process of design in chapter 3, but for now, and since these antennas are quite common, a light description of its layout will allow to continue the exposure of the state-of-the-art. These antennas are composed of a driven element, the dipole, a reflector (backing the driver) and may have a variable number of directors (in front of the dipole). This scheme guarantees the end-fire beam [32] making of these structures good candidates for beamforming applications.

In this sense, it is safe to say that Yagi antennas present several advantages in the 5G context. They are not only highly directive, but they also have considerably more gain than typical patches [32] and reasonable bandwidth at moderated costs [34]. Due to all these facts, it was decided to implement Yagi-Uda antennas.

2.3 Multilayer motivation

Throughout this work three antenna prototypes will be developed and presented in this document. The last of those structures will be a multilayer implementation of a Yagi-Uda antenna.

Figure 2.18 depicts a multilayer implementation of a radiating structure. In this case, by simply stacking multiple layers of dielectric substrate, it is possible to implement a stacked Yagi-like antenna. Nevertheless, this figure serves only to clarify the concept, hence the number of dielectric layers between elements as well as the number of layers used (4) is only an example.

Multilayer structures have been are a growing tendency, as an attempt of increasing the antenna's gain. According to the work developed in [35], planar antennas suffer from a gain saturation, particularly planar antenna arrays. Potentially, using the vertical dimension in the antennas' design, this physical limitation can be overcome [36], which explains the increasing studies on this multi-layered layout.

Another interesting aspect of these multilayer antennas is the radiation pattern. As shown in Figure 2.18(a) a planar printed Yagi-Uda antenna would present a radiation pattern that might not be suitable for printed circuits. On the contrary, if the choice relied on a multilayer implementation, Figure 2.18(b), the radiation diagram clearly would be more suitable, even at the expense of adding some height.

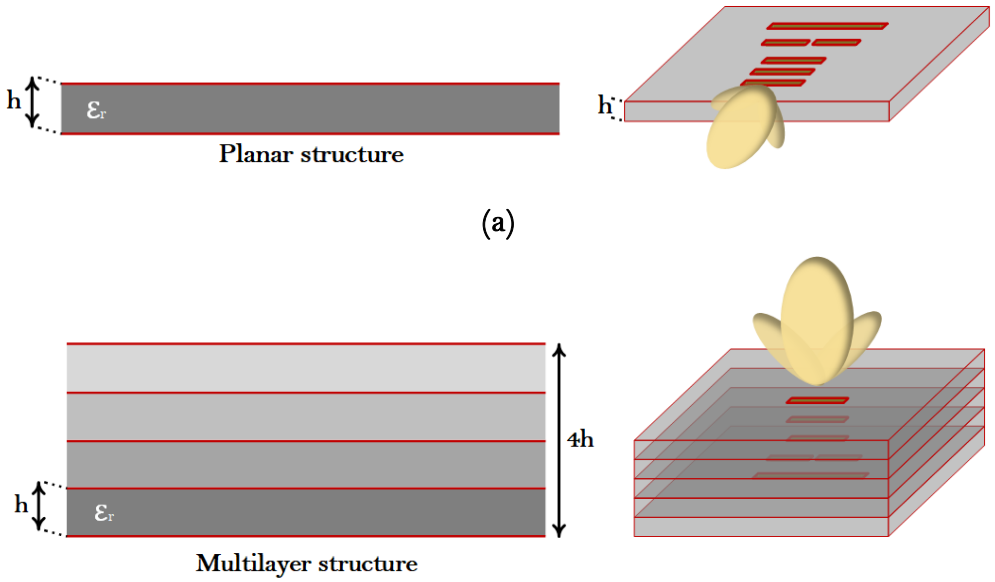

Figure 2.18: Structures: (a) planar and (b) multilayer.

Microstrip patch antennas, mainly due to their high versatility, have been presented in the multilayer configuration. As an example, in [37], authors designed a multilayer patch antenna, operating around 3 GHz, composed by two stacked rectangular patches above a ground plane, using a low-cost substrate. Here the information on the antenna's final gain is not provided, however measured results show a bandwidth of 14% around the frequency of operation.

On the contrary, in [38] an antenna based on a microstrip patch is presented and gain results are shown. The approach includes, not only a multilayer microstrip structure, but also the implementation of a V-shaped ground plane to further improve the results on the reflection coefficient. Furthermore, this prototype is composed by three parasitic patches, which work as director elements, separated by foam to ensure their spacing, and it is built to operate at 10 GHz. This antenna achieved a gain of 11.85 dB and 190 MHz of bandwidth, however, any prototype built is not shown and so these results seem to be only obtained in simulation, and they come at the expense of some complexity.

Clearly in [39] multilayer technology has been tested, since in this work a structure of eight layers in Low Temperature Co-fired Ceramic (LTCC) technology is presented, and its resonant frequency is also 10 GHz. The gain achieved was only 3.43 dBi and also a S_{11} of -11.52 dB at 10 GHz was reached. Moreover, it exhibits a narrow bandwidth and so, the sum of all these results was not satisfying.

Given the results above mentioned, multilayer technology does not seem to produce significant improvements when compared to the planar structures. However, in [40] authors propose a slot Yagi-like structure. This prototype has an operation frequency of 4.2 GHz and its geometry includes two director elements, as well as a reflector. A measured bandwidth of 27.8% was reached, from 3.68 up to 4.87 GHz. Also, a maximum measured gain of 12.20 dB was obtained. Apart from these promising results, simple air gaps form the distances between parasitic elements, sustained by metal and plastic cylinder sticks. This choice of design turns this antenna into a bulky and complex structure and, most importantly, likelier to vary over time, mainly physically, but also in its global properties.

With an increase on the degree of complexity, authors propose in [41] a multilayer substrate integrated waveguide (SIW) horn antenna array, in a 4×4 array configuration. The design strategy consisted on using multilayer cavities where permittivity is gradually decreased, whereas the aperture size expands above the slots to increase the bandwidth. This work also contemplates the migration to the mmWave region, since this structure

operates from 22.4 up to 29.8 GHz, representing a 28.4% bandwidth. Additionally, in terms of the antenna's radiation pattern, it shows a maximum gain of 15 dBi, and the overall results shown are good, apart from the prototype's complexity.

In the field of the multilayer Yagi-like antennas, the work done in [42] shows a Yagi antenna suitable for local positioning systems (LPS), where the goals include building an antenna with compact size and small footprint. Operating at 5.8 GHz, this antenna is a three-element Yagi, built as it was done in [40], using air gaps. In fact, the distance between the antenna's elements, and hence the height of the air gaps, is a function of the operation frequency, and in this case it represents a significant space. Apart from the disadvantage of being bulky, this antenna presents a 11 dBi gain and 14% of bandwidth.

On the other hand, in [43], a Yagi-like antenna was designed and implemented. Here authors decided to use foam to create the distances between elements, instead of air gaps, as done previously. This option turns the antenna less likely to vary over time, however, due to the foam's low permittivity, this antenna's volume is increased. This Yagi's frequency of operation is around 10 GHz, and authors achieved a quite reasonable bandwidth of nearly 20%, and a gain of 11 dBi. Since it operates in the X-band, it is still a low frequency for the 5G expected scenarios.

On the contrary, the Yagi antenna shown in [36] operates at 60 GHz, which is a significantly higher frequency than the one of the prototypes presented earlier, and clearly functioning in the mmWave region. As a direct consequence of the spectrum region, the antenna has a reduced size. Authors also propose its integration in a 4×4 array, confirming the potential utilization of these antennas in such scenarios. This antenna was built by stacking multiple layers of the dielectric substrate used, which means that, once again, air gaps do not appear. The prototype itself, presented an acceptable individual gain of 11 dBi. Still, the measured bandwidth is only of 4.2%, hence, despite the frequency of operation being suitable, the bandwidth represents an important disadvantage, given the high data traffic rates that will be witnessed.

Considering the constant evolution of wireless communications, and the increasing volume of information traded on a daily basis, bandwidth is a necessity which is becoming scarcer in the more conventional areas of the electromagnetic spectrum. Upcoming applications such as 5G, presented in chapter 2.1, demand the exploration of lesser used bands. Therefore, it is possible, due to the reduced wavelength, to ease the process of integrating antennas in systems which operate at mmWave, by using structures based on

printed circuits technology and multilayer, that allow better gain, efficiency and compactness.

Chapter 3

3 Yagi-Uda antennas: design

This chapter focuses on the design of three antennas to be implemented on Computer Simulation Technology (CST) Studio Suite. All of them are Yagi-Uda antennas, and their implementation steps are the ones described here. Despite all being Yagi-Uda antennas, they've got different characteristics, for example, operation frequency, and so, they're not built for the same applications. The process of designing each antenna is described in each sub-chapter.

3.1 Overall design of a Yagi-Uda antenna

3.1.1 Yagi-Uda antennas

Yagi-Uda antennas are a direct way of obtaining more gain from dipoles. They were firstly introduced in 1928 with an article written by H. Yagi and Shintaro Uda and mainly due to their low-cost fabrication, these antennas were used in the years before World War II, for very high frequency (VHF) radars [44].

In a certain way, this type of antennas can be described as a parasitic array of parallel dipoles [45], where only one element is driven, the active dipole. All the other elements are in fact parasitic elements, among them there is a reflector element, and there can be several elements acting as directors.

Commonly, the reflector is singular since the antenna's performance is not much improved when using more reflectors. On the other hand, using several directors improves significantly the overall performance of the antenna. There is not a limit for the number of directors used, however it comes to a point where the improvements are too few when compared to increasing the antenna's size. The combination of all components creates an antenna that generates an end-fire beam formation [32].

This work is focused on matching the advantages of Yagi-Uda antennas with the advantages of printed antennas, in order to study the already known characteristics in new applications.

3.1.2 General considerations on the design steps

When designing a Yagi-Uda antenna, the main aspects to have in account are the length of all the elements and the distance that separates those elements. In the end, this will sum up the main design variables.

As described earlier, a Yagi-Uda antenna is composed of a driven element, the dipole, a reflector and several directors (Figure 3.1).

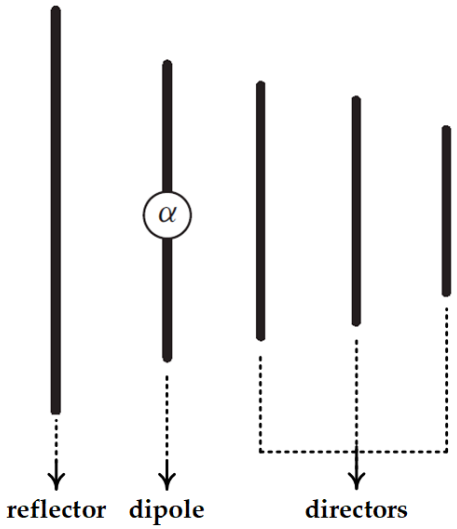

Figure 3.1: Yagi-Uda structure (adapted from [34]).

There can be many variants when designing this type of antenna. As an example, some structures include directors with different lengths, and in other cases all the directors have the same measure.

As can be seen in Figure 3.1, directors are slightly shorter than the active element, the dipole, and the reflector is, by opposition, a little bigger. Theoretically, the length of the dipole is 0.5λ. However, typical values for the lengths of printed dipoles are somewhere between 0.45λ-0.49λ [46].

Moreover, some authors had already observed that in printed antennas, the dipole's length is in fact significantly smaller than 0.5λ, for example, in [47] authors claim an

empirical model for the optimal dipole's length given by the Equation (3.1), where it is confirmed that the dipole effectively should have a length smaller than the traditional 0.5λ.

$$L_{dip} = 0.38\frac{c}{f} \tag{3.1}$$

This consequent reduction, due to the fact that antennas are to be printed instead of wired, is verified throughout all the elements of Yagi antennas, in the driven element, the reflector and directors.

When it comes to the director elements, there are several considerations to do, either in their number, or in their length. First, regarding the number of director elements that will be used. The quantity of these parasitic components will essentially produce alterations in the radiation pattern: the more director elements exist, the more gain the antenna achieves. However, there is a practical limit from which little is gained by adding more directors, especially when talking about dozens of director elements [32], where the consequent bigger size of the antenna starts to be a disadvantage.

While in wired Yagi-Uda antennas it is usual to find them having between 6 to 12 directors [32], in printed Yagi antennas typically, structures with more than 5 directors are not implemented. This is due to the applications for which these antennas are destined. By using printed antennas, such as the ones that are presented in this work, it is possible to reduce both weight and cost, making possible to include them in satellites, as a singular element or as a basic block of larger arrays [48].

Therefore, the choice on the number of director elements, to include in the antenna, needs to fulfil a balance between the antenna's size and its final gain. So, it was decided to include, as a first approach, 3 director elements on all Yagi-Uda antennas built. If later the radiation pattern does not satisfy what is aimed, this number could be changed. Thus, the number of director elements was fixed in 3, and that decision is valid for the 3 prototypes designed.

Concerning now the structure of each director, there are two different approaches when designing these parasitic elements. One of the alternatives is to use the same length for all directors, however, opting by progressively smaller lengths is also a possible option (Figure 3.2). In the case of the work developed, it was decided to use directors with equal lengths, and that was maintained in all the 3 antennas produced.

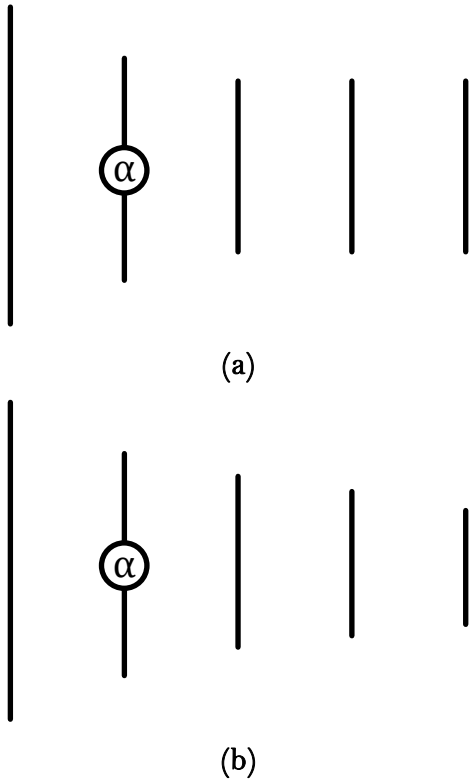

Figure 3.2: Yagi-Uda structures with (a) the same length for all directors and (b) progressivelly smaller lengths.

The decisions of maintaining both the number of directors and their length relation (equal) is vital so that later, when analysing the results, especially regarding the gain achieved, there exist enough common characteristics between all the antennas that allow a valid comparison.

As easily noticed, directors exist so that the end-fire beam formation is achieved. Therefore, these parasitic elements are smaller than the driven element, the dipole. Typical values for this length are around 0.4λ and 0.45λ [32],[46]. Yet, in [49], an interesting example of these structures in printed antennas is presented. There, authors studied the ideal director length in Yagi antennas. It was found that this parameter depends on the dielectric constant of the substrate used. It was noticed that if $\varepsilon_r = 4$ the optimal length of the dipole is 0.22λ, but if $\varepsilon_r = 2$ the optimal length of the same parameter changes to 0.32λ.

Lastly in this topic, the spacing between directors was studied. The optimal distance will be the one where directors are not too far, making each director able to provide an increase in the gain, but simultaneously, it cannot be too small, since if it were, it would cause a deformation on the radiation pattern. Bearing this in mind, the distance between

these elements is not unanimous in literature. It can be found that normal values for this parameter vary between 0.3λ and 0.4λ in [32], but it is also seen in [50] that these distances vary between 0.1λ and 0.3λ.

At this point, the element left to analyse is the reflector. As mentioned in the earlier sub-chapter, reflector elements are often singular in a structure, this comes from the fact that very little is gained when implementing more than one of these elements [32]. The reflector effect is achieved by placing a parasitic element, with a slight greater length in the rear of the dipole. Thus, the theoretical value for the reflector length can vary from equal up to 5% greater than the length of the active element [50].

The lines' width is still left to examine. The antennas built will have two different sections: a microstrip area, formed by the feeding structure, and a coplanar strips part with the Yagi antenna itself. The starting point of the distance between the dipole's arms and the lines' widths was obtained through a line calculator provided by National Instruments named TXLine [51].

This way, the Yagi's dipole is fed by two coplanar lines, each one feeding each of the dipole's arms. As explained in Figure 3.3, if between the coplanar lines the impedance seen is, for example, Z_c, then the impedance tested from one coplanar line and the ground plane of the microstrip area, is $Z_c/2$. This fact led to designing the lines of the balun with an impedance that was half of the input impedance saw in the coplanar area.

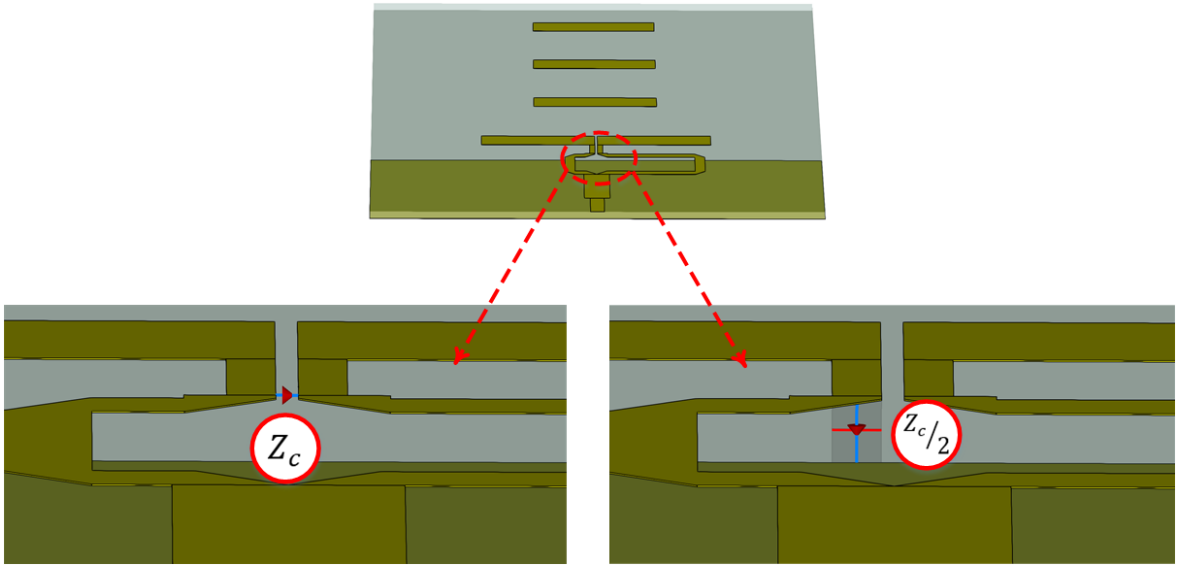

Figure 3.3: Highlight of the coplanar lines.

3.1.3 Implementing a Balun

In this work, it is intended to implement a centre-fed dipole. The goal is to design a printed dipole where its geometry is an equivalent of the free-space cylindrical dipole [48]. Since it is aimed to implement a centre-fed dipole, the dipole's arms are the key part of the design. A dipole is composed of two symmetrical radiating arms, and the distance between those arms is crucial because it is from there that coplanar lines are designed. In turn, these coplanar strips will allow the transition between the microstrip section of the feeding structure and the Yagi antenna.

In order to work properly, dipoles also require a balance feeding. However, a coaxial cable is inherently unbalanced, since its inner and outer conductors are not coupled to the antenna in the same way [32]. This leads to a current flow to ground in the outer conductor. A balun is simply a structure able to do the transition from balanced (in this case, the dipole) to unbalanced systems (here, the coaxial cable).

In practice this behaviour is achieved by feeding each arm of the dipole with two different paths, one of them $\lambda/2$ longer, at the operation frequency, than the other. This T-junction will split the input signal in two paths and it guarantees that the current in each of the dipole's arms is equal in magnitude and opposite in phase, as desired.

3.2 Design of a Planar Yagi-Uda antenna for 2.4 GHz

The earlier chapter presented the general design steps of a Yagi-Uda antenna. Those concerns will allow to obtain the parameters to proceed with the implementation of a printed Yagi-Uda antenna, resonant at 2.4 GHz.

3.2.1 Choice of substrate

One of the main topics when building printed antennas is the choice of dielectric substrate. Here, it was chosen to build the prototype on FR-4, a low-cost substrate. Even though its usage has disadvantages from the point of view of the dielectric constant, since it varies more than desired, it was thought that at this frequency of operation, these substrate's characteristics are enough. The main features of this material are summed up in Table 3.1:

TABLE 3.1: Characteristics of FR-4		UNITS
ε_r	4.30	-
h	1.60	mm
Copper thickness	30.00	µm
$\tan(\delta)$	0.025@10 GHz	-

Table 3.1: Characteristics of the FR-4 substrate used.

Where ε_r is the dielectric constant, h is the substrate's thickness and $tan(\delta)$ is the dissipation factor.

3.2.2 Designing the antenna's elements

Considering the typical values for the dipole's length, described earlier, and the operation frequency of 2.4 GHz, it is possible to estimate a value, which as a first approach, will be equivalent to 0.47λ, where the wavelength is equivalent to 125 mm. The theoretical value for the dipole's length is shown in Equation (3.2).

$$L_{dip} = 58.75\ mm \tag{3.2}$$

Reminding that the value for the wavelength at this frequency is 125 mm, consequently half-wavelength is 62.5 mm, and as can be observed, the theoretical length of the dipole is slightly shorter than the traditional half-wavelength dipole, clearly agreeing with the theoretical considerations.

On the other hand, regarding the length of the directors, a Yagi-Uda with equal lengths for all its director elements was implemented. By this, the optimization of these parasitic structures is narrowed down to three parameters: director's width, spacing between elements and directors' length. As a start, it was decided to implement director elements with a length correspondent to 0.22λ, separated from each other by 0.2λ, doing accordingly to what was presented in [42].

Lastly, and so that the antenna built presents the traditional scheme of a Yagi antenna, it is necessary to use a reflector. However, a reflector is simply a parasitic element that enhances the end-fire beam formation seen in Yagi antennas. Here, a typical reflector element was found to be unnecessary. Instead, and to obtain the desired radiation pattern, the microstrip section that will compose the feeding structure of the antenna (to be presented next), acted as a reflector element [52]. Roughly, instead of having a specific reflector element, this structure has a microstrip area, which allows to discard the usage of a reflector.

The starting point of all design parameters mentioned is presented in Table 3.2. Later in chapter 4, the optimal values obtained through successive iterations will be shown.

TABLE 3.2: Theoretical Design Parameters (UNITS: mm)

L_{dip}	58.75
L_{dir}	27.5
DirSpa	25
t_{dip}	5
gap	1

Table 3.2: Values of the design parameters for the planar 2.4 GHz antenna.

Where L_{dip} and L_{dir} represent the dipole's and the directors' lengths, respectively. The variable named *DirSpa* characterises the distance from the dipole to the first director and between directors. Finally, *gap* is the variable with the distance between the dipole's arms. Figure 3.4 clarifies these variables.

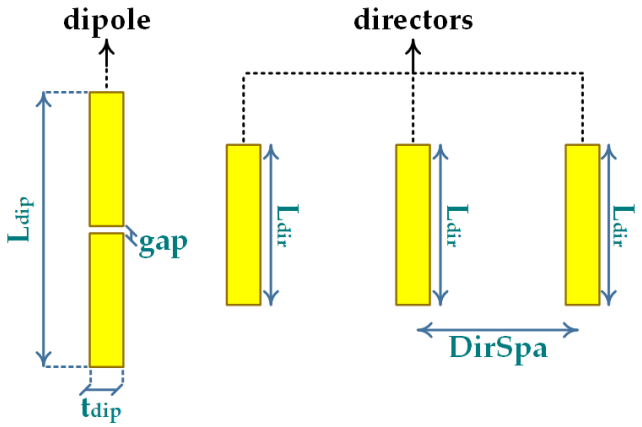

Figure 3.4: Yagi's schematic with the respective design parameters.

3.2.3 Feeding structure

Firstly, and as mentioned, it was decided to build a balun, so that the dipole would be correctly fed. The principle was to have the dipole's arms fed by different paths, one of them being $\lambda/2$ longer than the other.

To design this microstrip structure the input impedance of the Yagi antenna was simulated and, from there, the balun was built.

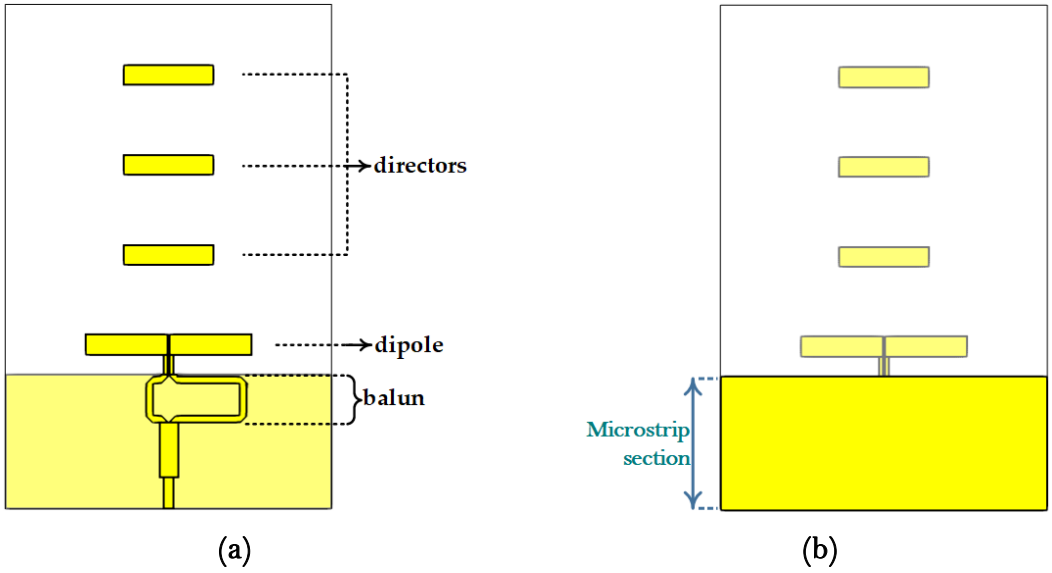

Figure 3.5: 2.4 GHz Yagi-Uda schematic, highlighting the microstrip area: (a) top and (b) bottom view.

To finish, a quarter-wavelength transformer was used, making possible to transform the output impedance of the balun into the desired 50 Ω of the coaxial cable used. Lastly, a 50 Ω line was designed, so that the connector could be attached accordingly.

3.3 Design of a Planar Yagi-Uda antenna for 24 GHz

The migration to higher frequencies was justified mainly in Chapter 2 of this work, where the advantages, and needs, of working in the mmWave region are shown. Thus, it was decided to implement a Yagi-Uda antenna, suitable for scenarios such as 5G.

One of the challenges found is due to the antennas' small size, which for this frequency range, naturally, require a more cautious design so that an appropriate performance at 24 GHz is reached.

3.3.1 Choosing the substrate

The substrate used was Rogers RO4350B. To choose properly, and within the available options, it was held in account its good performance in high frequencies (since it presents low dielectric tolerance and loss) and also its stable electrical properties versus frequency.

The main characteristics of this substrate are summed up in Table 3.3:

TABLE 3.3: Characteristics of RO4350B

		UNITS
ε_r	3.48 @ 10 GHz	-
h	0.762	mm
Copper thickness	30	µm
$\tan(\delta)$	0.0037 @ 10 GHz	-

Table 3.3: Characteristics of the RO4350B substrate used.

Where ε_r is the dielectric constant, h is the substrate's thickness and $\tan(\delta)$ is the dissipation factor.

3.3.2 Designing the antenna's elements

Since the structure remains equal to the one of the antenna designed to operate at 2.4 GHz, and that the theoretical principles are the same for all Yagi-Uda antennas, the principles described in the earlier sub-chapter are again used. By this, it is possible to obtain the length of the dipole.

Bearing all the considerations on the desired frequency of operation, and the inherent wavelength of 12.5 mm, it is viable to calculate the length of the dipole which is again equivalent to 0.47λ and it is exhibited in Equation (3.3).

$$L_{dip} = 5.88\,mm \tag{3.3}$$

The considerations on the number of directors and their length are also the same. Their proportion with the wavelength was maintained, meaning that $L_{dir} = 0.22\lambda$ and DirSpa = 0.2λ were the starting point for the design process.

TABLE 3.4: Theoretical Design Parameters (UNITS: mm)

L_{dip}	5.88
L_{dir}	2.8
DirSpa	2.5
gap	0.3

Table 3.4: Values of the design parameters for the planar 24 GHz antenna.

Where L_{dip} and L_{dir} represent the lengths of the dipole and the directors respectively. The variable named *DirSpa* characterises the distance from the dipole to the first director and between directors. Lastly, *gap* variable represents the distance between the dipole's arms. These variables follow the same line of thought of the previous Yagi antenna presented.

3.3.3 Feeding structure

According to what was made in the construction of the previous antenna, at first, to design the balun the input impedance of the new planar Yagi antenna was held in account.

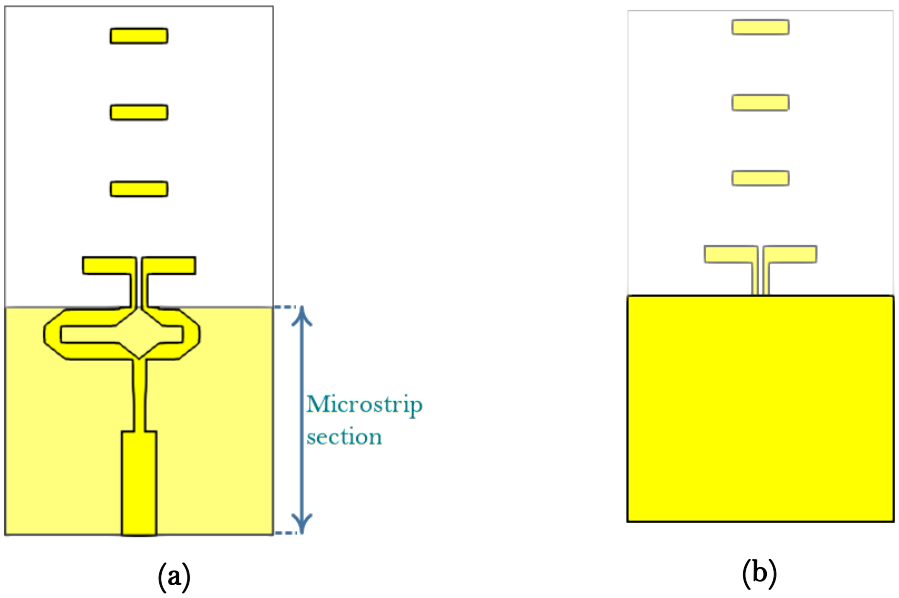

Figure 3.6: Planar 24 GHz Yagi-Uda: (a) top view and (b) bottom view.

Following the same theoretical principles, the width of the balun (*Wmsc*) lines was calculated and from there the balun structure implemented. Now, regarding the impedance matcher, a similar approach was attempted. However, here, the operation frequency changed, and as easily noticed, with this, several consequences arise.

One of those evident consequences is the fact that at this central frequency, lines of low impedances become too large to be implemented. Truth be told, these lines are not too wide, their width is simply too large when compared with the width of the dipole or the balun. So, even though their width appears to be small, this value, when compared to the entire antenna, is too large.

As a result, it was decided to implement a pair of impedance transformers, instead of only one (as it was done in the 2.4 GHz Yagi-Uda antenna). The first impedance transformer ($Lt1 \times Wt1$) allows the transformation of the balun's output impedance in an higher impedance, and the second one ($Lt2 \times Wt2$) adapts that same higher impedance to the 50 Ω of the input line. Then the input line, with 50 Ω, attaches the antenna to the coaxial connector. All the design variables are exposed and clarified in Figure 3.7.

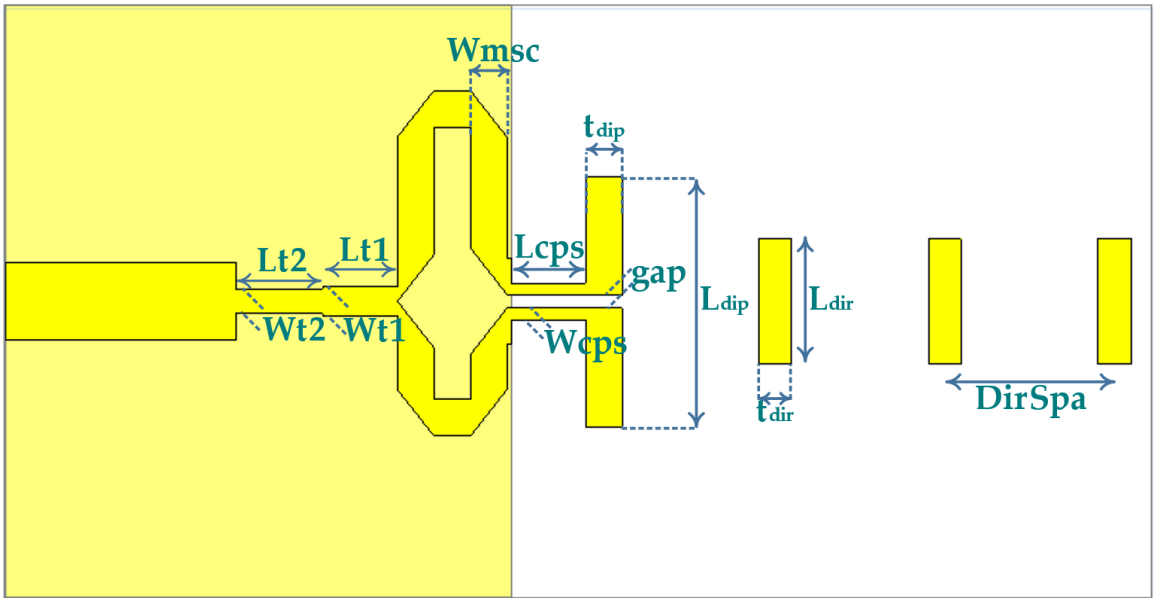

Figure 3.7: Planar 24 GHz Yagi antenna: schematics.

3.4 Design of a Multilayer Yagi-Uda antenna for 24 GHz

In line with what was done previously, it was decided to implement a Yagi-Uda antenna, however, here, a multi-layered structured Yagi antenna was designed. It was considered relevant to identify the advantages and disadvantages of a multilayer structure when compared to a planar antenna.

Initially the implementation was done using the same substrate as in the planar 24 GHz antenna. Later, tests will be shown, where the substrate was varied, in order to verify, or not, the adequacy of this dielectric substrate.

3.4.1 Designing the antenna's elements

The goal is to build a multilayer antenna without air gaps between elements. This type of structure will cause the elements (namely the dipole, the directors and the reflector) to be surrounded in substrate. Evidently there will be an impact on the antenna's radiation, mainly because the propagation will occur not in the air but in the dielectric substrate.

Thus, it is imperative in this application, to consider the wavelength in the specified dielectric substrate. This means that if a traditional Yagi antenna uses a close to half-wavelength dipole, here, its dipole will theoretically be near the value of half-wavelength in this substrate (λ_d). For example, in the 24 GHz planar antenna the theoretical length of the dipole is around 0.47λ, where λ represents the wavelength in the air. Now, the

theoretical value would be close to $0.47\lambda_d$, in the first approach, a value which is presented in Equation (3.4).

$$L_{dip} = 3.15\ mm \tag{3.4}$$

Regarding the director's length, the line of thought was kept, and as a first approach, directors with $L_{dir} = 0.22\lambda_d$ were designed.

This method of construction has some drawbacks, the first one affects directly the distance between the elements of the Yagi antenna. Even though it can be optimized, this parameter is limited to be a multiple of the substrate's thickness. This means that the optimal distance between the dipole and the directors, or between directors themselves, could be 3.5 layers of dielectric substrate but that would compromise the antenna's construction. Therefore, the method is to calculate the number of layers which produce a distance between the antenna's elements close to the theoretically expected distance in millimetres.

Meaning that, typically on Yagi antennas directors are separated from each other by 0.3λ to 0.4λ. Nevertheless, in printed Yagi antennas these values tend to be smaller [47] than in wired antennas. Naturally the distance between directors would be equivalent to vary between from $0.3\lambda_d$ up to $0.4\lambda_d$.

Bearing in mind the substrate's height, h=0.762mm, these distances represent values equivalent to 2.6 and 3.4 layers of substrate. Evidently, in practice it means that the optimal distance between directors would be around having 3 or 4 layers of substrate. As a start it is predicted to use 3 or 4 layers, but surely tests and simulations will guarantee the optimal number of layers to use.

In line with what was said regarding the dipole's length, the directors' dimensions will have in account that the antenna will be surrounded in substrate. Therefore, if theoretically directors can present lengths 5% to 30% shorter than dipoles [53], than, possibly, the proportion will be kept in these vertically stacked antennas.

On the contrary of the other 2 antennas designed, here it is necessary to implement a reflector element. This is due to the fact that in the other antennas implemented, the microstrip area of the antenna (composed by the balun, impedance transformers and input line) acted as a reflector element [52]. However, in this case, the microstrip area will naturally be horizontally levelled with the dipole, and hence this microstrip section will not be in the same vertical plane as the dipole and directors (Figure 3.8).

This way, this part of the antenna that in other implementations acted as a reflector element here, due to the antenna's layout will not perform accordingly. Thus, it is imperative to implement a reflector element, so that the radiation pattern of the antenna is as vertical as expected and the final gain is improved, as it is aimed.

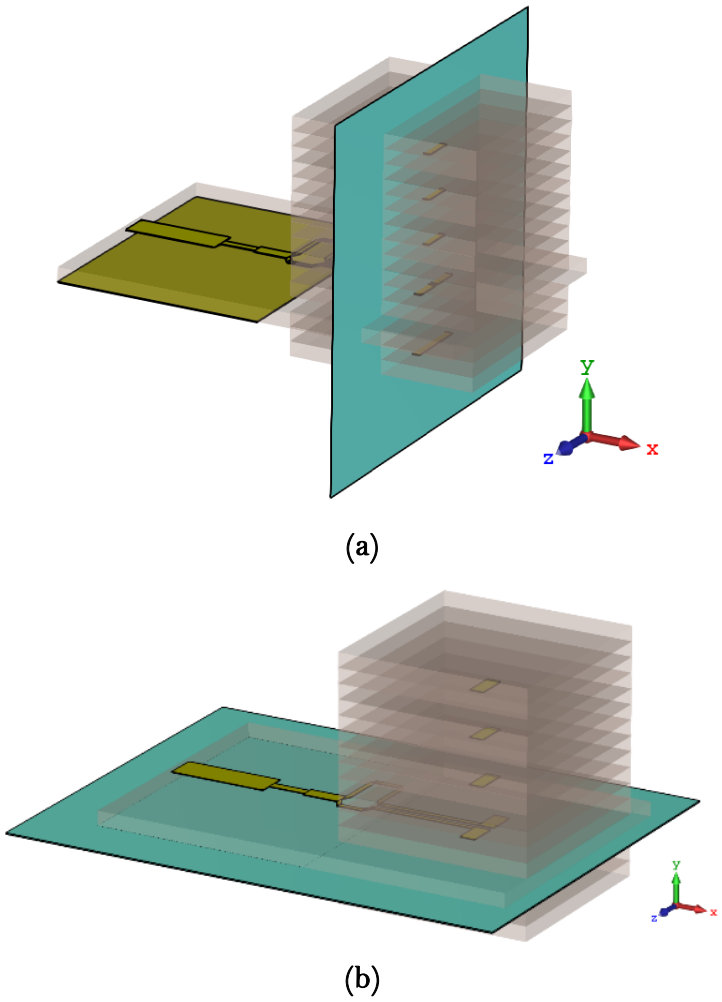

Figure 3.8: Highlight of the multilayer antenna design planes: (a) vertical and (b) horizontal.

Setting aside the discussion on the reflector's need, it is important now to decide this element's characteristics regarding its length and distance to the driven element, the dipole. Bringing back what was mentioned on the general considerations, a reflector can be up to 5% longer than the dipole, and so, to start, it was decided to implement a reflector with $1.02L_{dip}$, vertically aligned with the remaining antenna's elements.

The initial values on the design parameters of the multilayer antenna are summed up in table 3.5.

TABLE 3.5: Theoretical Design Parameters (UNITS: mm)

L_{dip}	3.15
L_{dir}	1.50
L_{ref}	3.21
h_{dir}	2.286
h_{ref}	3.048
gap	0.30

Table 3.5: Values of the design parameters for the multilayer 24 GHz antenna.

Where L_{dip}, L_{dir} and L_{ref} represent the lengths of the dipole, the directors and the reflector, respectively. The variables named h_{dir} and h_{ref} characterise the distance from the dipole to the first director and between directors, and also, the distance between the dipole and the reflector. Respectively, h_{dir} and h_{ref} are equivalent to $0.34\lambda_d$ and $0.45\lambda_d$. Finally, *gap* is the parameter that represents the distance between the dipole's arms.

3.4.2 Feeding structure

The feeding strategy of the antenna was the same. A structure formed by a balun, two impedance transformers and an input line was designed. Again, it was necessary to use two impedance transformers since a single transformer would result in a line too wide to be included in the antenna. Thus, two quarter-wavelength transformers were considered, and were responsible for the transformation from the output impedance of the balun to the 50 Ω, seen in the input line.

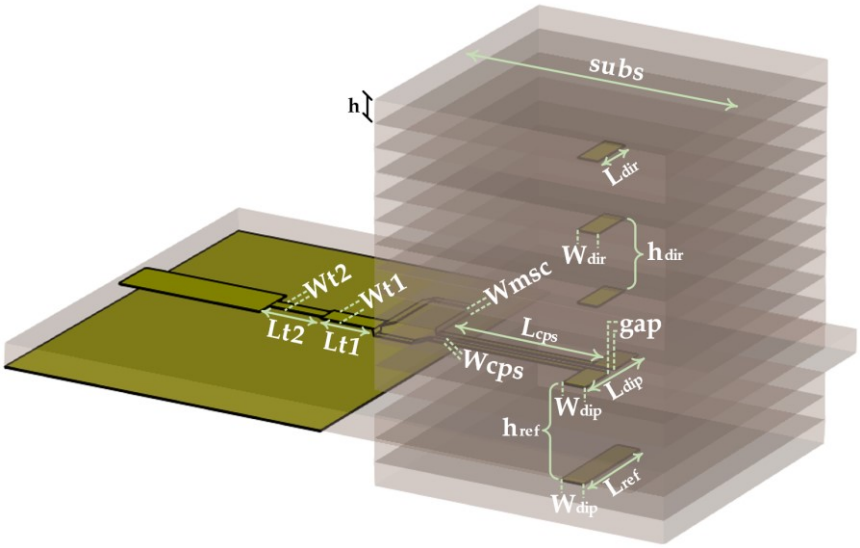

Figure 3.9: Full Yagi's schematic and design variables.

Where (*Lt1* × *Wt1*) and (*Lt2* × *Wt2)* identify the parameters of both quarter-wavelength transformers, *Wmsc* is the balun's width, which here equals *Wcps*, the width of the coplanar lines. Lastly, *Lcps* clarifies the coplanar lines' length.

In fact, one of the critical aspects of designing the feeding structure of the multilayer Yagi antenna is the length of the coplanar striplines, corresponding to the parameter *Lcps* (Figure 3.9). The accuracy of the microstrip-to-coplanar stripline transition is critical to properly match the antenna.

If the microstrip section was designed surrounded by substrate (which is not), it is believed that it would affect the radiation pattern, mainly the direction of the main lobe of radiation. With the aim of minimizing that effect it was decided to build the portion of the feeding structure outside the dielectric substrate block with dimensions *subs* × *subs* (Figure 3.9).

Furthermore, *Lcps* lines are responsible for the coplanar stripline-to-microstrip transition, connecting the antenna to the feeding structure. The length of these lines is crucial to achieve an adequate performance. Mainly, it is important to accomplish a real entrance impedance in these lines, Figure 3.10 intends to highlight *Lcps* as well as to show that this design includes considering two different dielectric constants. Meaning that, *Lcps* line is divided in *Lcps1* which is enclosed in dielectric substrate, and *Lcps2*, surrounded by air.

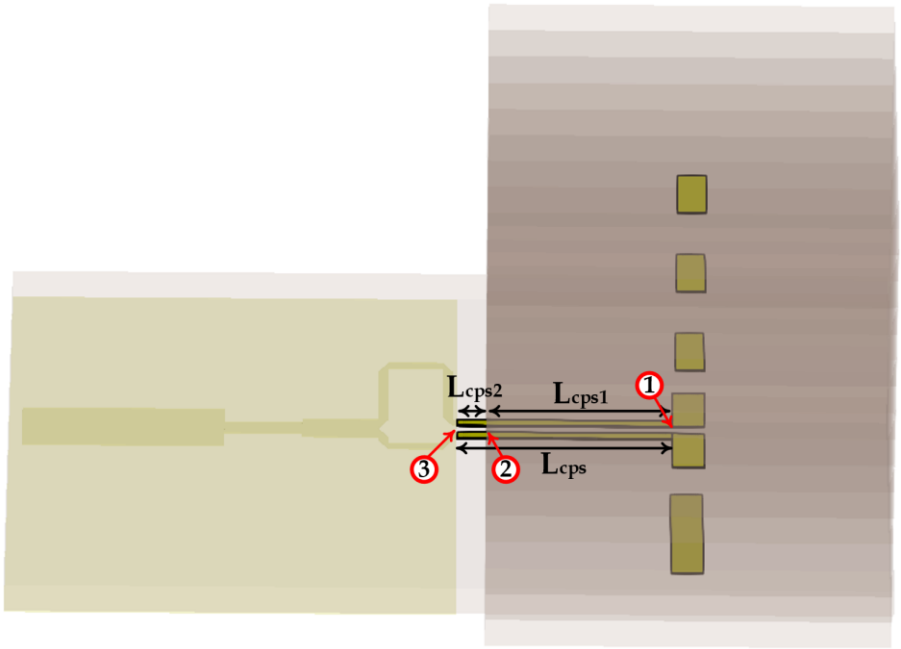

Figure 3.10: Highlighted design parameter Lcps.

The design strategy included analysing this line in a Smith Chart. Starting with obtaining the simulated impedance in **1** (Figure 3.10) and implementing a line with minimal width up to the frontier of the dielectric vertical block, corresponding to the length *Lcps1*. In the Smith Chart attached in Appendix B, the impedance in point **1**, named *Za*, was normalized using $Z_0 = 121.2\ \Omega$ (the characteristic impedance of the lines) and then marked as *za*. The physical length *Lcps1* was obtained as a function of λ_d and it was found to correspond to $0.68\lambda_d$. This way, the theoretical impedance in point **2** is reached, highlighted and named *zb*, lastly denormalization was made, allowing to obtain *Zb*.

This led to using the second Smith Chart presented in Appendix B, where *Zb* was normalized but now using $Z_0 = 136.4\ \Omega$. Marking *zb* in a Smith Chart, allowed to realize that the implementation of a line with $Lcps2 = 0.093\lambda_{air}$ would provide a real impedance in point **3**. This length corresponds to 0.837 mm. All these calculations were performed considering λ_d and λ_{air} where the effective dielectric constant was held in account in both scenarios.

This method allows to create a theoretical prediction for the *Lcps* parameter. Thus, *Lcps1* will have, mandatorily, 4.6 mm, the length from the edge of the dipole up to the extremity of the unevenly cubic structure. Then *Lcps2* will be responsible for the appropriate matching, and predictably will measure 0.837 mm. Overall, *Lcps* line should measure 5.437 mm.

Chapter 4

4 Implementation and results discussion

This chapter will focus on the presentation of the obtained results, both by means of simulation and practical. Results are shown according to the same order as the antennas were presented in the earlier chapter. It was decided to report results from each antenna within each subchapter. Moreover, simulation and practical results are exposed sequentially to each antenna, since the method was to implement the antenna on CST, optimize it, and then built it.

4.1 Planar antenna for 2.4 GHz

As mentioned in chapter 3, this is a Yagi-Uda antenna whose parameters and theoretical fundaments were already presented. The point of building this antenna within this dissertation's context was to get familiarized with the demands of Yagi-Uda antennas and the simulation environment.

The starting point of the design parameters has a theoretical basis already discussed in the earlier chapter. From there, several simulations were performed in order to achieve the optimal dimensions for this antenna.

The final scheme for this Yagi antenna, and its final (optimized) dimensions are presented in Figure 4.1 and in Table 4.1 the intention is to show how far are the final values from the ones previously predicted. Additionally, Table 4.2 contains the values used for the remaining design parameters.

Lastly, in Figure 4.2 is possible to visualize the antenna built.

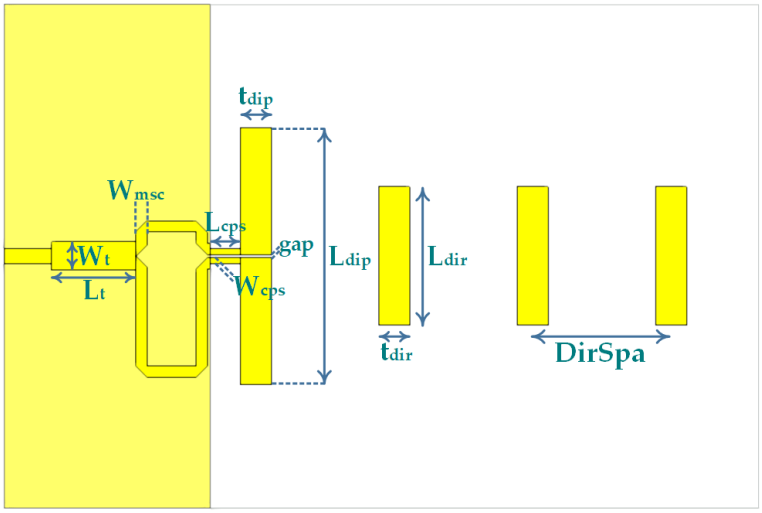

Figure 4.1: Schematics of the Yagi antenna for 2.4 GHz.

TABLE 4.1: Theoretical and optimal parameters of 2.4 GHz antenna (UNITS: mm).

Parameter	L_{dip}	L_{dir}	DirSpa	t_{dip}	t_{dir}	gap
Theoretical	58.75	27.5	25	5	5	1
Optimized	51	27.5	27.5	6.2	6.2	0.55

Table 4.1: Comparison between the optimal and theoretical parameters for the 2.4 GHz antenna.

TABLE 4.2: Remaining design parameters for the 2.4 GHz antenna (UNITS: mm).

Parameter	Lcps	Wcps	Wmsc	Lt	Wt
Optimized	6.00	1.20	2.24	16.70	5.65

Table 4.2: Final values of the design parameters.

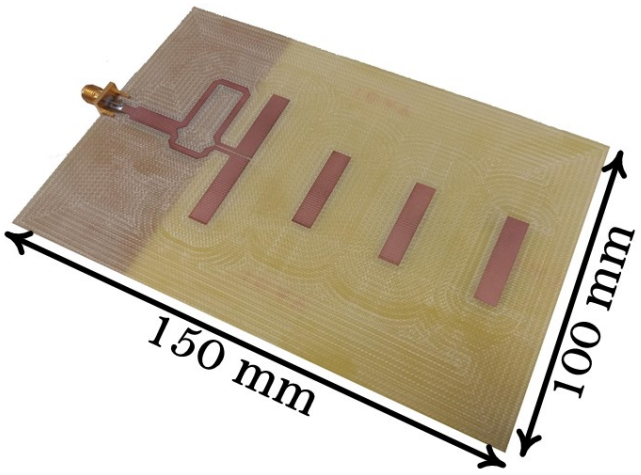

Figure 4.2: Printed prototype of the 2.4 GHz Yagi-Uda antenna.

The overall antenna's dimensions are, as highlighted in Figure 4.2, $100 \times 150 \times 1.6\ mm^3$.

4.1.1 Simulation results

In what concerns the |S11| parameter, results are shown in Figure 4.3. There, two markers allow to display the antenna's bandwidth, considering the -10dB criteria, and the third one is set at 2.4 GHz.

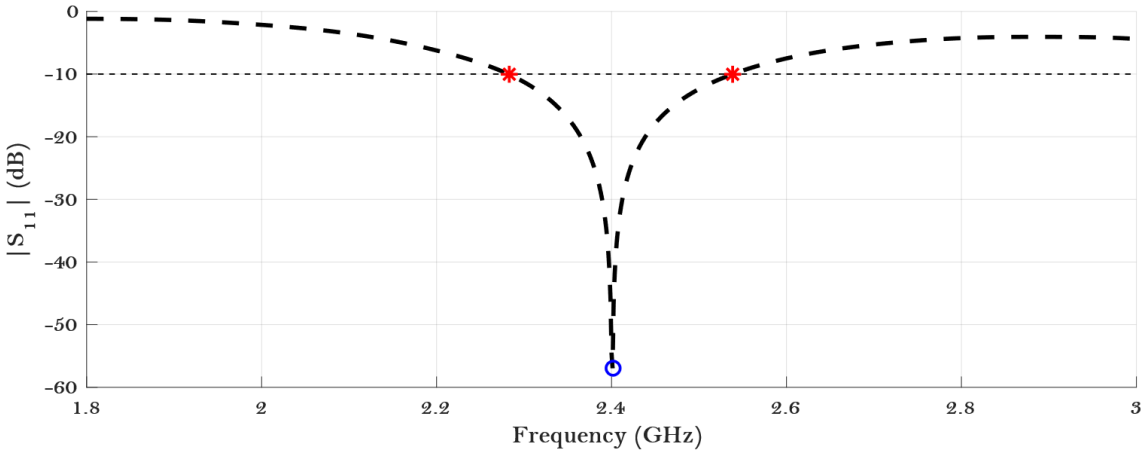

Figure 4.3: Simulated |S11| of the designed planar Yagi-Uda antenna for 2.4 GHz.

By the graphic of the antenna's reflection coefficient it is noticeable that the bandwidth achieved in simulation, considering the -10 dB criteria, is approximately 260 MHz, from 2.28 GHz up to 2.54 GHz. This represents a simulated bandwidth of 10.6%.

In terms of impedance matching, the third marker allows the observation of the antenna's reflection coefficient which for the frequency of operation (2.4 GHz) is -53.9 dB. Simultaneously, the simulated impedance seen at the input is near to the desired 50 Ω, being the one in Equation (4.1).

$$Z_{in} = 50.15 + i0.05\ \Omega \tag{4.1}$$

Regarding the radiation diagram, the three-dimensional scheme can be seen in Figure 4.4, where the antenna is also shown. In order to complement the information on the antenna's gain, the polar graphic is showed in Figure 4.5.

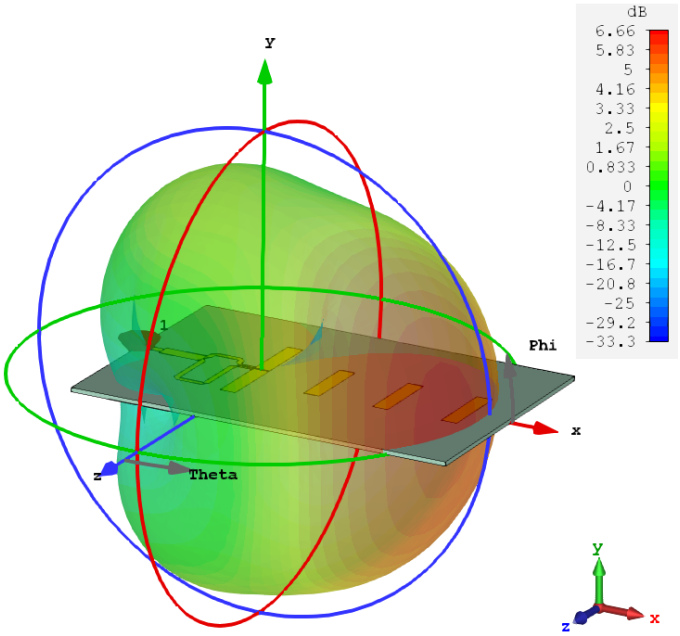

Figure 4.4: 3D view of the radiation diagram of the 2.4 GHz antenna.

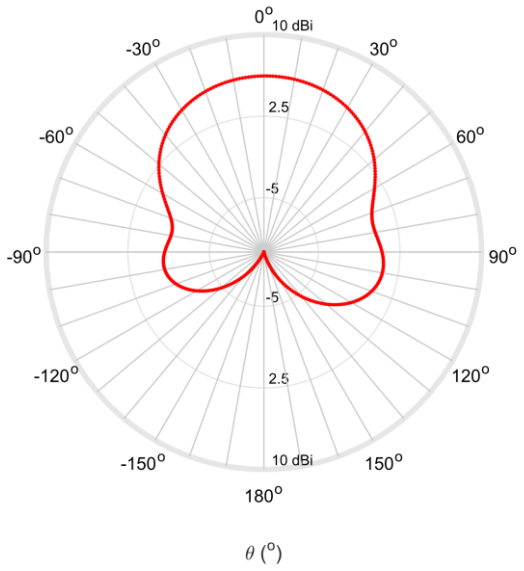

Figure 4.5: Polar diagram of the radiation pattern of the 2.4 GHz antenna (plane $\varphi = 0°$).

Through analysis of both Figure 4.4 and Figure 4.5 it is possible to conclude that the gain obtained with this Yagi antenna is 6.66 dBi at 2.4 GHz. Easily, it is observed that the end-fire beam formation was accomplished making of this a directive antenna, as it was expected.

Still in simulation environment, Figure 4.6 and Figure 4.7 both clarify the information concerning the gain variation and the antenna's efficiency, respectively, over

the same frequency range. The maximum efficiency occurs at the frequency of operation and its value is quite high, 99.7%. On the other hand, the maximum gain of this antenna doesn't happen at 2.4 GHz.

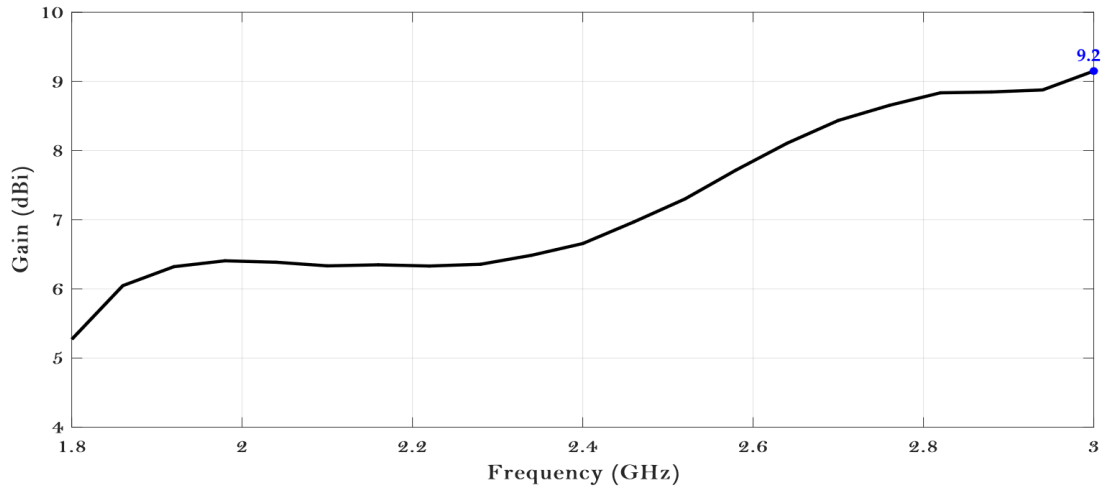

Figure 4.6: Gain variation over frequency for the 2.4 GHz Yagi antenna.

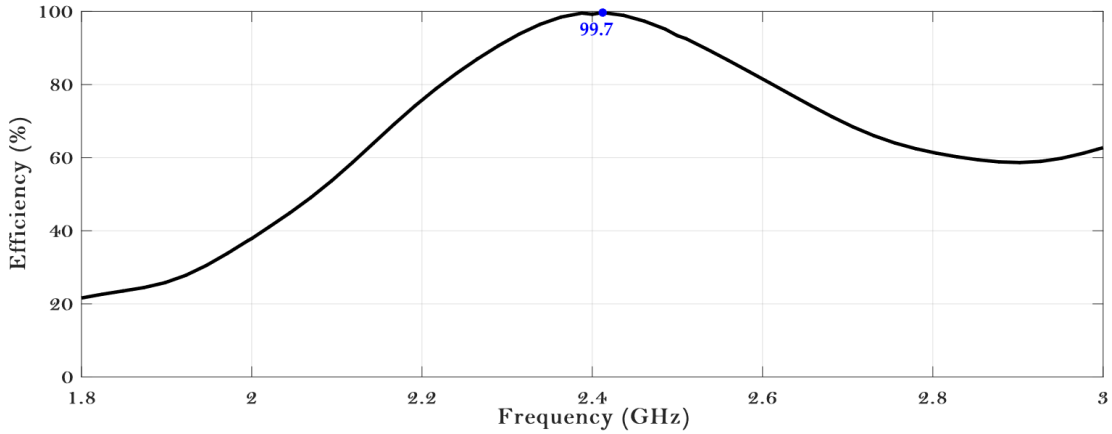

Figure 4.7: Efficiency variation over frequency for the 2.4 GHz Yagi.

4.1.2 Measured results

The antenna was built and it was possible to measure its reflection coefficient using a Vector Network Analyser (VNA). The comparison between what was obtained through simulation and what was measured, is presented in Figure 4.8. Markers indicating the simulated and measured bandwidths are enhanced in red and green, respectively.

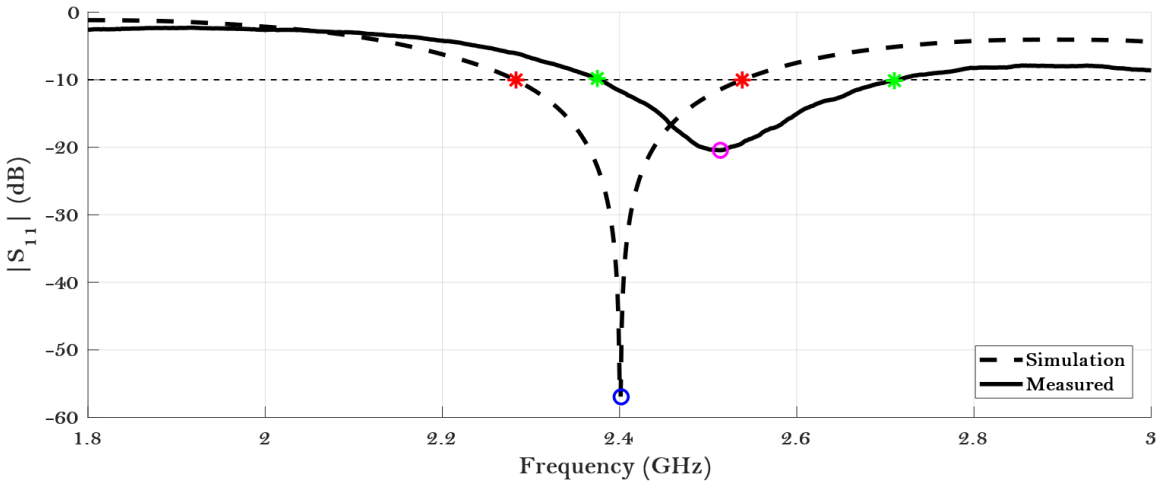

Figure 4.8: Simulated and measured reflection coefficient (|S11|) of the planar 2.4 GHz antenna.

Evidently the results obtained in practice differ not only in the $|S_{11}|$ value but also regarding the bandwidth achieved.

In practice, it was possible to obtain the minimum reflection coefficient of -20.45 dB at 2.51 GHz, and at the operation frequency, the antenna presented a measured $|S_{11}|$ of -12.3 dB, so a reasonable impedance matching was accomplished.

Even though the measured and simulated reflection coefficient present the same behavior, a shift in frequency of the minimum value of $|S_{11}|$ happened, since in simulation the minimum was seen at 2.4 GHz and in practice that minimum occurred at 2.51 GHz. This mismatch is probably due to the ε_r of the substrate used. The truth is that FR-4 does not have a very precise dielectric constant, making this type of disparities unpredictable.

Mainly, this shift in frequency could be corrected by simulating an antenna resonant near the 2.3 GHz, and that would cause, probably, a better $|S_{11}|$ at 2.4 GHz. Once again, as said, the dielectric constant of this substrate is too unstable, and there would still be the chance of producing an antenna with a minimum S11 coefficient far from 2.4 GHz. In the end, this was not made because the main goal of building this antenna was to get familiarized with CST and Yagi-Uda antennas, and that had been accomplished.

When it comes to differences observed on the antenna's bandwidth, graphically it is seen that the bandwidth of the antenna built presents better results than the antenna simulated. If through simulation a bandwidth of 260 MHz was obtained, in practice it was possible to achieve 335 MHz, equivalent to 13.2%. This corresponds to an improvement of 75 MHz.

Lastly, on the topic of the planar Yagi antenna for 2.4 GHz, it is left to present the measured radiation diagram. Through the measurements performed and having in account the gain of the reference antenna (G_{ref}) and its S21 parameter (S_{21_ref}), using Equation (4.2), it was possible to obtain the measured gain of the antenna (G_{AUT}), showed in Equation (4.3).

$$G_{AUT} = G_{ref} - (S_{21\_ref} - S_{21\_aut}) \tag{4.2}$$

$$G_{AUT} = 5.92\ dBi \tag{4.3}$$

Compared to the gain reached in simulation (6.66 dBi), this value is slightly lower. However, when it comes to the radiation pattern itself, Figure 4.5 presents clear similarities with Figure 4.9, thus it is possible to conclude the proper functioning of the antenna.

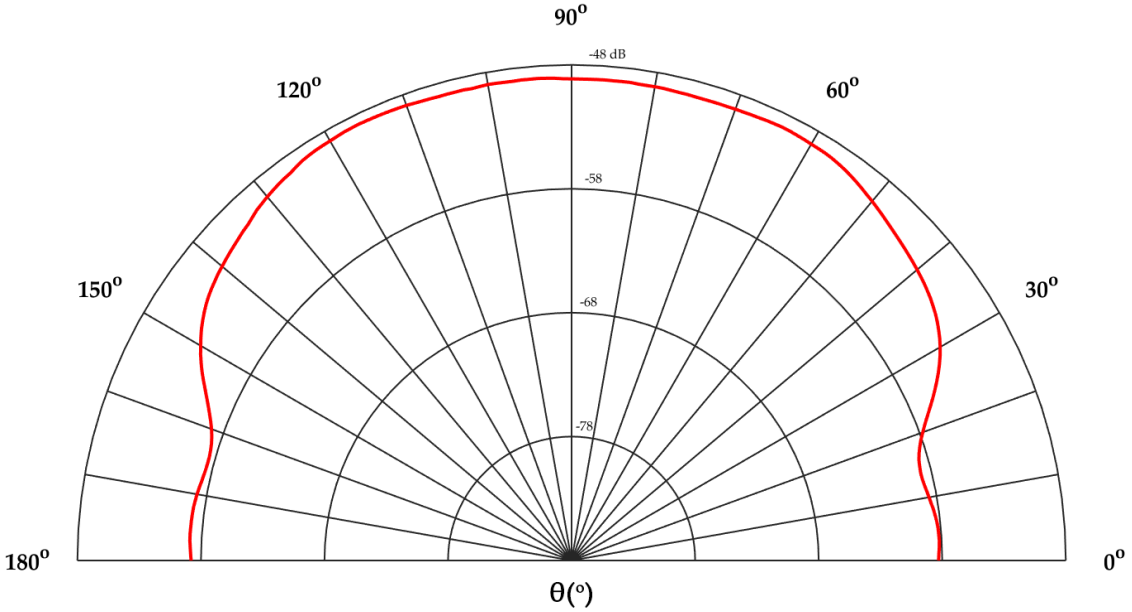

Figure 4.9: Radiation pattern of the 2.4 GHz Yagi (plane $\varphi = 0°$).

4.2 Planar antenna for 24 GHz

Once again the starting point when building this antenna were the theoretical values presented in the earlier chapter. From there, several simulations were performed to achieve the optimal dimensions.

The final scheme for this Yagi-Uda antenna and its global dimensions are presented in Figure 4.10. In Table 4.3 it is possible to establish a comparison between the theoretical

results and the optimal ones, obtained throughout the simulations. Additionally, in Table 4.4 the optimal values of the remaining design parameters are presented.

Then, in Figure 4.11 it is possible to see the antenna prototype.

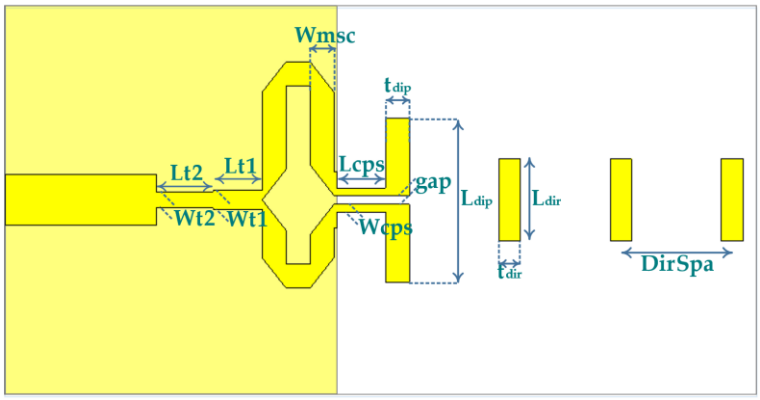

Figure 4.10: Schematics of planar 24 GHz Yagi-Uda antenna.

TABLE 4.3: Theoretical and optimal values for the 24 GHz antenna (UNITS: mm).

Parameter	L_{dip}	L_{dir}	DirSpa	t_{dip}	t_{dir}	gap
Theoretical	5.88	2.8	2.5	0.5	0.5	0.3
Optimized	5.185	2.75	3	0.8	0.715	0.3

Table 4.3: Comparison between the optimal the estimated values for the planar 24 GHz antenna.

TABLE 4.4: Remaining parameters for the planar 24 GHz Yagi (UNITS: mm).

Parameter	Lcps	Wcps	Wmsc	Lt1	Lt2	Wt1	Wt2
Optimized	1.63	0.25	0.8	1.64	1.91	0.65	0.54

Table 4.4: Optimized values for the design parameters for the 24 GHz planar antenna.

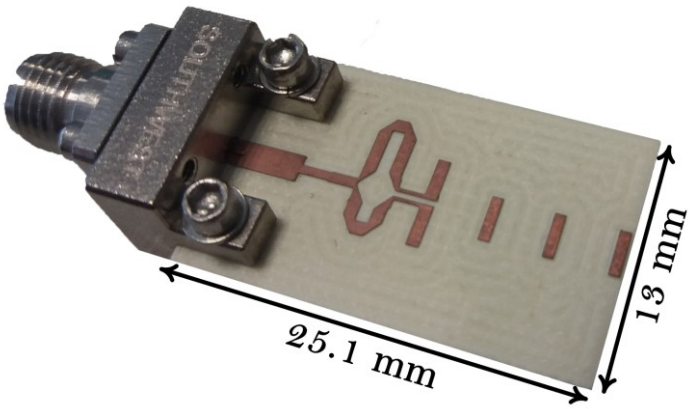

Figure 4.11: Planar Yagi-Uda antenna for 24 GHz.

The overall dimensions of this antenna are: $25.1 \times 13 \times 0.762\ mm^3$.

4.2.1 Simulation results

Regarding the reflection coefficient of the planar Yagi-Uda for 24 GHz, it is important to analyse Figure 4.12:

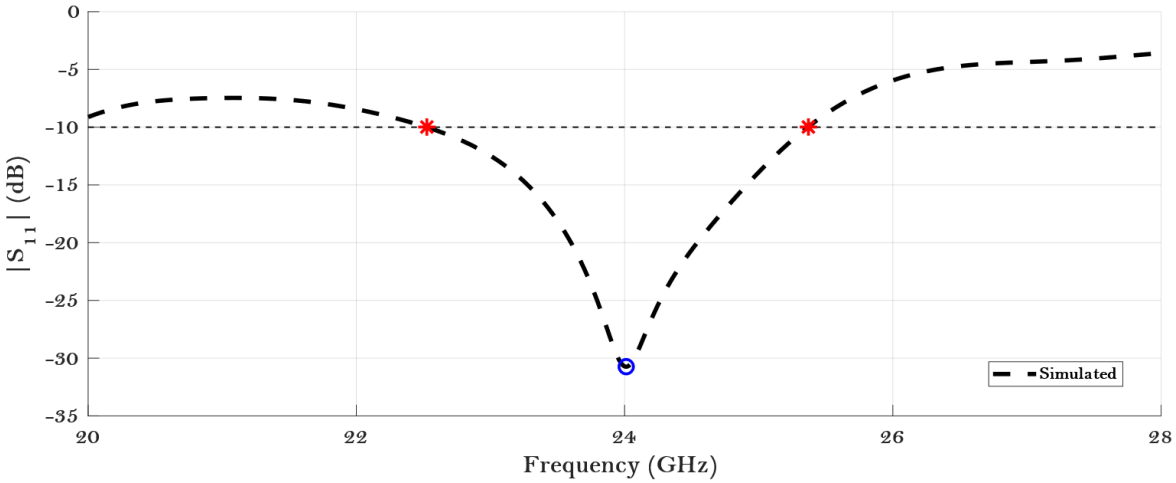

Figure 4.12: Simulated S11 of the designed planar Yagi-Uda antenna.

Following the same presentation used in the 2.4 GHz antenna, markers highlight the simulated bandwidth (in red), maintaining the -10 dB criteria, and the minimum $|S_{11}|$ found (blue circle).

Through direct observation, an appropriate impedance matching is confirmed, since at the frequency of operation the $|S_{11}|$ is minimum and equals to -30.74 dB. Moreover, at 24 GHz, the input impedance is once again close to 50 Ω, being the specific value showed in Equation (4.4).

$$Z_{in} = 47.53 + i1.40\ \Omega \tag{4.4}$$

Still considering Figure 4.12, the simulated bandwidth can be examined. Noticing the markers in red, the bandwidth obtained is approximately 2.85 GHz, from 22.53 GHz up to 25.37 GHz, representing a simulated bandwidth of 11.9%.

Another important parameter is the gain obtained, and for that, Figure 4.13 presents the 3D radiation diagram, and complementing this information, Figure 4.14 shows the polar scheme of the radiation pattern.

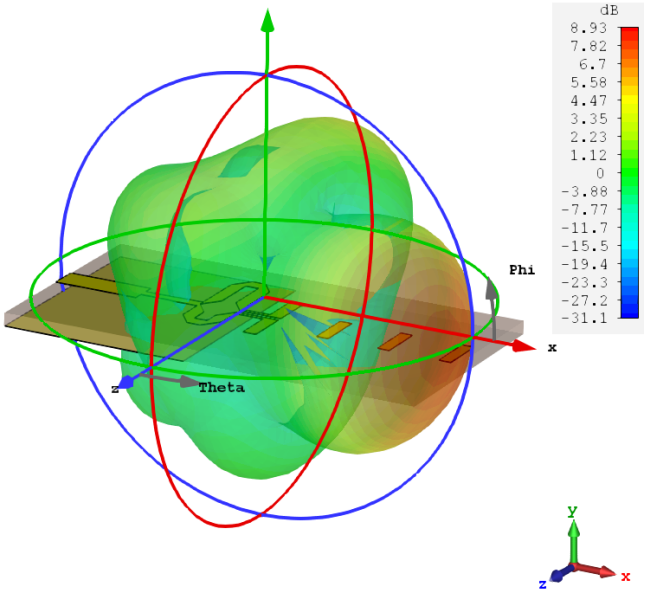

Figure 4.13: 3D view of the radiation pattern of the designed antenna for 24 GHz.

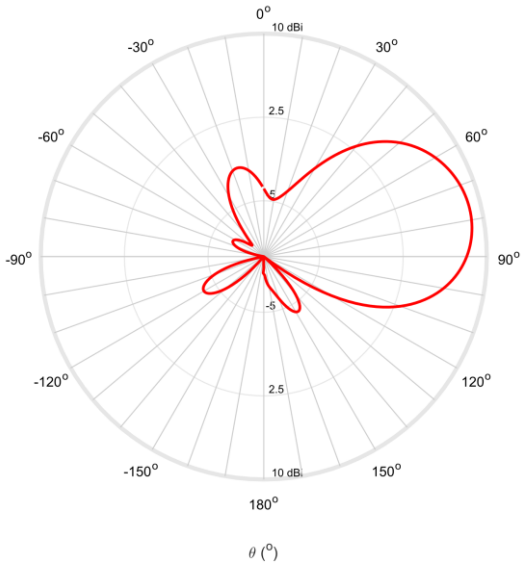

Figure 4.14: 24 GHz antenna's polar diagram of the radiation pattern (plane $\varphi = 0°$).

Both in Figure 4.13 and in Figure 4.14 it is again possible to confirm the adequate radiation pattern obtained with the Yagi antenna, since the high directivity observed and the gain obtained, 8.93 dBi, are satisfactory results for a three-director printed Yagi antenna.

However, a misalignment with the directors can be observed in the radiation diagram. Looking at Figure 4.14, and knowing that the directors and the dipole are aligned with $\theta = 90°$, the lobe with maximum gain has a slight deviation from that direction.

One possible explanation for the deviation observed is the implementation of the balun. As explained in Chapter 3, the microstrip section of the antenna acts as a reflector element, hence there's no physical reflector element. Since the microstrip section is not perfectly symmetrical, due to the balun's arms, the antenna's diagram deviates, as if there was a reflector element which wasn't aligned with the directors, causing the radiation pattern to escape the side with more copper. Another aspect that bears with this hypothesis is the fact that before building the balun, the radiation pattern was perfectly aligned with all the Yagi's elements.

The only thing left to analyse is the gain variation over frequency, shown in Figure 4.15.

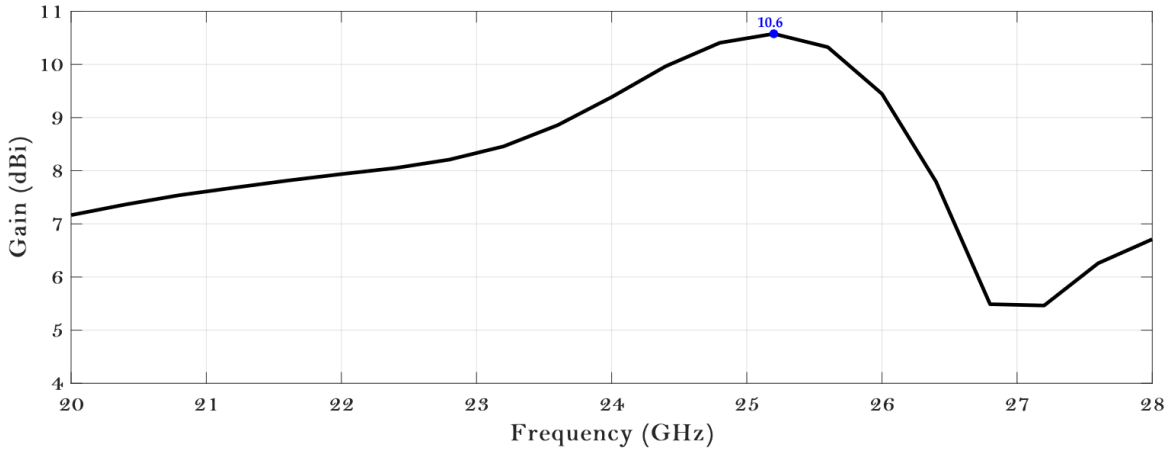

Figure 4.15: Gain variation over frequency of the 24 GHz planar antenna.

It is possible to verify that the maximum gain occurs at 25.2 GHz and not at the operation frequency. Moreover, in the range between 24.4 and 25.8 GHz the antenna's simulated gain is higher than 10 dBi. As seen in Figure 4.16, between 20 and 30 GHz, the antenna's total efficiency presents high values, especially from 22.3 up to 25.3 GHz since it's where the efficiency is more than 80%, the peak being of 90% at 24 GHz.

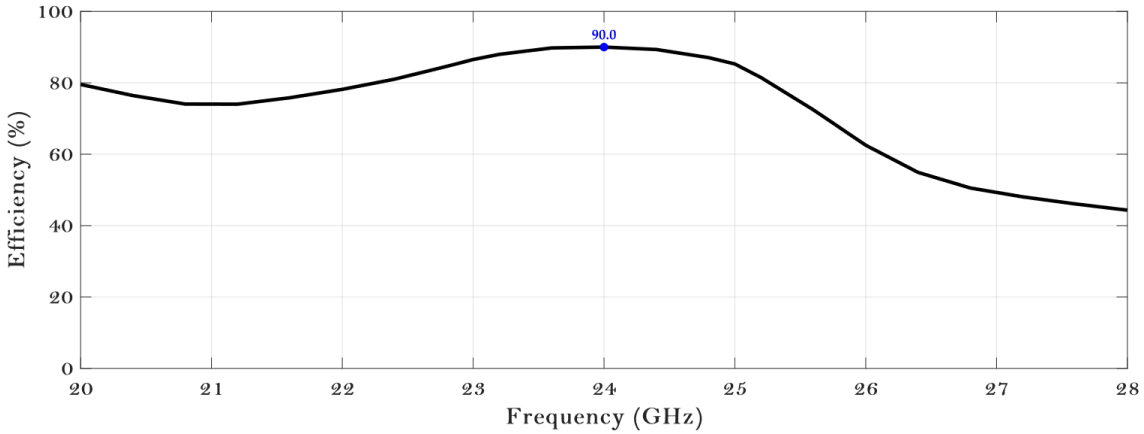

Figure 4.16: Efficiency over frequency of the 24 GHz planar antenna.

4.2.2 Measured results

Figure 4.17 allows to compare the results obtained through simulation and the measured ones, after building the antenna according to what was planned.

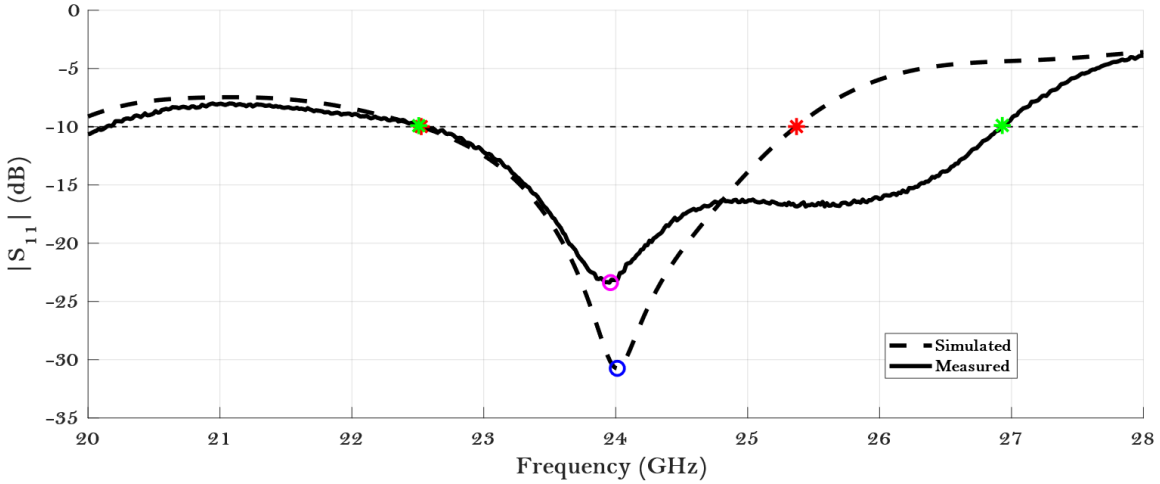

Figure 4.17: Simulated and measured reflection coefficient (|S11|) of the planar 24 GHz antenna.

Firstly, regarding the minimum $|S_{11}|$ and the impedance matching achieved. Blue and pink circles highlight the minimum reflection coefficient, respectively simulated and measured. Since the frequency of operation is 24 GHz, results obtained fulfil the initial goals for this structure. Moreover, it is easily seen that a good impedance matching was attained since the minimum value for $|S_{11}|$ occurred at 23.96 GHz, clearly close to the desired operation frequency, 24 GHz.

Meanwhile, the absolute value of the reflection coefficient differed roughly in 7.4 dB between the simulated and measured values, at 24 GHz. This is a somewhat expectable and reasonable difference.

Furthermore, these results show a significant improvement on the bandwidth obtained. While in simulation a bandwidth of 2.85 GHz was found, here, using the same criteria, 4.42 GHz were achieved, representing a 17.9% bandwidth, from 22.51 GHz up to 26.93 GHz, hence, the measurements made show significant improvements.

Lastly, the radiation diagram of this antenna is left to analyse. Due to the lack of an anechoic chamber suitable for this frequency of operation it was decided to test this prototype in a simplified version of an anechoic chamber, built in the laboratory. To implement it a VNA, absorbent material and two horn antennas (placed on top of two tripods) were used. The setup described can be seen in Figure 4.18, and it is important to mention that the far-field distance for this frequency of operation was held in account, hence, the transmitter and the receiver antennas were separated by 80 cm.

(a)

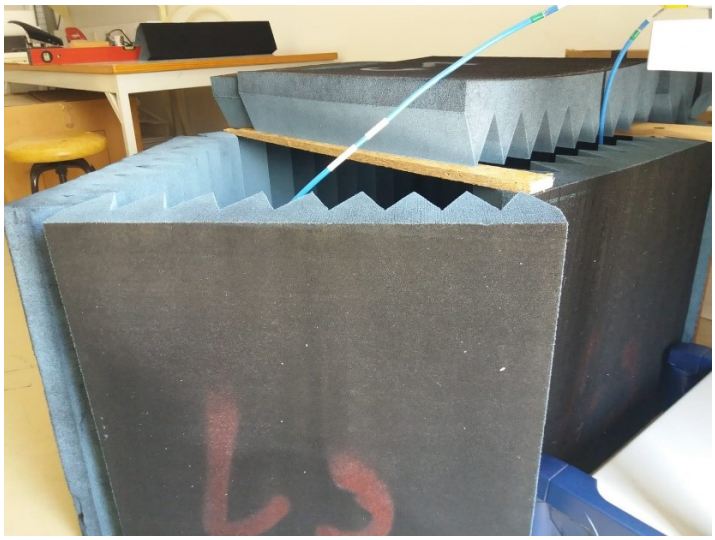

(b)

Figure 4.18: Simplified anechoic chamber: (a) chamber and VNA and (b) side view.

The planar 24 GHz Yagi was fixed as highlighted in Figure 4.19.

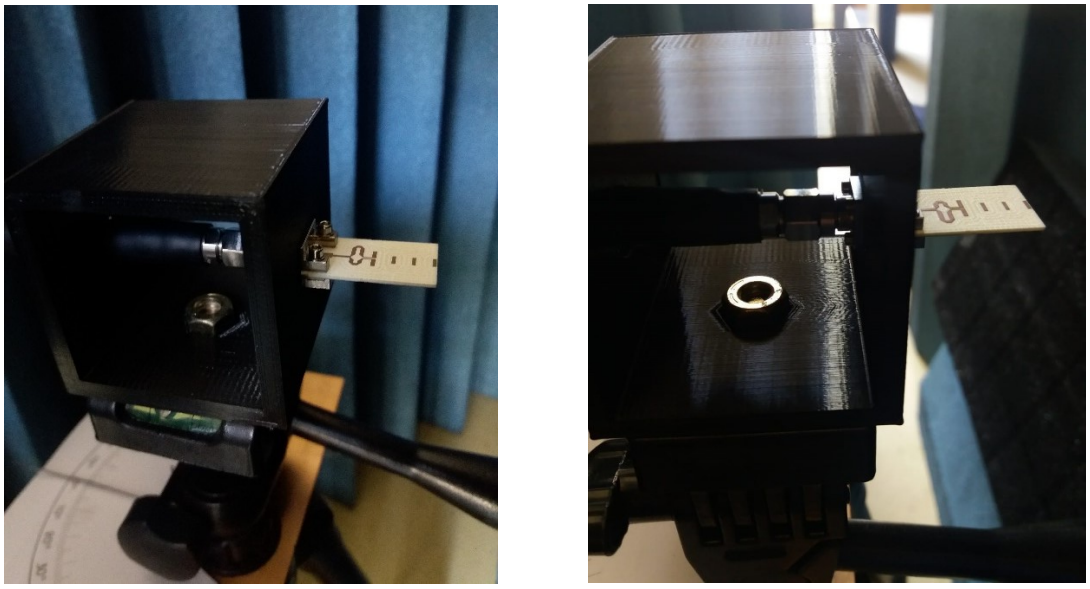

(a) (b)

Figure 4.19: Planar Yagi-Uda antenna's fixation.

Clearly, as observed in the pictures above, this prototype of anechoic chamber presents flaws. Nevertheless, the results obtained, when measuring the planar prototype, are compiled in Figure 4.20. There, a comparison between the simulation results and the ones obtained during the measurement process is made.

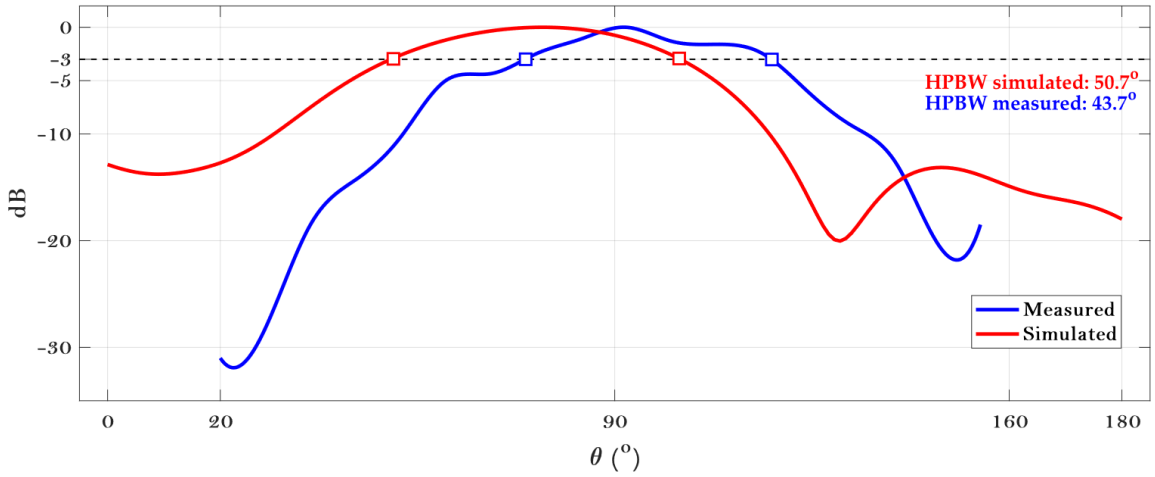

Figure 4.20: Radiation diagram of the 24 GHz planar Yagi antenna (plane $\varphi = 0°$).

It is possible to observe a shift in the main lobe of radiation, when comparing the simulated and measured results. However, when talking about the Half Power Beamwidth

(HPBW), results show a great match since the measured and simulated angles for this parameter are close.

Moreover, it was possible to obtain the measured gain, using one of the horn antennas as a reference, and once again, using Equation (4.2), while considering the datasheet of the horns.

$$G_{AUT} = 8.57\ dBi \tag{4.5}$$

Bringing back the simulated value of 8.93 dBi a difference of 0.36 dB is witnessed. Considering the context of the measurements performed, this is a significantly close value of the simulation predictions. Moreover, measures were taken by hand, reading the S21 parameter in the VNA, thus, possibly, errors occurred because, this device is highly sensitive, and thus the value read was constantly showing slight variations.

4.3 Multilayer antenna for 24 GHz

As a start, theoretical values presented in Chapter 3 allowed to design the antenna. Later, several simulations were performed, in order to achieve the optimal values for the design parameters.

However, since the construction of multi-layered antennas has a relative novelty, a study on the dielectric substrate and other possible design solutions was important.

4.3.1 Analysis of other substrates and other possibilities of construction

This first sub-chapter intends to clarify the antenna's behavior and the changes produced by structural alterations, such as the number of directors, the height between the parasitic elements and the substrate used to build the antenna.

Firstly, an analysis on the number of substrate layers used to separate the parasitic elements was done. In theory, the distance between parasitic elements has a direct relation with λ_d, but here, due to the construction process, there are limitations. As a result, simulations were performed where the distance between directors was varied, and the number of directors used was kept constant.

Additionally, since all elements were designed to radiate between layers of substrate, a comparison between having a few extra dielectric layers on the top of the last director, or not, was performed (the number of extra layers was varied). Figure 4.21 (a) and (b) clarifies the options between having or not having the extra layers of substrate.

Moreover, Figure 4.21 (b) highlights the layers identification. Thus, layers E_n constitute the extra dielectric layers (which are to be studied), layers named $D_{n.m}$ represent the distance between each director and the following element, meaning, the parameter h_{dir}, and lastly, R_n layers are representing the distance between the dipole and the reflector, h_{ref}.

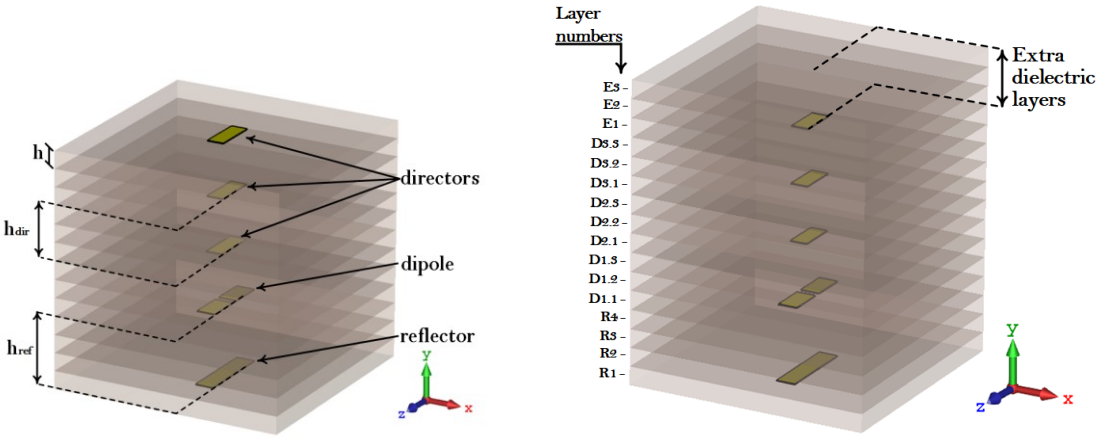

(a) (b)

Figure 4.21: Yagi antenna (a) without or (b) with the extra substrate on top of the 3rd director.

Figure 4.22 shows the information collected, in simulation, considering a three director Yagi-Uda antenna. The number of director elements was maintained in 3, for now.

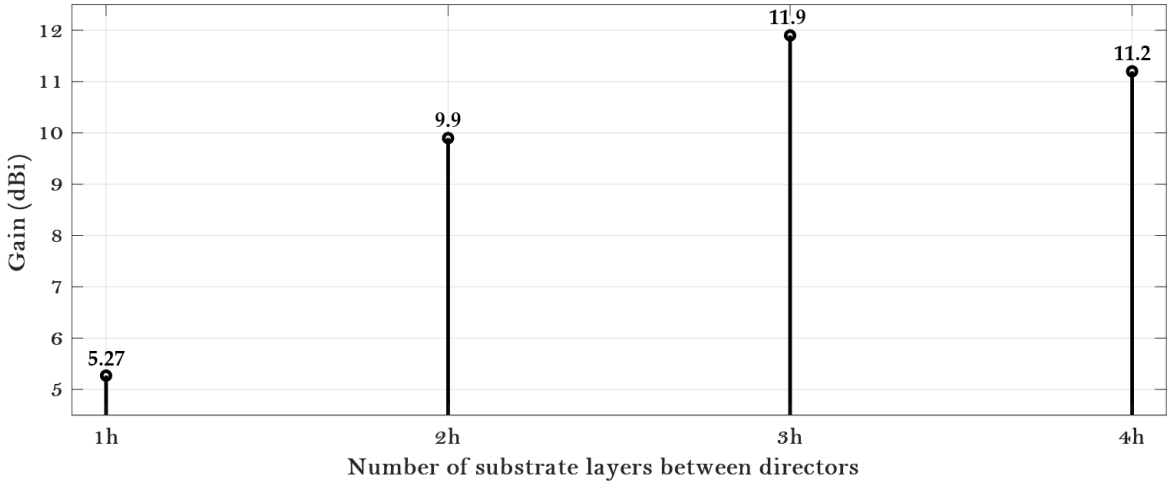

Figure 4.22: The gain variation with the distance between directors on a multilayer antenna.

With this, it is possible to assume that 3 layers of substrate separating each director might be the best choice, since it provides the maximum gain.

Figure 4.23 shows two different scenarios where the number of director elements was varied. In this case, tests were made with and without the extra layer of substrate (see

Figure 4.21). In both scenarios, the distance between directors was maintained in 3 layers, the optimal value found through Figure 4.22.

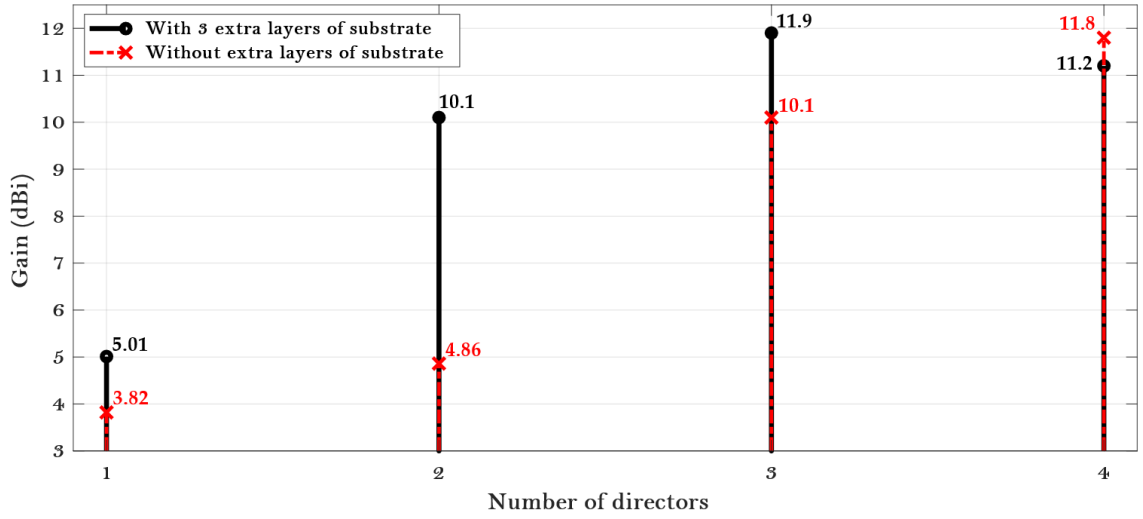

Figure 4.23: The gain variation with the number of directors on a multilayered antenna.

It is seen that the extra top layers enhance the antenna's gain being its importance major when talking about fewer directors. Moreover, it can be noticed that opting by 3 directors is the decision that will lead to a higher gain.

Up until this point the analysis started with deciding the distance between directors, how many should be used, and if opting by placing a few extra layers on the antenna's top was a good choice or not. Since in simulation, implementing these layers seems an adequate decision, so the optimal number of extra layers to include in the prototype was studied.

Figure 4.24 gathers the results obtained, where the number of substrate layers that composed the extra part of dielectric was varied. In these tests, 3 directors were used and the distance between them was composed of 3 substrate layers.

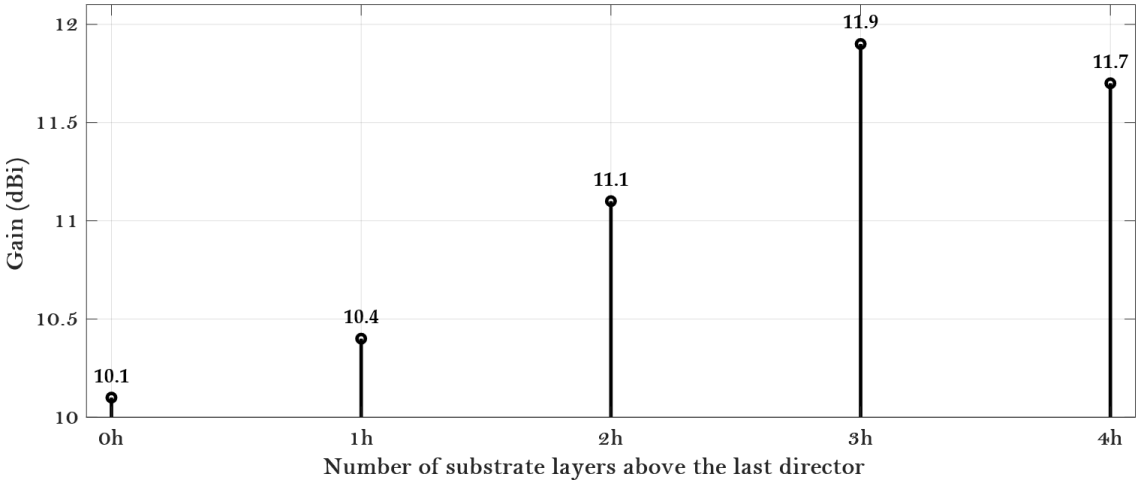

Figure 4.24: Gain variation with the variation of the number of substrate layers topping the last director.

Through Figure 4.24 it is observed that using only 1 layer of substrate toping the 3rd director already increases the gain significantly, since the marker in *0h* indicates a gain of 10.1 dBi and with *1h* 10.4 dBi are reached. So, the simple placement of one layer of substrate immediately enhances the gain by 0.3 dBi.

This analysis' main goal was to study the antenna's performance and at this point, and with this dielectric substrate, the optimal trade-off regarding the number of directors is 3, the number of layers that should separate each director is 3, as well as the distance between the 1st director and the dipole, equivalent to 2.286 mm. Also, it is possible to decide that 3 extra layers of substrate on top of the 3rd director will be used, since that provides extra gain of 1.8 dBi and the impact on antenna's size is adding less than 3 mm of height.

The other parasitic element is the reflector and alternatively to this element, a ground plane could be used. Figure 4.25 shows the differences on the antenna design.

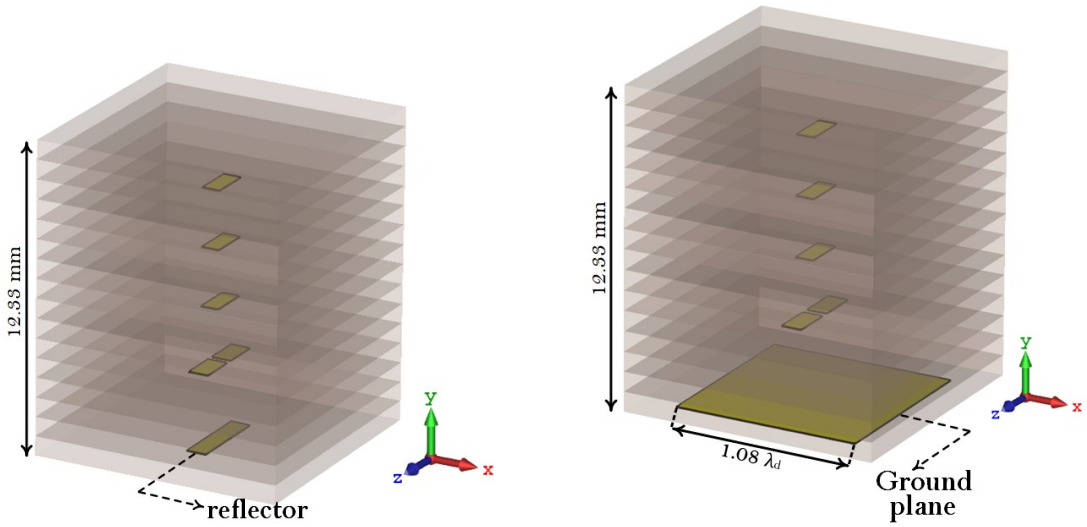

Figure 4.25: Multilayer antenna (a) with reflector or (b) ground plane.

Simulations were performed to optimize the area of the ground plane, and here the analysis made in [42] was attained. There it is concluded that the ground plane should have between $1.2\lambda^2$ and $1.4\lambda^2$. Therefore, a copper square as in Figure 4.25 (b) was designed.

After a few simulations it was possible to conclude that the best distance between the reflector and the dipole is composed of 4 layers of substrate, h_{ref}. So, both a ground plane and a reflector, were designed and equally separated from the dipole, and this distance is one layer bigger than the distance between directors (h_{dir}). This last separation, h_{ref}, is equivalent to 3.048 mm.

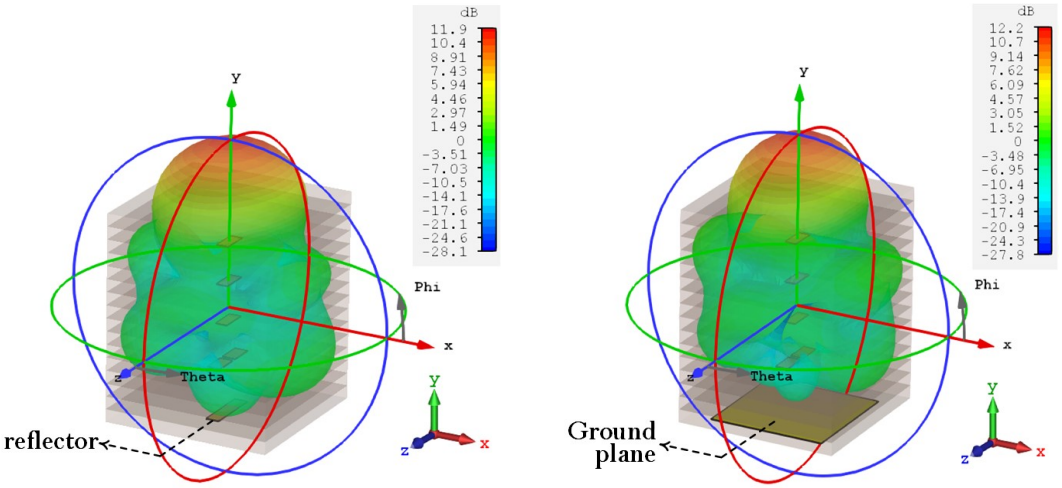

(a) (b)

Figure 4.26: 3D view of the antenna's radiation pattern (a) with reflector and (b) with ground plane.

The gain achieved with the presence of a reflector element, with an optimized length of $1.05\lambda_d$, was 11.9 dBi. On the other hand, the result obtained with the implementation of a ground plane was 12.2 dBi. Regarding the radiation pattern, its shape is similar. Since the difference observed is only of 0.3 dBi, the implementation with the ground plane was not significantly different, and so the traditional scheme of a Yagi-Uda antenna was maintained.

Lastly, and after deciding the structure to use on the multilayer Yagi-Uda antenna for 24 GHz, possible alternatives of dielectric substrate were analysed in simulation. Within the available choices, two other substrates were chosen, one of them with higher dielectric constant (ε_r) and another with lower.

Reminding that, until this point, throughout all simulations and designs, Rogers RO4350B was the dielectric substrate used. Table 4.5 compiles the basic electrical characteristics of the other substrates chosen: Rogers RO4360G2 and Isola Astra.

TABLE 4.5: Main characteristics of the substrates tested.

Substrate	Rogers RO4350B	Rogers RO4360G2	Isola Astra
ε_r (@ 10 GHz)	3.48	6.15	3
h	0.762 mm	0.813 mm	0.76 mm
Copper thickness	35 µm	18 µm	35 µm
$\tan(\delta)$ (@ 10 GHz)	0.0037	0.0038	0.0017

Table 4.5: Physical and electrical characteristics of the substrates tested.

Through the information in Table 4.5 it is seen that substrates vary not only their ε_r, but also their height (h) and their losses, described in the parameter $\tan(\delta)$. Since h varies, the optimal number of layers between the Yagi's elements will need to be analysed for each substrate. Moreover, tests need to be performed to guarantee that the ideal lengths are optimized for the new substrates, because the wavelength in each dielectric changes, as a direct consequence of the change in ε_r.

After iterating the designs, the values for all the design parameters, that provided the maximum gain observed, were compiled on Table 4.6. It is noticeable that these dimensions are also presented as a function of each λ_d, so that distances can be compared.

TABLE 4.6: Parameters which maximized the gain for each antenna. UNITS

Substrate	**Rogers RO4350B**	**Rogers RO4360G2**	**Isola Astra**	-
L_{dip}	3	2.25	3.23	mm
	0.448	0.447	0.448	λ_d
L_{dir}	1.68	1.26	1.80	mm
	0.25	0.25	0.25	λ_d
L_{ref}	3.47	2.68	3.71	mm
	0.52	0.53	0.51	λ_d
Number of layers between directors	3	2	4	-
Number of layers between dipole and reflector	4	3	4	-
Equivalent distance between directors	0.34	0.32	0.42	λ_d
Equivalent distance between dipole and reflector	0.45	0.48	0.42	λ_d
Maximum gain	**11.90**	**9.07**	**11.20**	dBi

Table 4.6: Main results obtained when designing a multilayer antenna with different substrates.

Firstly, considering the antenna's active element, even though the length of the dipole presents a different dimension for each substrate, if that value is written as a function of each λ_d, rapidly it is concluded that the relation with the wavelength is kept constant, since all 3 directors present an optimal length around $0.44\lambda_d$.

This observation can also be made regarding the parasitic elements of the antenna. At first glance, dimensions seem to be totally divergent but, when converting them as a function of λ_d their similarities are found. For all substrates chosen the best length for the director is $0.25\lambda_d$ and for the reflector, the best design would be with an element whose length is near $0.5\lambda_d$. These results confirm, once again, that for a vertically stacked Yagi antenna, the traditional theoretical considerations are valid, if the necessary variations are held in account.

Regarding the number of layers between elements, naturally, there are significant changes, mainly because substrates tested present not only a different dielectric constant (ε_r) but also a different height (h), as already mentioned. Once again, when transcribing the number of layers to the distance as a function of each λ_d, comparable results are seen.

Reminding that the optimal distance is the one that within the options available (since the construction process is confined to separate each element by a multiple of h), provides better gain, it is relevant to analyse the relation between h_{dir} and h_{ref} for each dielectric substrate.

Both for Rogers RO4350B and for Rogers RO4360G2 the maximum gain is achieved when the reflector element is slightly more apart from the dipole than the directors, as normally witnessed in Yagi antennas. On the contrary, in Isola Astra, maximum gain is obtained when using the same spacing between directors and between the reflector and the dipole, meaning that for this substrate maximum gain is obtained when $h_{dir} = h_{ref}$.

Still, it can be noticed that values are consistent when comparing the specified distances and the respective wavelength in each the dielectric. Once again, the idea is to build an antenna that allows to obtain the higher gain possible, so, on the prototype built, Rogers RO4350B was the chosen substrate.

4.3.2 Simulation results

This process of analysing the multilayer Yagi antenna allowed to obtain the design scheme, shown in Figure 4.27, with its respective design parameters. As it was done in the previous implementations, those dimensions are compared with the theoretical ones in Table 4.7.

At this point, it is relevant to enhance the comparison on the *Lcps* parameter, where it can be confirmed that the method of analysis, and the optimal value for this parameter is clearly close to the one predicted using the Smith Charts in Appendix B.

The remaining design parameters are presented in Table 4.8. Lastly, in Figure 4.28, the multilayer prototype is revealed.

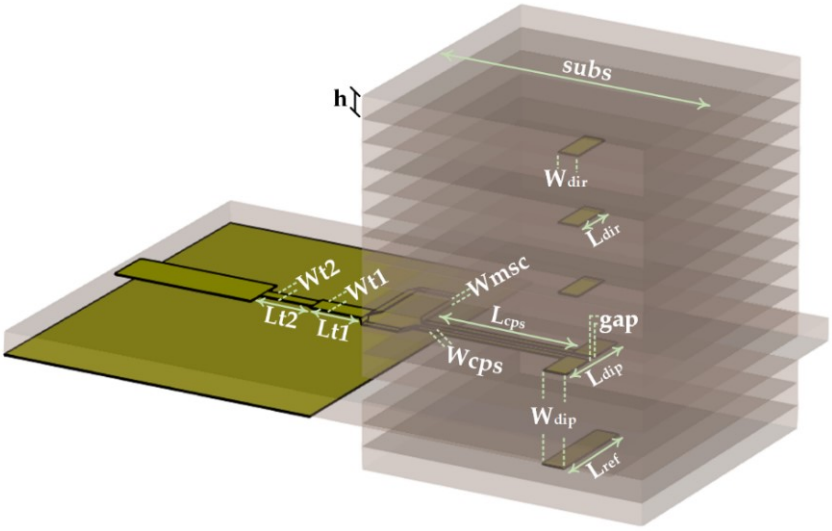

Figure 4.27: Schematics of multilayer Yagi-Uda antenna.

TABLE 4.7: Theoretical and optimal values for the multilayer Yagi (UNITS: mm).

Parameter	L_{dip}	L_{dir}	L_{ref}	Lcps	h_{dir}	h_{ref}	gap	subs
Theoretical	3.15	1.5	3.21	5.437	2.286	3.048	0.3	-
Optimized	3	1.67	3.47	5.32	2.286	3.048	0.3	10

Table 4.7: Optimal parameters and the ones estimated theoretically for the multilayer Yagi.

TABLE 4.8: Design parameters for the multilayer 24 GHz Yagi (UNITS: mm).

Parameter	W_{dip}	W_{dir}	Wcps	Wmsc	Lt1	Lt2	Wt1	Wt2
Optimized	0.80	0.72	0.25	0.25	1.88	1.92	0.78	0.48

Table 4.8: Optimized values for the design parameters for the 24 GHz multilayer antenna.

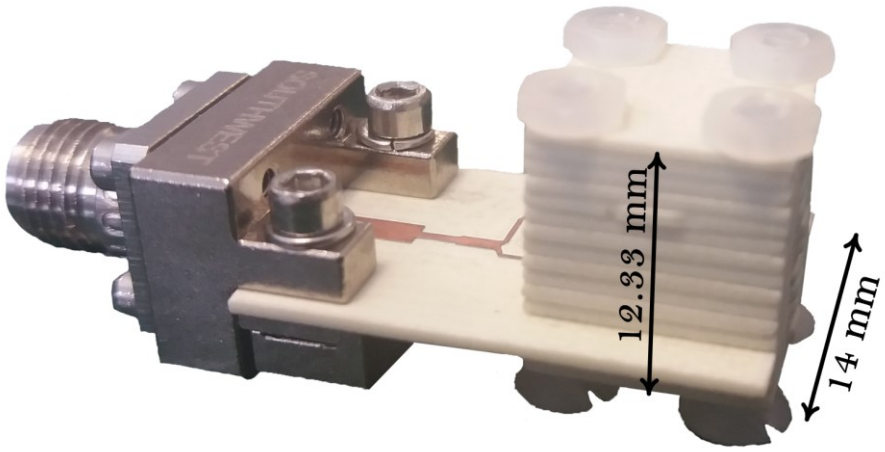

Figure 4.28: Prototype of the antenna built and its measurements.

In this case, the overall dimensions of this antenna are: $21.8 \times 14 \times 12.3\ mm^3$.

Again, to start, it is important to analyse the antenna's impedance matching at the operation frequency, and so, Figure 4.29 shows the simulated reflection coefficient.

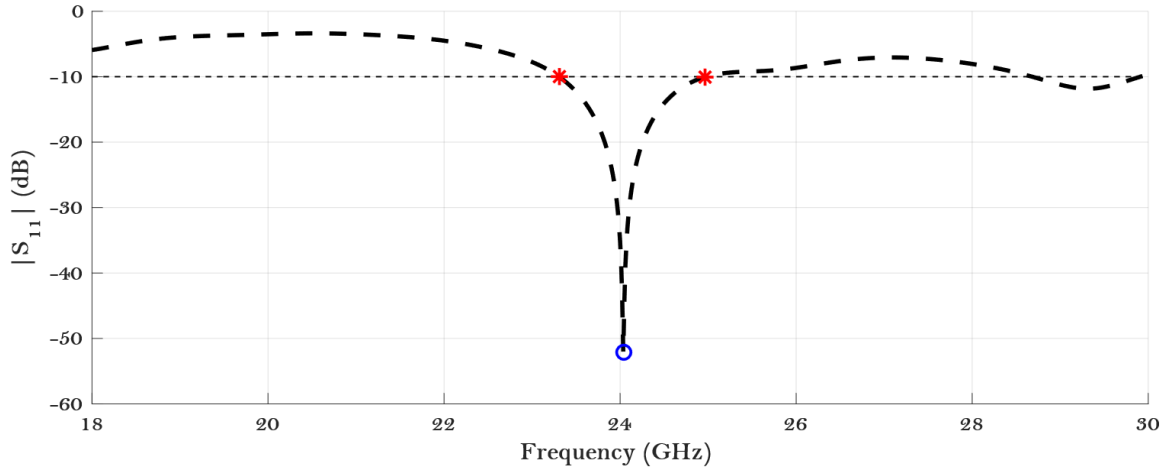

Figure 4.29: Simulated S11 of the designed multilayer Yagi-Uda antenna for 24 GHz.

Here, and once more, red markers identify the bandwidth of the antenna according to the -10 dB criteria. Simulation results present an antenna with 1.56 GHz of bandwidth, approximately 6.5%, between 23.31 and 24.86 GHz, a significant reduction when comparing these results with the ones of the planar Yagi-Uda antenna, for the same resonant frequency.

Simultaneously, the impedance matching accomplished is accordingly, since the antenna's input impedance, specified in Equation (4.6), is near the 50Ω of the coaxial cable.

$$Z_{in} = 50.54 - i0.11\ \Omega \tag{4.6}$$

Considering the implementation using a multilayered structure, one of the most important results to expose is in fact the radiation diagram obtained, and this is shown in Figure 4.30, as a 3D view, and in Figure 4.31 in a polar diagram, where the main lobe is highlighted.

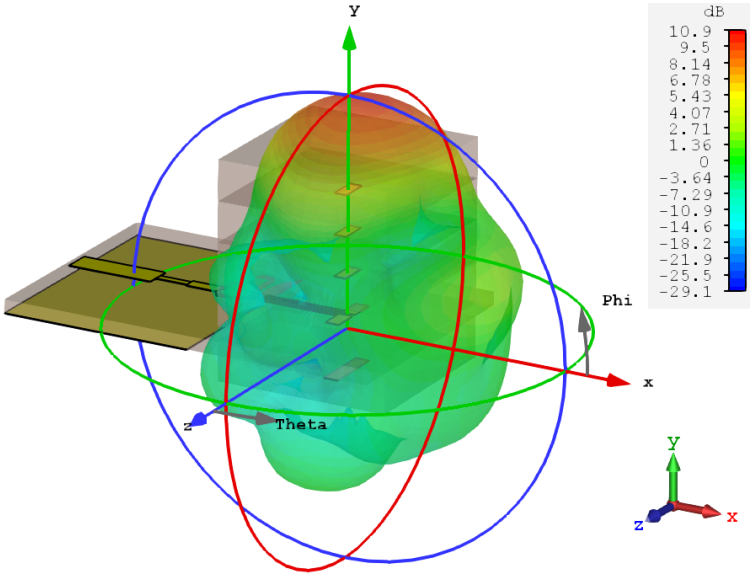

Figure 4.30: 3D view of the radiation diagram of the multilayer antenna for 24 GHz.

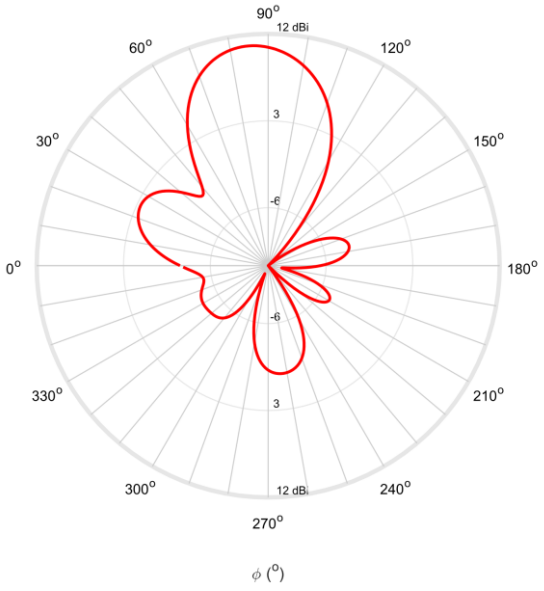

Figure 4.31: Polar diagram of radiation pattern of the 24 GHz multilayer antenna (plane $\theta = 90°$).

It is possible to notice that the maximum gain obtained is 10.9 dBi, and now, the direction of the lobe with maximum gain is aligned the Yagi's elements, in fact, vertically aligned. Secondary lobes of the diagram are all significantly smaller than the main lobe,

and therefore, once again, the radiation pattern obtained, satisfies the initial goals of the design.

Furthermore, another important aspect is given on Figure 4.32. There, the antenna's gain over frequency is presented. It is possible to confirm that this structure as a maximum gain at the frequency of operation equals to 10.9 dBi. Moreover, there's a range of about 2 GHz around the operation frequency where this antenna presents a gain of more than 10 dBi.

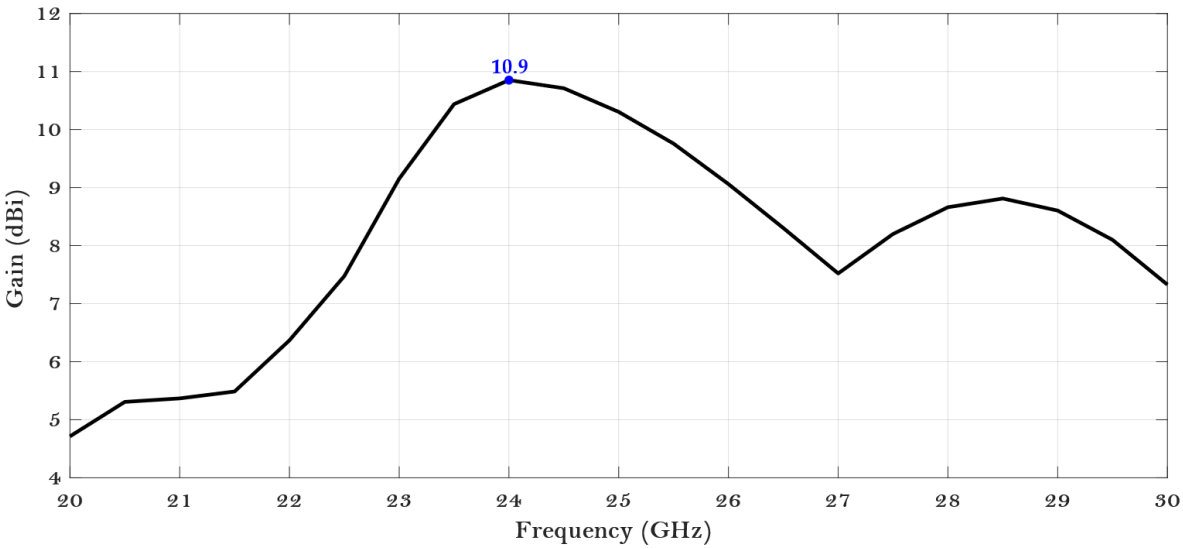

Figure 4.32: Gain over frequency of the 24 GHz multilayer Yagi.

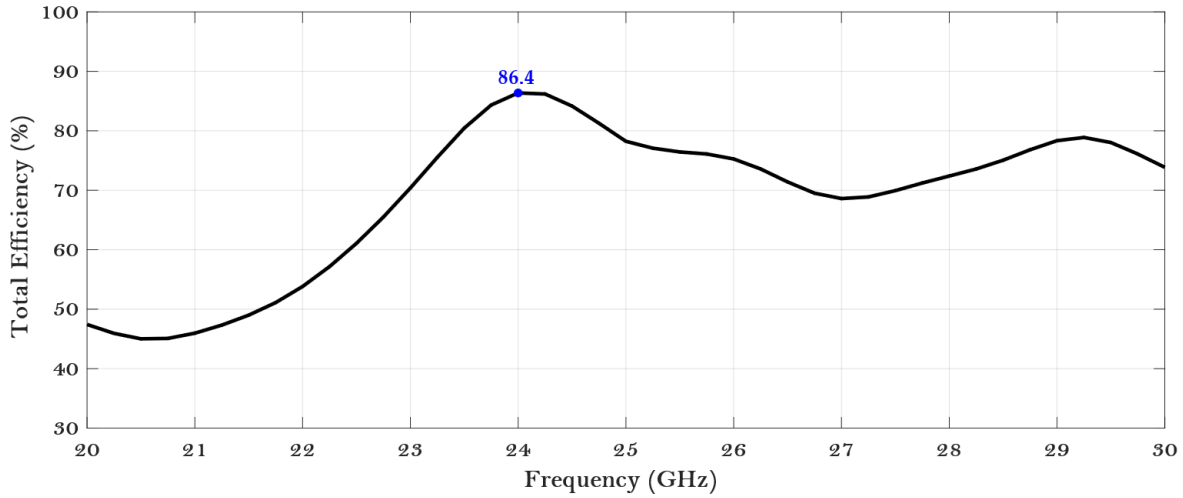

Figure 4.33: Efficiency over frequency of the 24 GHz multilayer Yagi.

Also, regarding the antenna's efficiency, Figure 4.33 indicates a maximum efficiency at the frequency of operation of about 86%, a high value. Also, between 23.5 and 24.9 GHz the antenna's overall efficiency is always greater than 80%. Given the structure's

complexity and its compactness, consisting of several stacked substrate dielectric layers, this is an important result.

4.3.3 Measured Results

Figure 4.34 highlights the results obtained through simulation and the ones that were measured using the VNA.

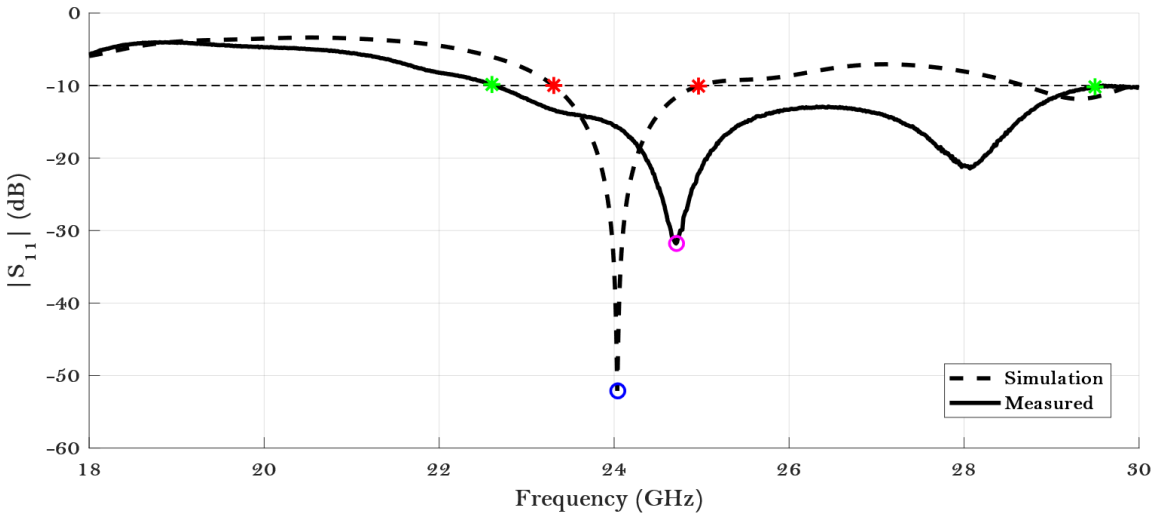

Figure 4.34: Simulated and measured reflection coefficient (|S11|) of the multi-layered 24 GHz antenna.

Again, a satisfactory level of impedance matching was obtained since for the operation frequency, the practical $|S_{11}|$ is -15.51 dB. Moreover, the minimum value for $|S_{11}|$ is -31.78 dB, even though it occurs at 24.71 GHz, and thus, a shift in frequency is observed.

The observation made concerning the minimum S_{11} value being 710 MHz apart from the desired 24 GHz can be justified by a slight variation on the effective dielectric constant from the value considered in simulation, where this dielectric substrate was confirmed as adequate. However, this construction method might be propitious to a change in the overall ε_r, for example if between the prototype's layers still exists air.

Regarding bandwidth, as shown by the green markers in Figure 4.34 this antenna showed 6.89 GHz, between 22.6 up to 29.5 GHz something that represents 26.5% bandwidth, an important and encouraging result.

Once again, the radiation diagram of this antenna was measured using the same conditions explained in the topic 4.2.2, for the planar Yagi antenna. In this case, the antenna's fixation was done as shown in Figure 4.35.

Figure 4.35: Multilayer Yagi antenna's fixation.

The results obtained regarding the 24 GHz multilayer antenna are compiled in Figure 4.36, where a comparison between the simulation results and the ones obtained during the measurement process is made.

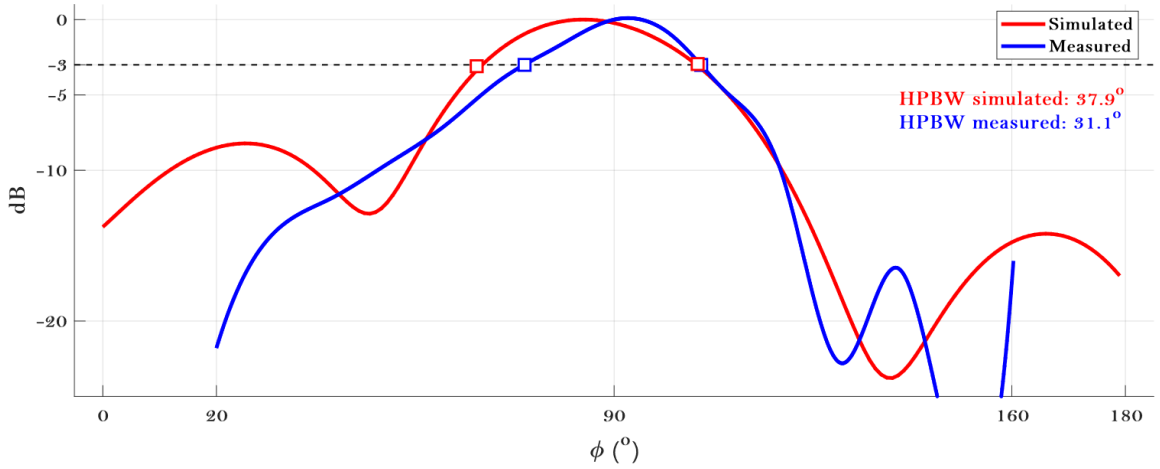

Figure 4.36: Radiation pattern of the multilayer Yagi antenna (plane $\theta = 0°$).

Here, in line with what was obtained for the planar prototype, a good match between the simulated and measured HPBW was achieved. Overall, the behavior observed in the radiation pattern seems adequate and agreeing with the expectations. However, regarding the maximum gain achieved, this antenna presented a value clearly not satisfying (remembering, the simulated value is 10.9 dBi), since in the measurement process a quite lower value was obtained (4.7)

$$G_{AUT} = 7.18\ dBi \tag{4.7}$$

There are several plausible justifications for the low value found. First of all, the construction process consisted in simply stacking multiple layers of substrate and assuring their compactness by using plastic screws (not considered in simulation). It is possible that this construction method created punctual air gaps in the antenna and that causes the discrepancies found between simulation and measurements.

Other possible explanation, and still regarding the construction method used, is the slight misalignment of the Yagi's elements. During the etching process, small variations can damage the elements' alignment leading to the differences observed.

Also important is the fact that the multilayer antenna is not perfectly tuned for 24 GHz, and the gain was measured for this frequency. Thus, it is possible that the maximum gain of the prototype was not measured, occurring in a different frequency than 24 GHz.

4.4 Discussion: results of the mmWave antennas

A planar Yagi-Uda antenna operating at mmWave frequency was designed and constructed (the construction process was similar, as well as the number of elements used). Here, the impedance matching obtained was perfectly tuned, since the minimum $|S_{11}|$ happened at 23.96 GHz in the measurements made. A careful choice of the dielectric substrate chosen was crucial to obtain these results. Moreover, a significant bandwidth was achieved, 4.42 GHz, representing a 17.9%, an encouraging outcome, considering the scenarios for which this antenna can be applied to.

Nevertheless, the main goal of this work was to design a multilayer Yagi-Uda antenna suitable for mmWave implementations such as the ones mentioned in Chapter 2. One of the main aspects to highlight throughout this last design is the analysis of the various dielectric substrates, where it was found that, within the ones tested, Rogers RO4350B provided the best gain for the Yagi antenna.

Also, within the design schematics, the usage of a ground plane was discarded since the improvement in the antenna's gain wasn't significant. From the other changes in design tested, the implementation of extra dielectric layers on top of the 3rd director is highlighted. In Figure 4.23 red markers show a progressively better gain, as the number of directors of the antenna increases, as it is expected in traditional Yagi-Uda antennas: the more directors, the more gain achieved. On the contrary, the few extra layers of substrate appear

to have a positive contribution only up to the point where 3 directors are used, since that with 4 directors the gain worsens.

This effect was noticed during the design process, and while testing the various possibilities, whether including or not the substrate layers. One possible justification for the observations made, is that the upper layers of substrate are creating a Dielectric Resonator Antenna (DRA) effect.

Considering the study made in [54], and taking into account the dimensions of the rectangular structure placed above the last director, it allows us to conclude that it can be seen as a DRA, which by its dimensions presents a resonant frequency around 20 GHz, not too far from the operation frequency, thus, some extra gain may be created by this additional structure.

This hypothesis is also sustained by the behavior witnessed in Figure 4.24, where the height of the extra structure is changed. The gain is reduced both for 2h and 4h, and for those dimensions the resonant frequency changes, being respectively 28 GHz and 16 GHz.

In the end, after all the design choices considered, the final prototype was designed and built. After the measurements made, is was confirmed an adequate impedance matching, however, the minimum reflection coefficient is a bit further from the desired 24 GHz than in the planar prototype, this might be due to a consequence of the construction method of this antenna, which was very simple, just to demonstrate the concept.

Despite having that slight deviation, an improvement in the antenna's bandwidth was accomplished, since this last prototype exhibits 6.9 GHz, meaning 26.5%, bandwidth. Overall, the concept of converting the planar into a multilayer structure, is clearly promising, since it is possible to reduce the antenna's overall size, while also improving both bandwidth and gain. In the Table 4.9, the results on the measured bandwidth and the simulated gain are exhibited.

TABLE 4.9: Measured bandwidth and simulated gain of the 24 GHz antennas.

Antenna	Bandwidth	Gain
Planar	4.42 GHz 17.9 %	8.9 dBi
Multilayer	6.9 GHz 26.5 %	10.9 dBi

Table 4.9: Comparison between both 24 GHz antennas.

Considering now the results on the measured gains, both for the 24 GHz planar and multilayer prototypes. In the first case the value obtained is quite reasonable, but on the other hand, in the multilayer antenna this value exhibited a discouraging result, since the value differed in more than 3 dB, from the simulation to the measurements. However, it is important to remember that the conditions where these measurements were performed are clearly not ideal. Moreover, several difficulties were faced, regarding the system's stability and the placement of the antennas, factors which can be improved for the coming measurements.

Chapter 5

5 Conclusions and Future Work

5.1 Conclusion

The main objective of this dissertation was to develop a multilayer antenna, operating in the mmWaves region. Within the context of this work, it was considered relevant the comparison between a planar and a multilayer prototype, with enough common characteristics so that in the end conclusions were fair. However, it was decided to firstly implement a 2.4 GHz Yagi antenna.

As said, the first implementation consisted on building an antenna suitable for the 2.4 GHz Industrial, Scientific and Medical (ISM) band. Its low-cost substrate is responsible for the results found, where a shift in frequency was observed, as a consequence of an inaccurate impedance matching. Even though it would have been possible to improve the prototype, by building a new antenna, which should compensate the frequency shift observed, that was considered unnecessary, mainly because the aim with this structure was only to find if the feeding scheme chosen was appropriate and to get familiarized with the simulation tools available.

Besides that, regarding the antenna's gain, measurements showed slight less gain than the simulation results. In simulation the antenna's gain at the frequency of operation is 6.66 dBi, whereas in practice 5.92 dBi were achieved.

Later, the mmWave migration was done and considering the framework of 5G, it was highly important to assure good characteristics regarding the antenna's efficiency, additionally to proper gain and bandwidth. Yagi-Uda antennas present several key features, interesting for implementation in 5G scenarios already exposed, however, if planar, their integration in printed circuits might be compromised due to their typical radiation pattern.

By simply stacking multiple layers of dielectric substrate, and using the same substrate in both prototypes, it is clearly stated by the results obtained that multilayer radiating structures are a valid and promising alternative.

In fact, a reasonable bandwidth had already been obtained in the planar prototype, since 4.42 GHz, at 24 GHz it is an interesting value. Nevertheless, the vertically stacked prototype improved this value, reaching 6.9 GHz of measured bandwidth. Possibly, the stacking of multiple layers of dielectric substrate causes, somehow, a more adequate mean of propagation, and this thesis is sustained by two facts.

The first one is that in this multilayer structure the transition between the antenna's elements is less abrupt, since in planar antennas there is a direct transition between dielectric substrate, the copper, and the air, and here, that transition is clearly smoother, since the elements are surrounded by dielectric substrate.

The second fact concerns the concept of the reflection coefficient. In fact, the bandwidth is measured having in account the S_{11} parameter, and it is important to remind that this S-parameter is a ratio between the transmitted and the reflected wave. There is the chance that this vertically stacked structure attenuates the reflected wave, and thus improves the bandwidth, however, this hypothesis is not confirmed.

Regarding the gain of both 24 GHz Yagi's, measurements were difficult, due to limitations on the anechoic chamber available, nonetheless, the shape of the radiation diagram and the antennas' gain were obtained. Both radiation diagrams measured were according to the ones obtained in simulation, however, the maximum gain measured was far from what was expected in the case of the multilayer prototype.

In the case of the planar prototype, a from the simulated gain to the measured one, an acceptable difference of 0.3 dBi was noticed, the simulated gain being greater and equal to 8.9 dBi. On the other hand, concerning the multilayer prototype, a difference of more than 3 dBi was seen, thus, it is important to consider the conditions where these measurements were made, and it is also important to have in account the slight deviation of the antenna from de 24 GHz.

Moreover, these results did not compromise the overall efficiency of the antenna, a key concern in the coming generation of mobile communications. Not only systems will have to guarantee spectrum efficiency, but it is also mandatory to reduce the cost per bit, and here, once again, these antennas achieve proper bandwidths without significantly increasing the costs.

Lastly, both prototypes showed a good matching regarding the simulated and measured radiation pattern, the half power beamwidth parameter clarifies that same match.

As a sum up, it is believed that this dissertation's main goals were accomplished since a multilayer Yagi antenna was built, as well as it was compared to an equivalent planar prototype. In the end, it has been proven that multilayer radiating structures are an individual element to be considered when designing an IoT or 5G system.

5.2 Future Work

Concerning the future work and the possible improvements to this work, three suggestions are made:

- Perform the antenna's measurements in an adequate anechoic chamber to verify the results obtained, specially about the 24 GHz multilayer Yagi antenna, to clarify the gain obtained.

- With the necessity of implementing this antenna in scenarios with thousands of structures, it is intended to turn this into a modular Yagi, and for that it is required to change the feeding structure. Mainly, the feeding method would change from a microstrip line feed into a traditional coaxial feed, meaning that the antenna's feed would be under the Yagi's elements. This strategy would allow to confirm these antennas' integration in arrays and their usage for instance in beamforming applications.

- Trying to further enhance the antenna's bandwidth the antenna from intended, starting by replacing the dipole by another active element, for instance, a slot element.

References

[1] "Maxwell, Hertz and Marconi", *Sounds in Communication*. [Online]. Available: https://katrinasiron21.wordpress.com/contributors-to-the-development-of-telephone/maxwell-hertz-and-marconi/. [Accessed: 17- Oct- 2018].

[2] "What is wireless communication technology and its types | Infrared, Satellite Communication & Broadcast Radio", *Engineersgarage.com*. [Online]. Available: https://www.engineersgarage.com/articles/wireless_communication. [Accessed: 17- Oct- 2018].

[3] "Types of Wireless Communication and Its Applications", *ElProCus - Electronic Projects for Engineering Students*. [Online]. Available: https://www.elprocus.com/types-of-wireless-communication-applications/. [Accessed: 17- Oct- 2018]. https://www.elprocus.com/types-of-wireless-communication-applications/

[4] J. Andersen, T. Rappaport and S. Yoshida, "Propagation measurements and models for wireless communications channels", *IEEE Communications Magazine*, vol. 33, no. 1, pp. 42-49, 1995.

[5] C. Rose, S. Ulukus and R. Yates, "Wireless systems and interference avoidance", *IEEE Transactions on Wireless Communications*, vol. 1, no. 3, pp. 415-428, 2002.

[6] K. Luk, "The Importance of the New Developments in Antennas for Wireless Communications", *Proceedings of the IEEE*, vol. 99, no. 12, pp. 2082-2084, 2011.

[7] "1st mobile phone call is made, April 3, 1973", *EDN Network*, 2018. [Online]. Available: https://www.edn.com/electronics-blogs/edn-moments/4411258/1st-mobile-phone-call-is-made--April-3--1973. [Accessed: 17- Oct- 2018].

[8] "45 years ago today, Motorola made the first mobile call", *Perfect New Gadgets - Best Gadgets / Best Buy / Perfect Combo*, 2018. [Online]. Available: https://www.perfectnewgadgets.com/news/45-years-ago-today-motorola-made-the-first-mobile-call/. [Accessed: 17- Oct- 2018].

[9] "The first mobile call was made 45 years ago today", *Android Authority*, 2018. [Online]. Available: https://www.androidauthority.com/first-mobile-call-motorola-851651/. [Accessed: 17- Oct- 2018].

[10] Qualcomm, "Making 5G NR a reality | Qualcomm", *Qualcomm*, 2016. [Online]. Available: https://www.qualcomm.com/documents/making-5g-nr-reality. [Accessed: 17- Oct- 2018].

[11] L. Ashiho, "Mobile technology: evolution from 1G to 4G", *Electronics for You*, pp. 94-98, 2003.

[12] "Remember your first Sprint phone?", *XDA-developers*, 2012. [Online]. Available: https://forum.xda-developers.com/showthread.php?t=1443800&page=5. [Accessed: 17- Oct- 2018].

[13] M. Arshad, A. Farooq and A. Shah, "Evolution and Development towards 4th Generation (4G) Mobile communication systems", *Journal of American Science*, vol. 6, no. 12, pp. 63-68, 2010.

[14] "GSM", *GSMA*. [Online]. Available: https://www.gsma.com/aboutus/gsm-technology/gsm. [Accessed: 17- Oct- 2018].

[15] V. Pereira, T. Sousa, P. Mendes and E. Monteiro, "Evaluation of Mobile Communications: From Voice Calls to Ubiquitous Multimedia Group Communications", *Proc. Of the 2nd International Working Conference on Performance Modeling and Evaluation of Heterogeneous Networks, HET-NETs*, vol. 4, pp. 4-10, 2004.

[16] "GSM: Global System for Mobile Communications", *4G Americas*. [Online]. Available: https://web.archive.org/web/20140208025938/http://www.4gamericas.org/index.cfm?fuseaction=page&sectionid=242. [Accessed: 17- Oct- 2018].

[17] "What is 3G (third generation of mobile telephony)?", *SearchTelecom*, 2009. [Online]. Available: https://searchtelecom.techtarget.com/definition/3G. [Accessed: 17- Oct- 2018].

[18] R. Gondane, "What is 4G LTE? - FD LTE vs TD LTE", *Cool PC Tips*, 2012. [Online]. Available: http://www.coolpctips.com/2012/12/what-is-4g-lte/. [Accessed: 17- Oct- 2018].

[19] "Evolution of the Mobile Phone", *Tiger Mobiles Limited*. [Online]. Available: https://www.tigermobiles.com/evolution/. [Accessed: 17- Oct- 2018].

[20] S. Sahoo, M. Hota and K. Barik, "5G Network a New Look into the Future: Beyond all Generation networks", *American Journal of Systems and Software*, vol. 2, no. 4, pp. 108-112, 2014.

[21] "Evolution of the Mobile Phone: Key Milestones", *Tiger Mobiles Limited*. [Online]. Available: https://www.tigermobiles.com/evolution/#footer. [Accessed: 17- Oct- 2018].

[22] "Mobile Communication: Types, History & Timeline", *Study.com*. [Online]. Available: https://study.com/academy/lesson/mobile-communication-types-history-timeline.html. [Accessed: 17- Oct- 2018].

[23] "History of Mobile Communications Timeline", *Timetoast*. [Online]. Available: https://www.timetoast.com/timelines/history-of-mobile-communications-08557899-99c2-4216-a518-80d38a0dfdba. [Accessed: 17- Oct- 2018].

[24] "5G Vision", *Samsung Global*, 2015. [Online]. Available: https://www.samsung.com/global/business/networks/insights/. [Accessed: 17- Oct- 2018].

[25] R. Crozier, "Father of IoT Kevin Ashton slams 'smart' devices", *IoT Hub*, 2015. [Online]. Available: https://www.iothub.com.au/news/father-of-iot-kevin-ashton-slams-smart-devices-411999. [Accessed: 17- Oct- 2018].

[26] "Redes NB-IoT", *T3 México*. [Online]. Available: https://t3mexico.mx/tag/redes-nb-iot/. [Accessed: 17- Oct- 2018].

[27] "Consumer cloud computing users worldwide 2018 | Statistic", *Statista*, 2018. [Online]. Available: https://www.statista.com/statistics/321215/global-consumer-cloud-computing-users/. [Accessed: 17- Oct- 2018].

[28] H. Chourabi, T. Nam, S. Walker, J. Gil-Garcia, S. Mellouli, K. Nahon, T. Pardo and H. Scholl, "Understanding Smart Cities: An Integrative Framework", *2012 45th Hawaii International Conference on System Sciences*, 2012.

[29] "The 5G Infrastructure Public Private Partnership: the next generation of communication networks and services", *5G PPP*, 2015. [Online]. Available: https://5g-ppp.eu/wp-content/uploads/2015/02/5G-Vision-Brochure-v1.pdf. [Accessed: 18- Oct- 2018].

[30] G. Liu and D. Jiang, "5G: Vision and Requirements for Mobile Communication System towards Year 2020", *Chinese Journal of Engineering*, vol. 2016, pp. 1-8, 2016.

[31] W. Roh, J. Seol, J. Park, B. Lee, J. Lee, Y. Kim, J. Cho, K. Cheun and F. Aryanfar, "Millimeter-wave beamforming as an enabling technology for 5G cellular communications: theoretical feasibility and prototype results", *IEEE Communications Magazine*, vol. 52, no. 2, pp. 106-113, 2014.

[32] C. Balanis, *Antenna Theory Analysis and Design*, 4th ed. New Jersey: John Wiley & Sons, 2016.

[33] M. Oliveira, "Soalho Inteligente e Sensores de Movimento, Backscatter e Piezoelétricos", Tese de Mestrado, Universidade de Aveiro, 2017.

[34] C. Balanis, *Modern Antenna Handbook*. New York, NY: John Wiley & Sons, 2008.

[35] P. Hall and C. Hall, "Coplanar corporate feed effects in microstrip patch array design", *IEE Proceedings*, vol. 135, no. 3, pp. 180-186, 1988.

[36] O. Kramer, T. Djerafi and K. Wu, "Very Small Footprint 60 GHz Stacked Yagi Antenna Array", *IEEE Transactions on Antennas and Propagation*, vol. 59, no. 9, pp. 3204-3210, 2011.

[37] G. Giunta, C. Novi, S. Maddio, G. Pelosi, M. Righini and S. Selleri, "Efficient Tolerance Analysis on a Low Cost, Compact Size, Wideband Multilayer Patch Antenna", *Proceedings of the 2017 IEEE International Symposium on Antennas and Propagation & USNC/URSI National Radio Science Meeting*, pp. 2113-2114, 2017.

[38] N. Pornprachatham and T. Theeradejvanichkul, "Enhancement of a reflection coefficient via modified ground plane of a multilayer microstrip patch antenna for x-band application", *Proceedings of the 2017 IEEE International Symposium on Antennas and Propagation & USNC/URSI National Radio Science Meeting*, pp. 2327-2328, 2017.

[39] N. Sukaimi, M. Ali, S. Subahir, H. Jumaat and N. Faudzi, "10 GHz Multilayer Antenna Proximity Coupled Feed Using Low Temperature Co-fired Ceramic Technology", *Proceedings of the 2013 IEEE Symposium on Wireless Technology and Applications*, pp. 240-244, 2013.

[40] Y. Liu, H. Liu, M. Wei and S. Gong, "A Novel Slot Yagi-Like Multilayered Antenna With High Gain and Large Bandwidth", *IEEE Antennas and Wireless Propagation Letters*, vol. 13, pp. 790-793, 2014.

[41] Y. Cai, Y. Zhang, C. Ding, Z. Qian and J. Liu, "Design of Multilayer SIW Cavity-Backed Slot Antenna Array", *Proceedings of the 11th European Conference on Antennas and Propagation (EUCAP)*, pp. 1189-1193, 2017.

[42] O. Kramer, T. Djerafi and K. Wu, "Vertically Multilayer-Stacked Yagi Antenna With Single and Dual Polarizations", *IEEE Transactions on Antennas and Propagation*, vol. 58, no. 4, pp. 1022-1030, 2010.

[43] J. Nessel, A. Zaman, R. Lee and K. Lambert, "Demonstration of a X-band Multilayer Yagi-Like Microstrip Patch Antenna with High Directivity and Large Bandwidth", *Proceedings of the 2005 IEEE Antennas and Propagation Society International Symposium*, 2005.

[44] W. Stutzman and G. Thiele, *Antenna Theory and Design*, 3rd ed. New York: John Wiley & Sons, 2013.

[45] G. Zheng, A. Kishk, A. Glisson and A. Yakovlev, "Simplified feed for modified printed Yagi antenna", *Electronics Letters*, vol. 40, no. 8, 2004.

[46] H. Karbalaee, M. Salehifar and S. Soleimany, "Designing Yagi-Uda antenna fed by microstrip line and simulated by HFSS", *2012 6th International Conference on Application of Information and Communication Technologies (AICT)*, 2012.

[47] E. Ávila-Navarro, J. Blanes, J. Carrasco, C. Reig and E. Navarro, "A new bi-faced log periodic printed antenna", *Microwave and Optical Technology Letters*, vol. 48, no. 2, pp. 402-405, 2006.

[48] M. Prasad, S. Amit, M. G, R. S and T. Rukmini, "Design and Fabrication of Printed Dipole Array for Smart Antenna Applications", *International Journal of Emerging Technology and Advanced Engineering*, vol. 2, no. 4, pp. 138-145, 2012.

[49] A. Hoorfar, "Analysis of a "Yagi-like" printed stacked dipole array for high-gain applications", Microwave and Optical Technology Letters, vol. 17, no. 5, pp. 317-321, 1998.

[50] N. Barbano, "Log periodic Yagi-Uda array", *IEEE Transactions on Antennas and Propagation*, vol. 14, no. 2, pp. 235-238, 1966.

[51] "TX-LINE: Transmission Line Calculator", *National Instruments*. [Online]. Available: https://www.awrcorp.com/products/additional-products/tx-line-transmission-line-calculator. [Accessed: 18- Oct- 2018].

[52] E. Ávila-Navarro, J. Carrasco and C. Reig, "Printed Dipole Antennas for Personal Communication Systems", *IETE Technical Review*, vol. 27, no. 4, pp. 286-292, 2010.

[53] A. Alshahrani, K. Alshahrani and F. Alshahrany, "Designing and Building a Yagi-Uda Antenna Array", *International Journal of Multidisciplinary Research and Development*, vol. 2, no. 2, pp. 296-301, 2015.

[54] S. Keyrouz and D. Caratelli, "Dielectric Resonator Antennas: Basic Concepts, Design Guidelines, and Recent Developments at Millimeter-Wave Frequencies", *International Journal of Antennas and Propagation*, vol. 2016, pp. 1-20, 2016.

Appendices

Appendix A

Article for Special Issue "Antenna Technologies for Microwave Sensors" by Sensors Journal

sensors

MDPI

Article

Compact Multilayer Yagi-Uda Based Antenna for IoT/5G Sensors

Amélia Ramos [1,2,*], Tiago Varum [2] and João N. Matos [1,2]

[1] Universidade de Aveiro, Campus Universitário de Santiago, 3810-135 Aveiro, Portugal; matos@ua.pt
[2] Instituto de Telecomunicações, Campus Universitário de Santiago, 3810-135 Aveiro, Portugal; tiagovarum@ua.pt
* Correspondence: ameliaramos@ua.pt; Tel.: +351-234-377-900

Received: 27 July 2018; Accepted: 30 August 2018; Published: 2 September 2018

Abstract: To increase the capacity and performance of communication systems, the new generation of mobile communications (5G) will use frequency bands in the mmWave region, where new challenges arise. These challenges can be partially overcome by using higher gain antennas, Multiple-Input Multiple-Output (MIMO), or beamforming techniques. Yagi-Uda antennas combine high gain with low cost and reduced size, and might result in compact and efficient antennas to be used in Internet of Thins (IoT) sensors. The design of a compact multilayer Yagi for IoT sensors is presented, operating at 24 GHz, and a comparative analysis with a planar printed version is shown. The stacked prototype reveals an improvement of the antenna's main properties, achieving 10.9 dBi, 2 dBi more than the planar structure. In addition, the multilayer antenna shows larger bandwidth than the planar; 6.9 GHz compared with 4.42 GHz. The analysis conducted acknowledges the huge potential of these stacked structures for IoT applications, as an alternative to planar implementations.

Keywords: Yagi-Uda; multilayered antenna; millimeter-waves; IoT

1. Introduction

People's interconnection was improved by 4G, making the communication more efficient, fluent, and natural. Nowadays, 5G intends to continue that demand and take it to a higher level. In this framework, 5G aims to guarantee people's interaction, devices interconnection, as well as the connection among people and devices. A network composed of users, daily gadgets, traffic information, personal health conditions, or the status of all the home electronic devices is only a small example of a possible scheme, shown in Figure 1, within many 5G scenarios that are not yet discovered. For now, it is known that 5G services will be divided in three categories; namely, enhanced mobile broadband, mission-critical control, and massive Internet of Things (IoT) [1].

Probably the most effective method to fulfil some demands for 5G cellular services, which are expected to be commercially available in 2020, is to increase the bandwidth [2]; hence, the migration to higher frequencies (in the mmWaves) is mandatory, mainly to support the required gigabit data rate service [3]. On the other hand, as a disadvantage, the frequency ranges of mmWaves present higher path-loss resulting in fragile link, due to weak diffractions at these frequency bands. To overcome these issues, high gain antennas and highly directive antenna arrays using several elements, as well as the application of beamforming techniques, can be used, in order to transmit the wave in the right direction. Yagi-Uda antennas present several characteristics that make them suitable for application in sensors or in larger antenna arrays.

Figure 1. Example of 5G communications and a massive Internet of Things (IoT) scenario.

Structurally Yagi-Uda antennas are well known. They are composed of a driven dipole, a reflector element, and a variable number of directors. This scheme guarantees the creation of an end-fire beam [4], appropriate for beamforming applications. This antenna's layout has been widely analyzed, and historically used, mainly because these structures present a reasonable bandwidth and relatively high gains at moderated costs [5]. With the emergence of printed circuits, several Yagi-like antennas have been proposed for different frequencies of operation and a wide number of applications [6,7].

In Internet of Things (IoT) scenarios, antennas are to be implemented in every small gadget or wearable gadget, mainly to assure the interaction between sensors placed in the most various devices and people. Because of their widespread use, it is highly recommended that antennas are small and compact.

Over the years, some effort has been made to find antenna miniaturization techniques that allow reducing antenna size, maintaining or improving its main characteristics. Some of these methods are described in the literature [8], presented in different classes, including techniques such as fractals, metamaterials, high dielectric constant substrates, slow wave structures, or engineered ground planes. A miniaturization technique described in the literature that is widely used because it also allows obtaining broadband characteristics is the use of reactive impedance substrates (RIS) [9]. In the works of [10,11], two patches are presented, designed on an RIS, which convert them into Ultra-wideband (UWB) antennas. In another work [10], the bandwidth increases over than 100 times, compared with the conventional patch antenna, while in the work of [11], the bandwidth is increased by a factor of 16. These solutions based on RIS are, however, complex to design in millimeter waves, and are used in antenna structures with ground planes.

In addition, for IoT and 5G applications, gain is a concern and even though Yagi antennas naturally present higher gains than microstrip patch antennas [4], this work intends to analyze the advantages of implementing a Yagi-Uda antenna in a multilayer configuration to further enhance its most important properties, such as the gain and the bandwidth.

Multilayer structures have been tested as an attempt to increase the antenna's gain. In the works of [12,13], two microstrip patch antennas are presented in a multilayer configuration. In the work of [12], an antenna composed of two stacked patches is proposed as a low-cost solution, operating around 3 GHz. The antenna's bandwidth is 14%, but the information about the radiation pattern and the gain is not provided. On the other hand, in another paper [13], an antenna based on a microstrip patch is presented. It is formed by three parasitic patches working as director elements, operating around 10 GHz. This antenna uses a dielectric foam to ensure the distance between directors, as well as a V-shaped ground plane to improve the reflection coefficient. This antenna has about 190 MHz bandwidth and gain of 11.85 dB, although at the expense of some complexity, and any prototype built is not shown. Additionally, in the work of [14], a structure of eight layers in Low Temperature Co-fired Ceramic (LTCC) technology is presented, also designed for 10 GHz. This antenna consists of a microstrip patch using a proximity coupled feed, presenting a gain of only 3.43 dBi and an S_{11} of −11.52 dB at 10 GHz, in addition to a narrow bandwidth. Moreover, a slot Yagi-like multilayered antenna is proposed by the authors of [15] for 4.2 GHz. This is a vertically stacked structure with

three patches, which uses slit slots as the parasitic elements. The prototype shows a bandwidth of about 28% and a gain of 12.20 dBi. However, this structure is bulky and complex. Furthermore, a multilayer substrate integrated waveguide horn antenna array is proposed in another paper [16], in a 4×4 array configuration. This antenna uses multilayer cavities with gradually decreased permittivity and expanded aperture sizes above the slots to increase the bandwidth. The array operates between 22.4 to 29.8 GHz (about 28.4% bandwidth) and presents a gain around 15 dBi; however, its complexity is huge.

The authors of [17] designed a Yagi antenna resonant at 5.8 GHz using air gaps, presenting a bandwidth of 14% and a gain of 11 dBi. These air gaps between layers are function of the operation frequency, and this antenna requires a huge spacing between the elements, turning the antenna bulky and likely to vary its physical structure and properties over the time.

The authors of [18] implemented a multilayer Yagi-like microstrip patch antenna, without air gaps. A gain of 11 dBi was reached and this antenna presents a reasonable measured bandwidth of nearly 20%. However, the structure uses foam between the directors, with low permittivity, which increases the volume of the antenna. No efficiency values are referred to in this work. This antenna is resonant at 10 GHz, which is still a low frequency for the 5G and the massive IoT referred scenarios. A multilayered antenna for 60 GHz is proposed in the work of [19]. This antenna has a reduced size and presents an individual gain of 11 dBi. However, its bandwidth is just 4.2%, which is a clear disadvantage considering the high traffic data rates that, predictably, will be witnessed.

In this paper, two printed antennas are presented for IoT sensors, operating at 24 GHz, and designed according to the theoretical principles of Yagi-Uda structures. A planar printed Yagi-Uda is designed and characterized, and its prototype is shown. This antenna has a gain of 8.9 dBi and a bandwidth of 18%. Then, a compact multilayer stacked antenna is presented. This antenna improves all the main properties of the planar printed Yagi and outperforms the previously referred antennas, showing a gain of 10.9 dBi, an operation bandwidth of 27%, and a total efficiency of 86%, besides its reduced size. This antenna is also an interesting element to be used in larger arrays, and is suited for beamforming applications.

This paper is divided into five sections, starting with an introduction regarding some of the possible applications for these prototypes, where our goals are settled. In the second section, the required features to design the proposed antennas are presented, and in Section 3, the simulation and measured results of both antennas built are shown. Then, the fourth section presents a light discussion on the results obtained, where mainly a comparison between both antennas is highlighted. Lastly, in section five, the main conclusions are reported.

2. Materials and Methods

A Yagi-Uda antenna is a directive radiating structure composed of an active element and a group of passive elements, commonly referred to as directors and reflector, with the objective to steer the radiation to a specific direction [5]. Traditionally, Yagi antennas were based on metallic wire structures, in which the directors, reflectors, and the half-wavelength dipole were created [4]. However, and because printed antennas and circuits are currently widely used in microwave applications, several researchers have implemented printed Yagi-like structures in a planar dielectric substrate. Printed antennas allow one to develop low-cost and low-profile antennas, highly versatile and with good efficiency, facilitating its integration in microwave circuits [20].

Design concerns of such antenna lie on the estimation of the lengths of the various constituent elements of the antenna, the distance between them, and, possibly, the number of directors needed to accomplish the goals. In this work, the optimal length for the dipole is not equivalent to half-wavelength in vacuum because these antennas are to be printed on a dielectric substrate, and its dielectric constant has a direct impact, causing a reduction on the dipole's length [21]. In fact, in the literature [21], it was found that the optimal length for a printed dipole would be 0.38 λ. Consequently,

an overall reduction on the antenna's size occurs, which is a clear advantage when considering the target applications for which these antennas can be applied.

When designing antennas for this frequency band, one of the main challenges is the choice of the dielectric substrate to use, as it has a strong impact in the design and in the performance of the antenna. Moreover, at these frequencies, because of the small size of the elements, a more cautious design is required to guarantee an appropriate performance at 24 GHz. In this work, the substrate used is the Rogers RO4350B, because of its good performance in high frequencies (as it presents low dielectric tolerance and loss), as well as its electrical stability properties over frequency. The main characteristics include a relative dielectric permittivity of $\varepsilon_r = 3.48$, a dissipation factor of $\tan(\delta) = 0.0037$ with a thickness of h = 0.762 mm.

Usually, in Yagi antennas, the spacing between directors varies between 0.1 λ and 0.3 λ and their length is 5% to 30% shorter than the active element [6]. On the other hand, the reflector typically is up to 5% longer than the dipole and it backs the driver [6]. This placement of the active and parasitic elements ensures the end-fire beam formation [4]. In this work, the design of two Yagi antennas is presented, where the first one follows a planar structure and the second is a multilayer assembly of dielectric substrates with the elements printed on them. Both antennas are composed by a dipole, a reflector and three director elements, which is a trade-off between the gain achieved and the overall size of the antennas.

2.1. Planar Yagi-Uda Design

The design of the antenna starts with the radiating element, by creating the two arms of the dipole (with global length L_{dip} and width W_{dip}) over a substrate layer, which are separated by a small gap, which should be carefully selected as it affects the input impedance of the dipole. Then, three strip directors (with size $L_{dir} \times W_{dir}$) were introduced after the dipole, separated by a distance DirSpa, which was adjusted in the simulation process to improve the radiation performance of the antenna. The number of directors was a trade-off between the global size of the antenna and its directivity.

Then, the feeding part, composed of an impedance matching network, a microstrip balun, and two coplanar printed lines, were connected to the dipole. The coplanar lines allow one to connect each arm of the dipole to each output of the balun, and also to separate the microstrip structure from the dipole of a distance Lcps. This is important because the microstrip section also acts as a reflector element of the Yagi [22]. The balun creates the balanced feeding, by splitting the input signal in two outputs with half-power and half-wavelength phase delay, and finally, a double microstrip transformer matches the input impedance of the antenna to a 50 Ω microstrip line.

The layout of the designed planar Yagi antenna is presented in Figure 2a. The planar Yagi-Uda antenna was simulated and its dimensions were optimized. After several simulations, the optimal values for the design parameters were accomplished and are summarized in Table 1. As function of the wavelength, it is found that the optimal value for the dipole's length is equivalent to 0.415 λ, which is reasonably close to theoretical approaches for printed Yagi antennas. The manufactured prototype is shown in Figure 2b.

Figure 2. Planar Yagi-Uda antenna: (**a**) layout and parameters; (**b**) photograph of the prototype.

Table 1. Parameters of the 24 GHz planar Yagi-Uda antenna (UNITS: mm).

L_{dip}	L_{dir}	W_{dip}	W_{dir}	gap	DirSpa	L_{cps}	W_{cps}	W_{msc}	L_{t1}	L_{t2}	W_{t1}	W_{t2}
5.19	2.75	0.8	0.72	0.3	3	1.63	0.25	0.8	1.64	1.91	0.65	0.54

2.2. Multilayer Yagi-Uda Design

A multilayer version of the printed Yagi antenna was designed with a view to improve the performance and to compact its structure. According to what has been analysed in the literature [23], a gain saturation occurs for planar antennas, especially planar antenna arrays, and developing antennas in a multi-layered arrangement can overcome this limit, because it uses the vertical dimension [19].

The design was based on converting a set of directors and the reflector, properly spaced around the printed dipole. The radiation will be conducted in the upper vertical plane, instead of the horizontal plane, as in the planar version. This radiation characteristic can reveal being a clear advantage for many of the sensors where the antenna will be placed. This type of structure implies that the elements are surrounded in the dielectric substrate. This is one of the differences regarding the planar structure, where the radiation in the antenna follows two different mediums, air and dielectric substrate. Avoiding some air gaps inside the antenna structure keeps it more robust and stable physically, but also in terms of its properties to the environment variations. Thus, in the design process, it is imperative in this application to consider the wavelength in the specified substrate (λ_d).

Considering that the construction of multilayer antennas has a relative novelty, a study on the dielectric and structure was carried out, as a way of better understanding the antenna's behaviour and the changes produced by structural modifications.

The design of this antenna was based on theoretical dimensions, which were then adjusted through simulation. As in the previous planar form, a dipole was printed on a substrate, and a reflector element using the same line width was placed below at a distance h_{ref}. This separation was guaranteed by using a number of layers of dielectric substrate between the elements.

Several simulations were performed varying the number of directors placed on the structure, with a length of 0.25 λ_d, and spaced by a distance h_{dir}. Additionally, the impact of adding a new layer of dielectric material over the last director element was studied. These two versions of structure are shown in Figure 3a,b, respectively. Moreover, Figure 3b highlights the layers identification. Thus, layers E_n constitute the extra dielectric layers (which are to be studied), layers named $D_{n.m}$, represent the distance between each director and the following element, meaning the parameter h_{dir}, and lastly, R_n layers are representing the distance between the dipole and the reflector.

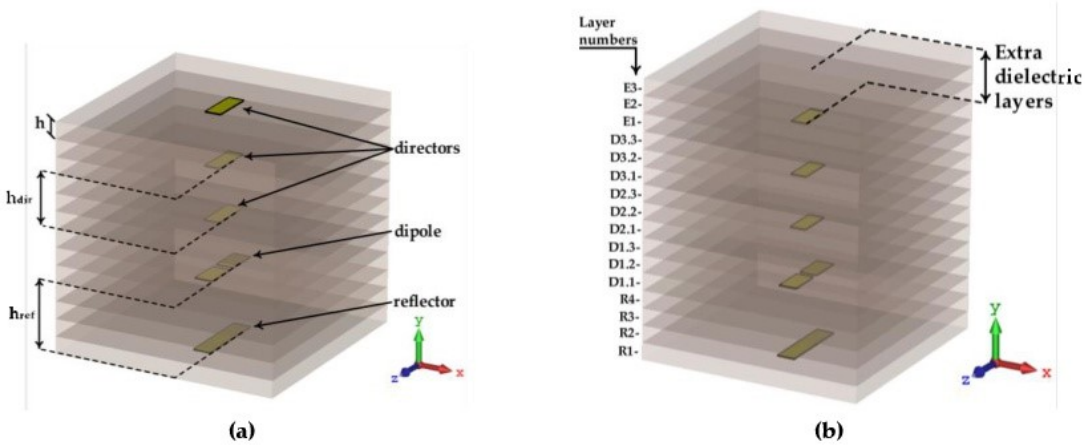

Figure 3. Vertically stacked Yagi antenna: (**a**) without the extra top layers of dielectric; (**b**) with extra layers of substrate.

The analysis was focused mainly on the radiation parameters of the antenna, particularly on its radiation pattern and the obtained gain, because it induces the directivity, which is one of the main parameters that it is required to enhance our application, thus maintaining the compactness of the structure. The results are shown in Figures 4–6.

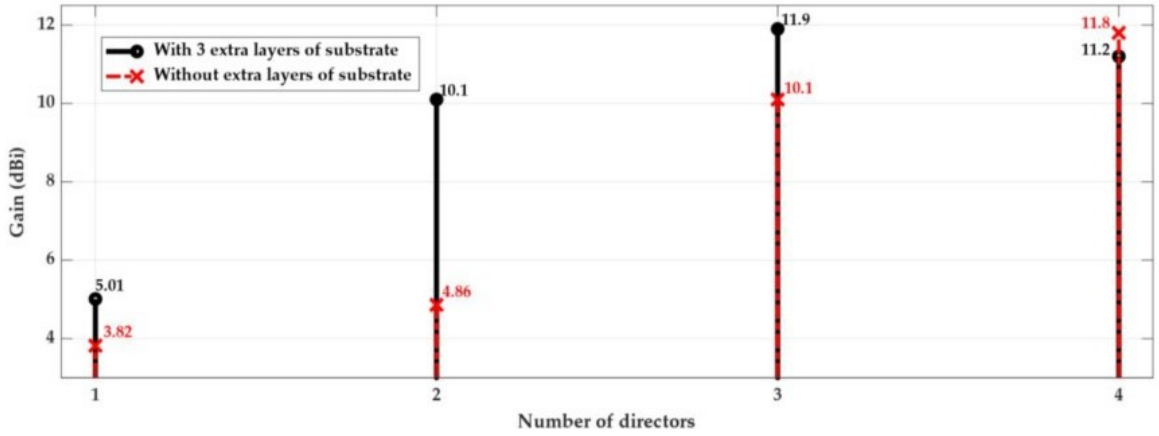

Figure 4. Gain variation with the number of director elements in the Yagi antenna.

Figure 4 (cross marker) shows the evolution of the antenna's gain as a function of the number of directors added after the dipole. As expected, the gain increases as the number of directors increases. In parallel, the volume of antenna structure also grows substantially. However, the directors were designed to guide the waves surrounded in dielectric, and the last director has the same length of all the others and is not surrounded as the others are, which led to implementing a slight different scheme.

An alternative design was proposed, as shown in Figure 3b, where on the top of the third director, a few extra layers of dielectric were used. Naturally, this alternative design increases the antenna's height, but as it is presented in Figure 4 (circle marker), it is clearly compensated by an increase of the antenna's gain, about 1.8 dBi, using up to three directors. On the other hand, when using four director elements, it is possible to observe a reduction of the gain when the extra dielectric layers are inserted.

Considering the results of Figure 4, and taking into account the obtained antenna's gain and its dimensions, using the two possible approaches of Figure 3, three directors were chosen as the optimal compromise for the multilayer Yagi antenna.

Using three directors in the multilayer structure, several simulations were performed mainly to understand the impact of increasing the thickness of the extra substrate layer on the top of the third director. The gain variation due to the number of substrate layers that form the extra dielectric (Figure 3b) is illustrated in Figure 5. The substrate used has a thickness of h = 0.762 mm, and so, the height that tops the last director, as well as the various distances between the other elements, are a multiple of this value.

According to Figure 5, it can be realised that there is a limit to the thickness of the last substrate layer above the last director. The value that maximizes the antenna gain corresponds to 3 h, which is equivalent to 2.286 mm. Finally, to understand the variation of the structure's gain (using three directors) with the distance between them, in multiples substrate layers (h), a few more simulations were performed, and the results are shown in Figure 6. In this figure, it is verified that the optimal separation between the several directors corresponds to three layers of substrate (3 h), equivalent to h_{dir} = 2.286 mm.

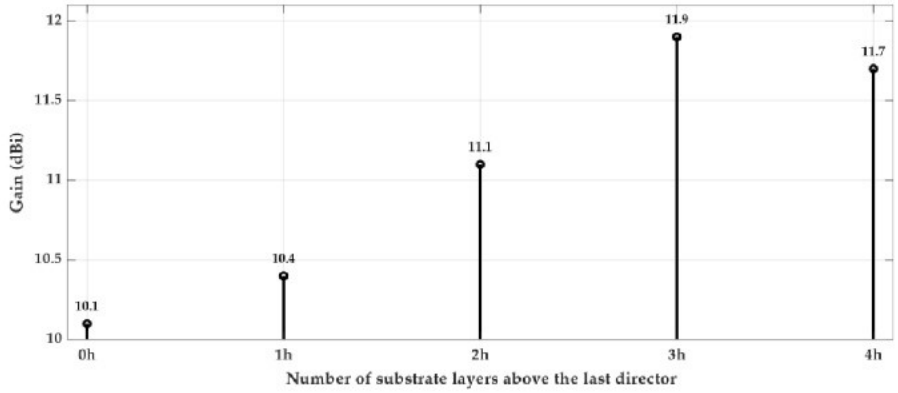

Figure 5. Variation of the gain with the usage of extra layers of substrate topping the last director.

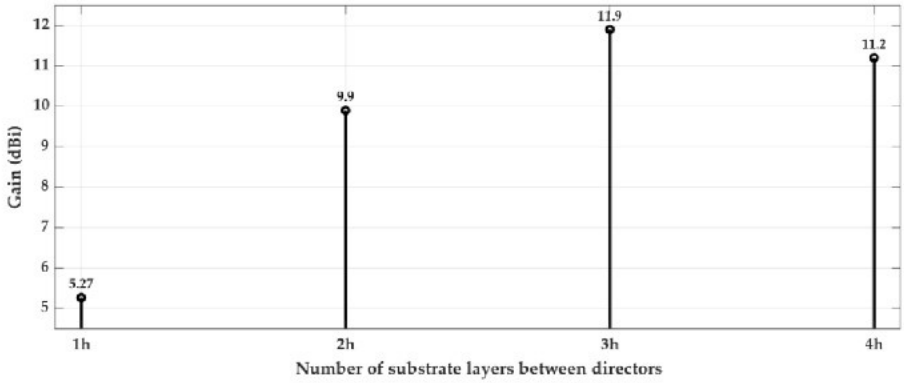

Figure 6. Variation of the gain with the number of dielectric layers between directors.

Considering the analysis presented above, the multilayer structure of a Yagi-Uda antenna was designed, as is shown in Figure 7a. The multilayer antenna features an optimized compromise between gain and functionality with compact dimensions. It consists of a printed dipole together with three director elements, spaced by a dielectric layer with thickness 3 h, and with a reflector element placed at an optimized distance of: h_{ref} = 4 h. The feeding part of antenna has the same basis of the design used for the planar antenna. Figure 7b shows the prototype of the proposed Yagi-Uda antenna and its final dimensions are mentioned.

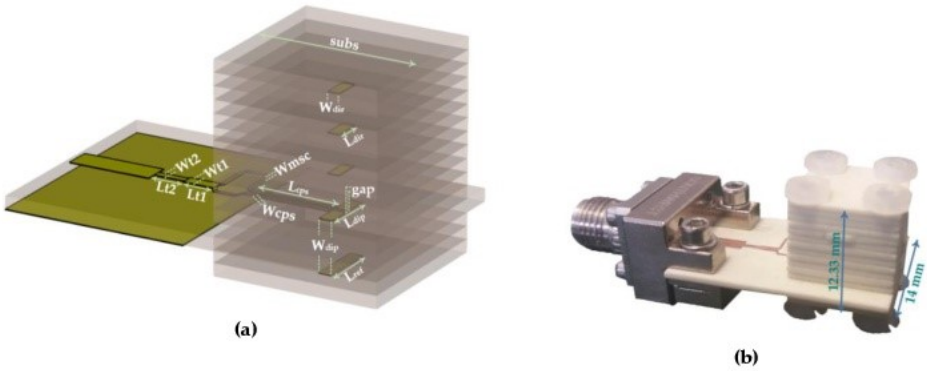

Figure 7. Multilayer Yagi-Uda antenna: **(a)** layout and parameters; **(b)** photograph of the prototype.

After an iterative simulation process, it was possible to achieve the optimal values for the parameters shown in Figure 7a, which are presented in Table 2. Regarding the dipole's length as a function of λ_d, the optimal length is equivalent to 0.45 λ_d.

Table 2. Parameters of the 24 GHz multilayer Yagi-Uda antenna (UNITS: mm).

Subtable 2.1. Lengths of the lines used.					
L_{dip}	L_{dir}	L_{ref}	L_{cps}	L_{t1}	L_{t2}
3	1.68	3.47	5.32	1.88	1.918
Subtable 2.2. Widths of the lines used.					
W_{dip}	W_{dir}	W_{cps}	W_{msc}	W_{t1}	W_{t2}
0.80	0.715	0.25	0.25	0.78	0.48
Subtable 2.3. Other parameters of design.					
h_{dir}		h_{ref}	subs		gap
2.286		3.048	10		0.3

3. Results

3.1. Planar Yagi-Uda: Simulated and Measured

The planar Yagi antenna depicted in Figure 2 was simulated and characterized in terms of its most important parameters. It was fabricated and measured, and the results are presented in Figures 8 and 9. Figure 8 shows the comparison between the simulated and measured reflection coefficient of the designed antenna. It is possible to observe that the antenna has a good impedance matching at 24 GHz, with a simulated S_{11} of −31 dB and a measured value of −23 dB.

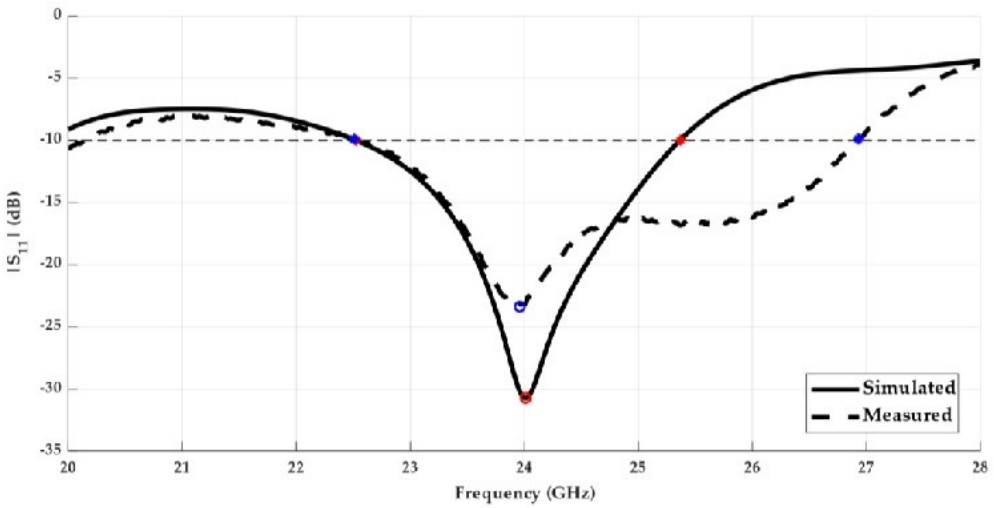

Figure 8. Simulated and measured S_{11} of the designed planar Yagi-Uda antenna.

In terms of operation bandwidth, this antenna presents considerable good results, where the prototype achieved a band of 4.42 GHz [22.5–26.9 GHz] in which it is properly matched, considering the $S_{11} < -10$ dB criteria, representing a bandwidth of 18%. Comparing these results with the simulated ones, an improvement in the bandwidth was obtained.

Regarding the radiation properties of the antenna, Figure 9 presents the simulated radiation pattern of the designed antenna, in terms of its 3D view (Figure 9a), and the plane $\phi = 0°$ in the 2D polar diagram (Figure 9b). A directive radiation pattern in the horizontal plane, the plane where the directors are placed is observed, with a simulated gain of 8.9 dBi at 24 GHz. The planar antenna also presents a total efficiency of 90%.

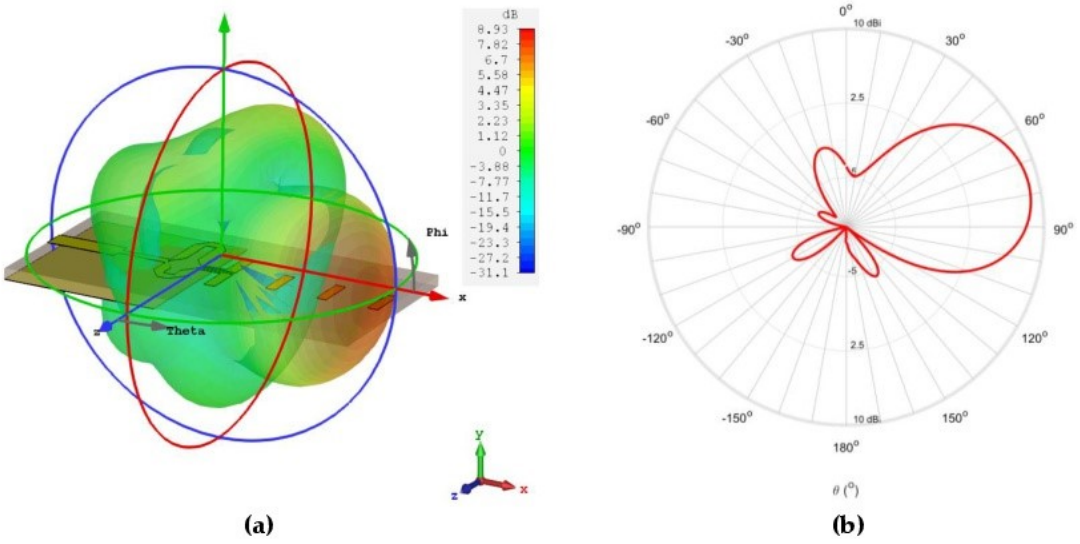

Figure 9. Simulated radiation pattern of the 24 GHz planar antenna: (**a**) 3D view; (**b**) polar diagram of plane $\phi = 0°$.

3.2. Multilayer Yagi-Uda: Simulated and Measured

Concerning the multilayer antenna from Figure 7, it was simulated and analysed according to its main properties. Figure 10 shows the comparison between the simulated and measured results of the reflection coefficient of the antenna.

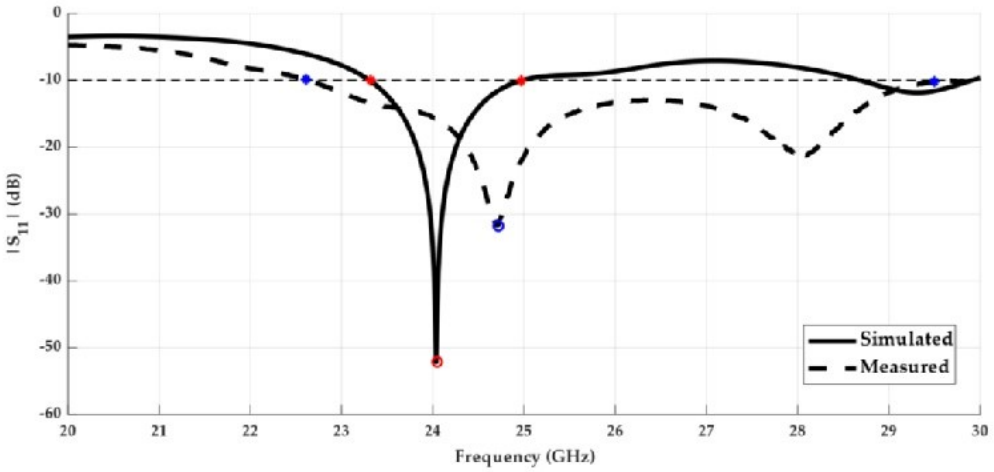

Figure 10. Simulated and measured reflection coefficient of the multilayer Yagi antenna.

A good impedance matching can be observed, showing that the antenna was perfectly tuned in terms of simulation despite the frequency shift of 710 MHz in relation to the measured curve. However, at the operation frequency, 24 GHz, a measured S_{11} of −15.51 dB makes these results satisfactory. Moreover, the designed multilayer antenna presents roughly 6.9 GHz of bandwidth, equivalent to 27%, from 22.6 GHz up to 29.5 GHz—a frankly encouraging result.

Looking at the radiation pattern, the simulated results are shown in Figure 11, where it is possible to verify the alignment of the main lobe with the directors of the antenna, in accordance with the vertical plane.

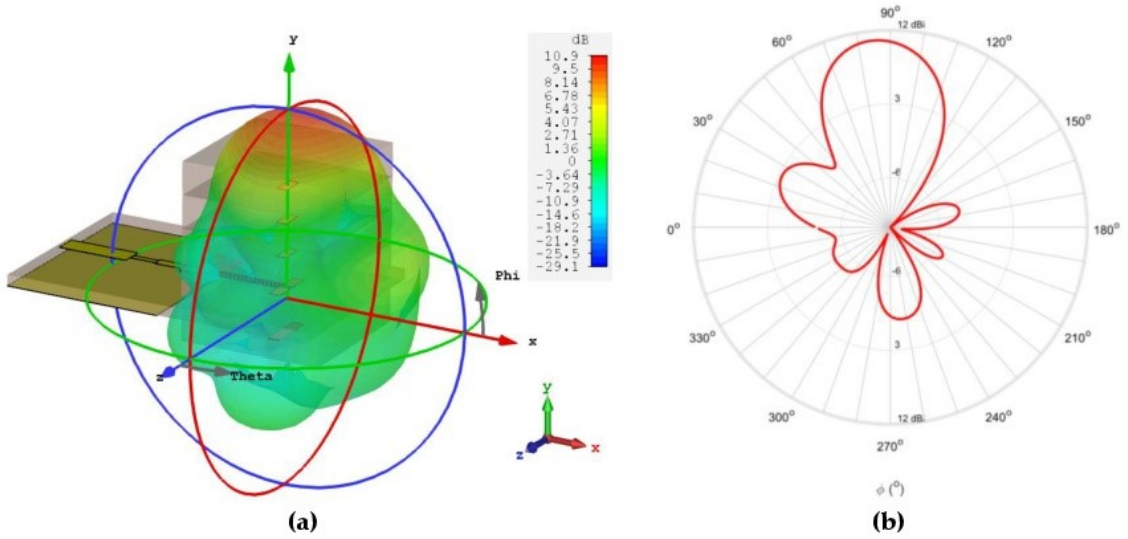

Figure 11. Simulated radiation pattern of the 24 GHz multilayer antenna: (**a**) 3D view; (**b**) polar diagram.

Figures 12 and 13 show the variation of the maximum gain of the antenna and its total efficiency, respectively, over the frequency. It can be seen that the structure has a maximum gain of 10.9 dBi at 24 GHz, the frequency for which it was designed. Furthermore, there is a range of about 2 GHz around the operating frequency where the gain is always greater than 10 dBi.

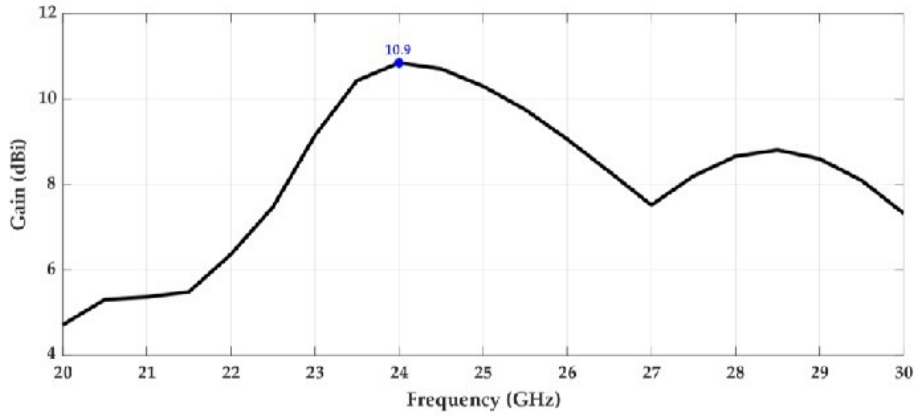

Figure 12. Gain over frequency.

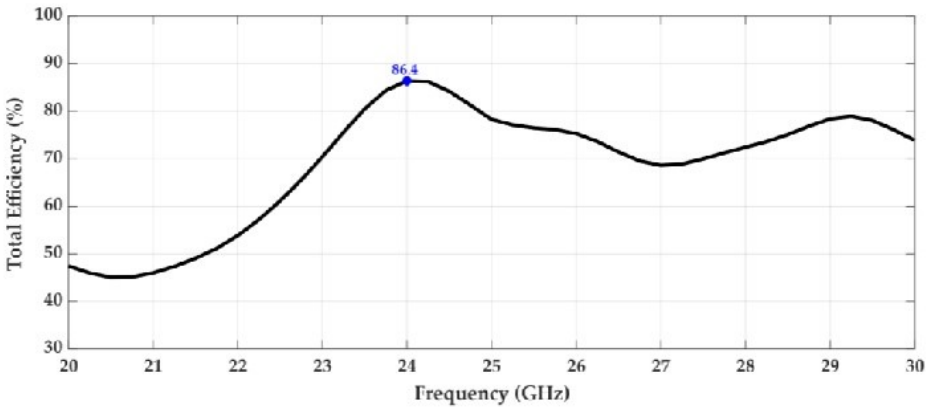

Figure 13. Total efficiency over frequency.

In terms of the antenna's efficiency, according to Figure 13, it is possible to see that it is high, about 86% at the 24 GHz frequency. This result is very important, given the complexity of the structure, its compactness, consisting of several stacked substrate dielectric layers. It should also be noted that between 23.5 and 24.9 GHz, the total efficiency of the antenna is always greater than 80%.

4. Discussions

Regarding the feeding structure, it was verified that the used microstrip-to-coplanar stripline transition provides good matching results between the simulated and practical measurements, for both designed antennas. However, this microstrip structure is not physically symmetrical, because of the balun's arms that cause the 180° phase shift. This asymmetry causes a slight deviation on the main lobe of the radiation pattern in the planar antenna. In the multilayer implementation, the influence of the balun in radiation is negligible, as a reflector element was used, and the main radiation lobe is vertically aligned with the directors.

Furthermore, the impedance matching made on the planar antenna is very accurate, however, in the multilayer antenna, a small frequency shift was observed. This might be a consequence of the construction method of this antenna, which was very simple, just to demonstrate the concept. In fact, this vertically stacked Yagi-Uda antenna has its elements surrounded in substrate, and, possibly, there may have existed a slight difference between the practical and theoretical, used in simulation, and as a result, the minimum return loss happens at a slight different frequency than in the simulation.

The concept of converting the planar into a multilayer structure, as shown in Table 3, is clearly promising, as not only it is possible to reduce the antenna's overall size, but also, improvements are seen, both in bandwidth and gain.

Table 3. Measured bandwidth and simulated gain of both antennas.

Antenna	Bandwidth	Gain
Planar	4.42 GHz 18%	8.9 dBi
Multilayer	6.9 GHz 27%	10.9 dBi

5. Conclusions

In this paper, two compact printed antennas, based on Yagi structures, were presented as a solution to integrate IoT sensors. A multilayer antenna, which is an adaptation of the conventional planar Yagi structure was designed, improving the most important properties compared with the planar antenna and with the state-of-the-art. The multilayer antenna designed provides more than 25% bandwidth, covering the entire 5G allocated band in Europe, allowing its usage for IoT applications. Its improved gain to almost 11 dBi in a cube structure of nearly 1 cm^3 of volume is a good achievement to combat the propagation issues of use mmWave frequencies, a gain considerably higher than the conventional microstrip patch antennas.

Moreover, the multilayer configuration permits to change the direction of radiation to the vertical plane, allowing it to be placed over the IoT sensors circuits. These results were not obtained at the expense of a reduction of antenna efficiency, because the multilayer structure shows an efficiency of 86%. Finally, the multilayer antenna has modular physical features that allow it to be easily grouped into high gain antenna arrays, or also arrays for 5G applications using beamforming techniques. Thus, the multilayer antenna presents better radiation performance, essentially, better gain and a wider bandwidth while being simultaneously smaller and more compact.

In conclusion, the possibility of using both Yagi antennas in 5G scenarios, physical sensors, or as a singular element of a larger array has been confirmed. Moreover, a multilayer implementation seems to be a promising chance for achieving better performances at higher frequencies.

Author Contributions: All the authors have contributed to this paper. Amélia Ramos has designed the proposed antennas, performed the simulations and the measurements, and wrote the paper. Tiago Varum and João N. Matos have supervised the entire research, the approach used, the results analysis, and discussion. Additionally, both have strongly contributed to the writing of the paper.

Acknowledgments: This work is supported by the European Regional Development Fund (FEDER), through the Competitiveness and Internationalization Operational Programme (COMPETE 2020) of the Portugal 2020 framework, Project, RETIOT, POCI-01-0145-FEDER-016432.

Conflicts of Interest: The authors declare no conflict of interest.

References

1. Making 5G NR a Reality. Available online: https://www.qualcomm.com/documents/making-5g-nr-reality (accessed on 17 July 2018).
2. Roh, W.; Seol, J.Y.; Park, J.; Lee, B.; Lee, J.; Kim, Y.; Cho, J.; Cheun, K.; Aryanfar, F. Millimeter-Wave Beamforming as an Enabling Technology for 5G Cellular Communications: Theoretical Feasibility and Prototype Results. *IEEE Commun. Mag.* **2014**, *52*, 106–113. [CrossRef]
3. 5G Vision. Available online: https://www.samsung.com/global/business/networks/insights/white-paper/?white-paper (accessed on 17 July 2018).
4. Balanis, C. *Antenna Theory Analysis and Design*, 4th ed.; John Wiley & Sons: New Jersey, NJ, USA, 2016.
5. Balanis, C. *Modern Antenna Handbook*; John Wiley & Sons: New Jersey, NJ, USA, 2008.
6. Ávila-Navarro, E.; Carrasco, J.; Reig, C. Design of Yagi-like printed antennas for wlan applications. *Microwave Opt. Technol. Let.* **2007**, *49*, 2174–2178. [CrossRef]
7. Grajek, P.R.; Schoenlinner, B.; Rebeiz, G.M. A 24 GHz High-Gain Yagi-Uda Antenna Array. *IEEE Trans. Antennas Propag.* **2004**, *52*, 1257–1261. [CrossRef]
8. Fallahpour, M.; Zoughi, R. Antenna miniaturization techniques: A Review of Topology-and Material-Based Methods. *IEEE Antennas Propag. Mag.* **2018**, *60*, 38–50. [CrossRef]
9. Mosallaei, H.; Sarabandi, K. Antenna miniaturization and bandwidth enhancement using a reactive impedance substrate. *IEEE Trans. Antennas Propag. Mag.* **2004**, *52*, 2403–2414. [CrossRef]
10. Yao, J.; Tchafa, F.M.; Jain, A.; Tjuatja, S.; Huang, H. Far-field interrogation of microstrip patch antenna for temperature sensing without electronics. *IEEE Sens. J.* **2016**, *16*, 7053–7060. [CrossRef]
11. Li, L.W.; Li, Y.N.; Yeo, T.S.; Mosig, J.R.; Martin, O.J. A broadband and high-gain metamaterial microstrip antenna. *Appl. Phys. Lett.* **2010**, *96*, 164101. [CrossRef]
12. Giunta, G.; Novi, C.; Maddio, S.; Pelosi, M.; Selleri, S. Efficient tolerance analysis on a low cost compact size, sideband multilayer patch antenna. In Proceedings of the 2017 IEEE International Symposium on Antennas and Propagation & USNC/URSI National Radio Science Meeting, San Diego, CA, USA, 9–14 July 2017.
13. Pornprachatham, N.; Theeradejvanichkul, T. Enhancement of a reflection coefficient via modified ground plane of a multilayer microstrip patch antenna for x-band application. In Proceedings of the 2017 IEEE International Symposium on Antennas and Propagation & USNC/URSI National Radio Science Meeting, San Diego, CA, USA, 9–14 July 2017.
14. Sukaimi, N.H.M.; Subahir, M.T.; Jumaat, H.; Faudzi, N.M. 10 GHz multilayer antenna proximity coupled feed using low temperature co-fired ceramic technology. In Proceedings of the 2013 IEEE Symposium on Wireless Technology & Applications (ISWTA), Kuching, Malaysia, 22–25 September 2013.
15. Liu, Y.; Liu, H.; Wei, M.; Gong, S. A novel slot Yagi-like multilayered antenna with high gain and large bandwidth. *IEEE Antennas Wirel. Propag. Lett.* **2014**, *13*, 790–793.
16. Cai, Y.; Zhang, Y.; Ding, C.; Qian, Z.; Liu, J. Design of a multilayer SIW Cavity-backed slot antenna array. In Proceedings of the 11th European Conference on Antennas and Propagation (EUCAP), Paris, France, 19–24 March 2017.
17. Kramer, O.; Djerafi, T.; Wu, K. Vertically Multilayer-Stacked Yagi Antenna with Single and Dual Polarizations. *IEEE Trans. Antennas Propag.* **2010**, *58*, 1022–1030. [CrossRef]
18. Nessel, J.; Zaman, A.; Lee, R.Q.; Lambert, K. Demonstration of a X-Band Multilayer Yagi-Like Microstrip Patch Antenna with High Directivity and Large Bandwidth. In Proceedings of the 2005 IEEE Antennas and Propagation Society International Symposium, Washington, DC, USA, 3–8 July 2005.
19. Kramer, O.; Djerafi, T.; Wu, K. Very Small Footprint 60 GHz Stacked Yagi Antenna Array. *IEEE Trans. Antennas Propag.* **2011**, *59*, 3204–3210. [CrossRef]

20. Zhong, Q.; Li, Y.; Jiang, H.; Long, Y. Design of a Novel Dual-frequency Microstrip Patch Antenna for WLAN Applications. *IEEE Antennas Propag. Soc. Symp.* **2004**, *1*, 277–280.
21. Ávila-Navarro, E.; Blanes, J.M.; Carrasco, J.A.; Reig, C.; Navarro, E.A. A New Bi-faced Log Periodic Printed Antenna. *Microwave Opt. Technol. Lett.* **2006**, *48*, 402–405. [CrossRef]
22. Ávila-Navarro, E.; Carrasco, J.A.; Reig, C. Printed Dipole Antennas for Personal Communication Systems. *IETE Tech. Rev.* **2010**, *27*, 286–292. [CrossRef]
23. Hall, P.S.; Hall, C.M. Coplanar corporate feed effects in microstrip patch array design. *IEE Proc. H (Microwaves, Antennas Propag.)* **1988**, *135*, 180–186. [CrossRef]

Appendix B

Smith Charts for the *Lcps* calculation

These Smith Charts were used to calculate the appropriate length of the coplanar lines used in the multilayer Yagi antenna. They're responsible for the coplanar stripline-to-microstrip transition.

→Characteristic impedance: 121.2 Ω
→Antenna's impedance in 1:
Za=52.955 - i8.62
za=0.437-i0.07

→Lcps1 length, meaning, from the dipole up to the edge of the cubic structure:
Lcps1=4.6mm
λ_d=6.7mm
→Thus, Lcps1=0.68λ_d

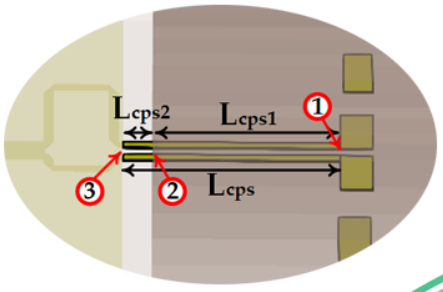

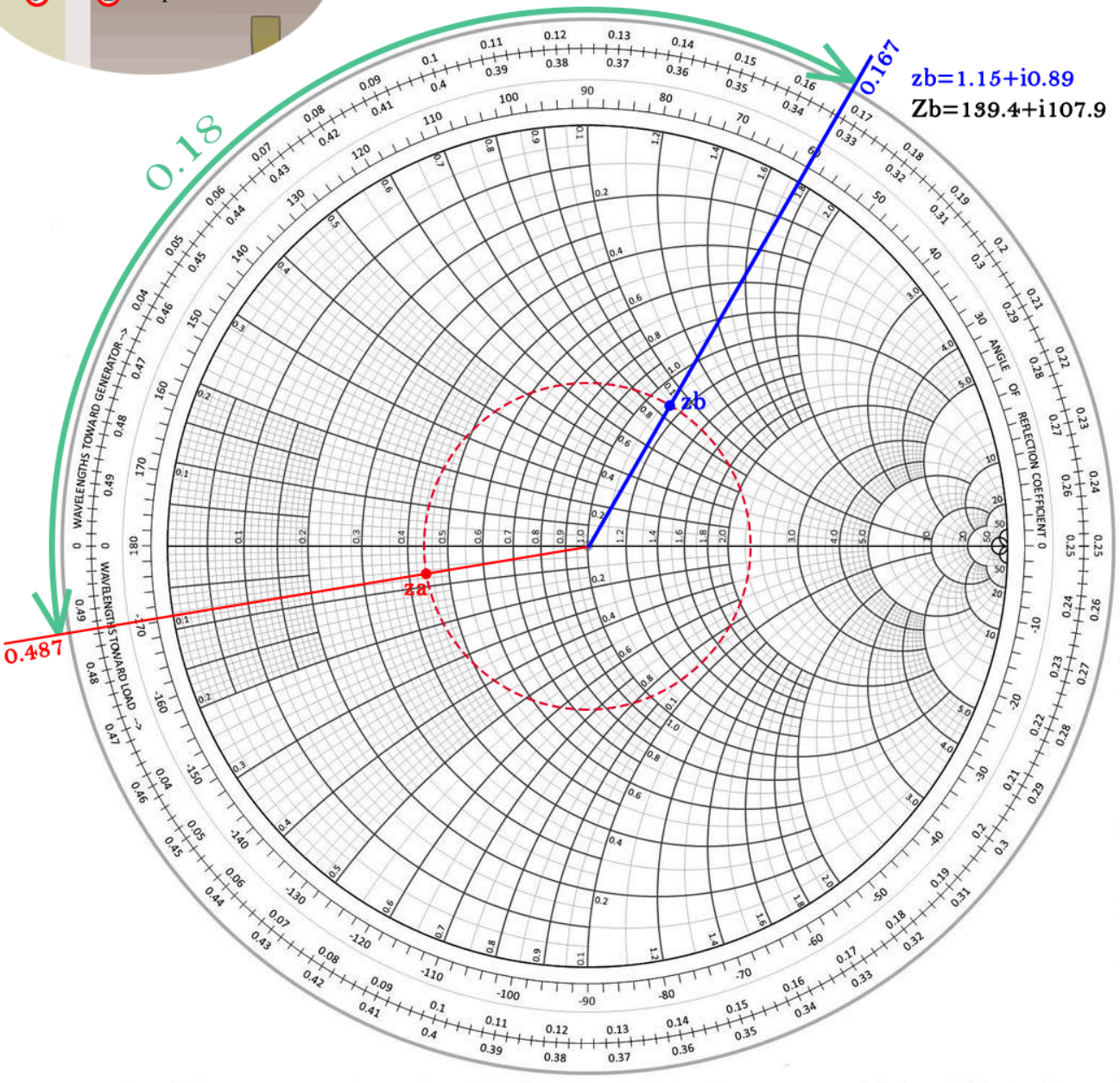

→Characteristic impedance: 136.4Ω
→Zb impedance in 2:
Zb= 139.4+i107.9
zb=1.02+i0.79

→Theoretical length of Lcps2 to achieve a real impedance in 3:
Lcps2=0.093
λ_{ar}=9mm
→ Therefore,
Lcps2=0.837mm

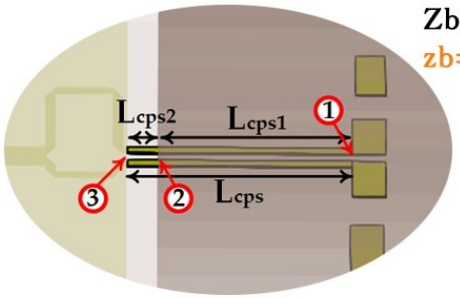

Lcps=Lcps1+Lcps2=
=4.6+0.837=
=5.437mm